

1-1-2008

Modeling the unsaturated zone at the Area 5 Radioactive Waste Management Site: Effects of climate change and vegetation on flow conditions

Amanda Marie Brandt
University of Nevada, Las Vegas

Follow this and additional works at: <https://digitalscholarship.unlv.edu/rtds>

Repository Citation

Brandt, Amanda Marie, "Modeling the unsaturated zone at the Area 5 Radioactive Waste Management Site: Effects of climate change and vegetation on flow conditions" (2008). *UNLV Retrospective Theses & Dissertations*. 2394.

<http://dx.doi.org/10.25669/udo5-xrtm>

This Thesis is protected by copyright and/or related rights. It has been brought to you by Digital Scholarship@UNLV with permission from the rights-holder(s). You are free to use this Thesis in any way that is permitted by the copyright and related rights legislation that applies to your use. For other uses you need to obtain permission from the rights-holder(s) directly, unless additional rights are indicated by a Creative Commons license in the record and/or on the work itself.

This Thesis has been accepted for inclusion in UNLV Retrospective Theses & Dissertations by an authorized administrator of Digital Scholarship@UNLV. For more information, please contact digitalscholarship@unlv.edu.

MODELING THE UNSATURATED ZONE AT THE AREA 5 RADIOACTIVE
WASTE MANAGEMENT SITE: EFFECTS OF CLIMATE CHANGE
AND VEGETATION ON FLOW CONDITIONS

by

Amanda Marie Brandt

Bachelor of Environmental Studies
York University
1999

A thesis submitted in partial fulfillment
of the requirements for the

Master of Science Degree in Water Resource Management
Water Resource Management
College of Sciences

Graduate College
University of Nevada, Las Vegas
December 2008

UMI Number: 1463497

INFORMATION TO USERS

The quality of this reproduction is dependent upon the quality of the copy submitted. Broken or indistinct print, colored or poor quality illustrations and photographs, print bleed-through, substandard margins, and improper alignment can adversely affect reproduction.

In the unlikely event that the author did not send a complete manuscript and there are missing pages, these will be noted. Also, if unauthorized copyright material had to be removed, a note will indicate the deletion.

UMI[®]

UMI Microform 1463497

Copyright 2009 by ProQuest LLC.

All rights reserved. This microform edition is protected against unauthorized copying under Title 17, United States Code.

ProQuest LLC
789 E. Eisenhower Parkway
PO Box 1346
Ann Arbor, MI 48106-1346



Thesis Approval
The Graduate College
University of Nevada, Las Vegas

November 20, 2008

The Thesis prepared by

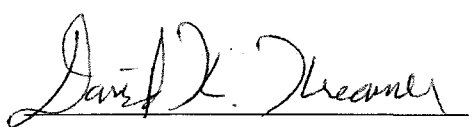
Amanda M. Brandt

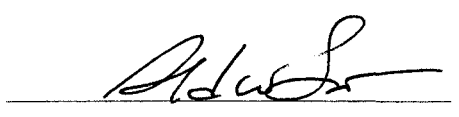
Entitled

Modeling the Unsaturated Zone at the Area 5 Radioactive Waste
Management Site: Effects of Climate Change and Vegetation on
Flow Conditions

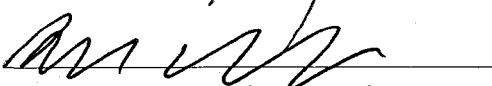
is approved in partial fulfillment of the requirements for the degree of

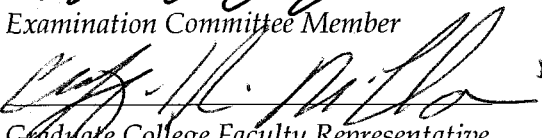
Master of Science in Water Resource Management


Examination Committee Chair


Dean of the Graduate College


Examination Committee Member


Examination Committee Member


Graduate College Faculty Representative

ABSTRACT

Modeling the Unsaturated Zone at the Area 5 Radioactive Waste Management Site: Effects of Climate Change and Vegetation on Flow Conditions

by

Amanda Marie Brandt

Dr. David Kreamer, Advisory Committee Chair
Professor of Hydrology
University of Nevada, Las Vegas

This thesis tests a series of potential future climate scenarios and associated environmental conditions that could result in the reversal of the present upward hydraulic gradient in the vadose zone at the Area 5 Radioactive Waste Management Site (RWMS) by implementing a one-dimensional model developed using the HYDRUS 1-D numerical modeling package. The research is divided into two phases. Phase I simulates the system from the Pleistocene to Holocene transition (approximately 13,000 years ago) to the present and is tested by independently varying precipitation, evaporation and transpiration rates. The results provide initial conditions for subsequent modeling under Phase II, which considers potential future flow conditions under a series of eight possible bioclimatic scenarios analogous to potential future climates for the next +1,000 years. Results indicate that the net upward hydraulic gradient is reversed under four of the future (Phase II) cases considered where vegetation does not effectively remove available soil moisture. This scenario can occur in periods of (1) warmer temperatures, higher precipitation rates and expanded vegetation cover, (2) warmer temperatures, lower precipitation rates and reduced vegetation cover, and (3) cooler temperatures, higher precipitation rates and expanded vegetation cover.

TABLE OF CONTENTS

| | |
|--|-----|
| ABSTRACT | iii |
| LIST OF FIGURES | v |
| LIST OF TABLES | vi |
| CHAPTER 1 INTRODUCTION | 1 |
| Study Area Description | 3 |
| CHAPTER 2 EXISTING WORK | 7 |
| Area 5 Vadose Zone Flow Modeling | 7 |
| Hydraulic Properties | 11 |
| Future Climate Prediction..... | 12 |
| Vegetation Profiling and Migration..... | 15 |
| CHAPTER 3 MODELING METHODS | 17 |
| Phase I: Paleomodel | 21 |
| Phase II: Future Cases | 22 |
| Selection of Probable Future Climates..... | 23 |
| Selection of Analog Climate Sites..... | 26 |
| Climate Inputs | 26 |
| Development of Representative Biomes | 29 |
| Calculation of Evapotranspiration..... | 35 |
| Numerical Flow Model Description..... | 39 |
| Plant Water Uptake..... | 42 |
| Model Performance Measures..... | 44 |
| CHAPTER 4 RESULTS..... | 45 |
| Phase I Paleoflow Model Results..... | 45 |
| Phase II Future Case Results | 50 |
| Model Validation and Performance..... | 61 |
| CHAPTER 5 CONCLUSIONS | 64 |
| Future Work..... | 67 |
| APPENDIX I COMPUTER CODE..... | 69 |
| REFERENCES | 81 |
| VITA..... | 90 |

LIST OF FIGURES

| | | |
|-------------|--|----|
| Figure 3.1. | Cumulative Probability Distributions for Predicted Changes in Temperature and Precipitation..... | 20 |
| Figure 3.2. | Projected Climate Responses at +100 Years Under a Doubled CO ₂ Scenario..... | 21 |
| Figure 3.3. | Comparison of Reference Evapotranspiration (<i>ET_o</i>) Calculation Methods Using the Case 1 Climate Data Set..... | 36 |
| Figure 3.4 | Composite Root Distribution for Cases 1-8..... | 39 |
| Figure 3.5 | Feddes Plant Uptake Parameters..... | 44 |
| Figure 4.1. | Simulated Soil Matrix Head from 13,000 Years Ago to Present..... | 45 |
| Figure 4.2. | Volumetric Water Content from 13,000 Years Ago to Present..... | 46 |
| Figure 4.3. | Simulated Flux from 13,000 Years Ago to Present..... | 47 |
| Figure 4.4. | Simulated Soil Matrix Head and Volumetric Water Content for Paleomodel Test Series..... | 48 |
| Figure 4.5. | Simulated Flux for Paleomodel Test Series..... | 49 |
| Figure 4.6. | Timeline for Cases 1-8..... | 52 |
| Figure 4.7. | Simulated Soil Matrix Head for Cases 1-3, +100 Years | 54 |
| Figure 4.8 | Simulated Volumetric Water Content and Flux for Cases 1-3, +100 Years...56 | |
| Figure 4.9 | Simulated Soil Matrix Head for Cases 4-6, +300 Years | 57 |
| Figure 4.10 | Simulated Volumetric Water Content for Cases 4-6, +300 Years..... | 58 |
| Figure 4.11 | Simulated Flux for Cases 4-6, +300 Years..... | 59 |
| Figure 4.12 | Simulated Soil Matrix Head and Volumetric Water Content for Cases 7-8, +1000 Years | 60 |
| Figure 4.13 | Simulated Flux for Cases 7-8, +1000 Years..... | 61 |
| Figure 4.14 | Paleomodel Performance: Pilot Well Matrix Heads..... | 63 |
| Figure 4.15 | Paleomodel Performance: Pilot Well Volumetric Water Content..... | 63 |
| Figure 4.16 | Model Performance Over Time | 64 |

LIST OF TABLES

| | | |
|------------|--|----|
| Table 1.1. | Canopy Cover near the Area 5 RWMS | 6 |
| Table 3.1. | Bioclimatic Scenario - Climate Description | 24 |
| Table 3.2. | Climatic Tolerances of Biomes in western North America | 25 |
| Table 3.3. | Bioclimatic Scenario - Vegetation Profile | 25 |
| Table 3.4. | Guild Composition, Case 1 | 32 |
| Table 3.5 | Guild Composition, Case 2 | 32 |
| Table 3.6 | Guild Composition, Case 3 | 32 |
| Table 3.7 | Guild Composition, Case 4 | 32 |
| Table 3.8 | Guild Composition, Case 6 | 33 |
| Table 3.9 | Guild Composition, Case 7 | 33 |
| Table 3.10 | Guild Composition, Case 8 | 33 |
| Table 3.11 | Root Distribution By Guild | 38 |
| Table 3.12 | Summary of Soil Hydraulic Properties | 42 |
| Table 4.2 | Water Balance for Paleomodel Test Series | 51 |
| Table 4.3 | Future Climate Case Summary | 52 |
| Table 4.4 | Water Balance for Future Cases 1-3, +100 Years | 54 |
| Table 4.5 | Water Balance for Future Cases 4-6, +300 Years | 57 |
| Table 4.6 | Water Balance for Future Cases 7-8, +1000 Years | 61 |
| Table 4.7 | Descriptive Statistics for PW Wells Soil Water Head and Volumetric Water Content Data | 63 |

CHAPTER 1

INTRODUCTION

The Area 5 Radioactive Waste Management Site (RWMS) has been the focus of several research studies and ongoing monitoring efforts to ensure continued compliance with environmental and safety regulations. Current understanding of deep arid zone hydrology in Southern Nevada indicates net recharge is not occurring under modern climatic conditions (Shott et al., 1995; Tyler, 1996) and net soil moisture flux is primarily upward in response to arid climate and plant root uptake (Edmunds and Tyler, 2002; Walvoord et al., 2002a; Young et al., 2002; Scanlon et al., 2003). Research based on paleohydrologic records of the region suggests the flow regime in the region was once characterized by a net downward flux associated with a wetter, cooler climate and mesic vegetation adapted to moderately moist soil conditions, followed by a transition to a warmer, drier climate and associated xeric vegetation tolerant of very dry conditions (Walvoord et al., 2002b).

Because the influence of high root suction by desert vegetation is a prominent feature of most conceptual models, there is a need to better understand how this zone might respond to future climate scenarios. This research hypothesizes that variations in environmental conditions affected by climate change, specifically alterations to vegetation cover, could result in a reversal of the hydraulic gradient, altering the current regime of near-surface upward flow. Understanding the influence of future climate on the deep hydraulic gradient is complimented by examining paleoflow responses by modifying past environmental conditions, encouraging a temporally expansive approach to the problem that considers both

past and future climate conditions. Specific objectives of the study to test the hypothesis are to:

- (i) evaluate the effects of wetter and drier climate inputs on paleoflow at the study site;
- (ii) evaluate the effects of higher and lower evapotranspiration rates on paleoflow;
- (iii) develop a method to represent possible environmental conditions under potential future climates, and;
- (iv) evaluate the effects of environmental conditions on flow for potential future climates.

These objectives are accomplished through the completion of three research tasks undertaken in two phases. Phase I focuses on paleoclimate modeling efforts and Phase II focuses on potential future climates. Phase I accomplishes objectives (i) and (ii) through the development and verification of a paleomodel. A one-dimensional, forward run hydrologic model representing paleoenvironmental conditions at the Area 5 RWMS is developed using a variably saturated, finite element modeling package (HYDRUS 1-D; Simunek et al., 2005) and observed soil properties. The paleomodel is used to evaluate the effects of varying boundary conditions, allowing independent comparison of the effects of altered climate and vegetation inputs as they would affect paleoflow. Different treatments of the upper boundary are undertaken for comparative purposes and include doubled precipitation from paleoclimatic levels, reduced precipitation from paleoclimatic levels, increased precipitation intensity, expanded vegetation cover from paleovegetation distributions, and removed vegetation cover. Phase II meets objectives (iii) and (iv) by presenting a method used to generate a series of bioclimatic analogs for future climate conditions, then implementing these coupled effects in a future climate model. This is accomplished by examining expected long-term climatic trends in the region, developing likely vegetation profiles for each climate stage, and modeling flow under these scenarios. Results are examined for changes in soil

water pressure head and water flux through the entire profile, with particular attention to the influence of vegetation at the root zone.

Existing research in the separate but related fields of climate change prediction, plant community evolution and deep arid zone hydrology is presented in Chapter 2, "Existing Research." This is followed by a description of the methodology used to develop and implement the hydrologic model found in Chapter 3, "Modeling Methods." Results from runs under each of the conditions are presented in Chapter 4, "Results." A discussion of determined hydraulic gradient and flux profiles conditions is presented in Chapter 5.

Study Area Description

The Area 5 Radioactive Waste Management Site (RWMS) is located in northern Frenchman Flat in the southeast corner of the Nevada Test Site (NTS), approximately 26 km (16 mi) north of Mercury, NV (US DOE, 1997), 105 km (65 mi) northwest of Las Vegas (Shott et al., 1995) at an elevation of 971 m (3186 ft). The disposal facility has been in operation since 1961 (Shott et al., 1995), and receives low-level, mixed-level and transuranic wastes deposited in pits, trenches and deep boreholes (Albright et al., 1994). Filled trenches are covered with a 2.4 m (8 ft) native soil cover to inhibit movement of gas or water (National Securities Technologies, 2007).

The site is located on approximately 2.96 km² (1.14 mi²) of alluvial basin fill in the Frenchman Flat drainage basin (Albright et al., 1994). The soil upon which the RWMS is built is primarily alluvial detritus from exposed Tertiary volcanic material from Massachusetts Mountain Range (Bechtel Nevada, 2005b). These unconsolidated soils are primarily sand with silt, some gravel, and no clay sized particles (Bechtel Nevada, 2005b). Several studies report composition did not vary significantly with depth (Shott et al., 1995; Bechtel Nevada, 2005a; Bechtel Nevada, 2005b), though recent work indicates that

heterogeneity may play a more significant role in flow than previous work suggests (Yucel and Levitt, 2001). The alluvial basin fill below the site extends to a depth of 360 – 460 m (1,200 – 1,500 ft), and is underlain by a layer of Tertiary volcanic tuff estimated at 550 m (1,800 ft) thick, sitting atop deep Paleozoic carbonate aquifer (Shott et al., 1995; Bechtel Nevada, 2001).

The uppermost aquifer in the unconsolidated alluvium has a water table located approximately 235 m (770 ft) beneath the surface (US DOE, 1997); multiple studies have shown aerial recharge is not occurring under current climate conditions (Bechtel Nevada, 2005a). Additionally, this aquifer has a relatively flat water table demonstrating a hydraulic gradient of nearly zero (Bechtel Nevada, 2005b); characterization studies of the region report no horizontal movement in the aquifer (Bechtel Nevada, 2005b). The underlying volcanic tuff acts as a large regional aquitard, and is considered to be a major barrier between the alluvial aquifer and the deep regional carbonate aquifer below (Bechtel Nevada, 2001).

Extreme arid conditions, including very low annual precipitation of approximately 123 mm (4.85 in) (reported for Area 5 weather station W5B in Soule, 2006) and extremely high annual potential evapotranspiration rates of 1625 mm (64 in) (Yucel and Levitt, 2001) are representative of the current interglacial climate state (Sharpe, 2003). The rain shadow effect of the Sierra Nevada Range to the west is considered the dominant climate control in the region (Miklas et al., 1995). Infrequent precipitation events are usually the result of moist oceanic air moving around the southernmost end of the Sierra Nevada Range from the Pacific Ocean or Mexico, or wet air masses moving southward from the Pacific Northwest (Miklas et al., 1995). Most rainfall occurs January – March, with a secondary maximum falling during summer months (Soule, 2006). The area averages 14 thunderstorm days per year (Soule, 2006). Though annual precipitation totals are quite low, intensity can vary greatly. Extreme precipitation events are occasionally recorded at the NTS, with 50 – 75 mm (2 -3 in) storm

totals being recorded at several sites (Soule, 2006). A 100-year storm event for this region is defined as 90 mm (3.5 in) in a 24-hour period, and was last recorded in Mercury, NV on 08/18/1983 (Soule, 2006).

Flora at the site is dominated by perennial desert vegetation including *Larrea tridentata* (creosote bush) accounting for 6% of ground cover, *Ambrosia dumosa* (white bursage) at 1.3% ground cover and *Acamptopappus shockleyi* (Shockley goldenhead) at less than 1% (Webb et al., 2003). Total live ground cover in the area is less than 9%, with an additional 12% of ground cover by dead shrub material (Webb et al., 2003). Vegetational composition has been relatively constant over the last 40 years at this site, with *Larrea tridentata* accounting for 6%, 7% and 6% ground cover when monitored in 1963, 1975 and 2002, respectively (Webb et al., 2003). When dead shrub material is included, total ground cover has remained constant at around 20% (Webb et al., 2003). Fauna surveys published in 2003 by Hansen and Ostler from two additional plots in the vicinity of the Area 5 RWMS identified many of the same dominant species but in varying proportions (Table 1.1).

Taken together, these unique geologic, hydrologic, and climatic features generally favor this region for waste disposal by minimizing the potential for offsite transport of contaminants. The generally inhospitable environment has historically precluded this area from human settlement; natural conditions, land accessibility and current and future use suggest it will remain an unlikely location for intensive human development. It is these features that make this a unique and interesting site for hydrologic research.

| | Site 1 - 600m N of Area 5 RWMS ^a | Site 2 – 1.25 km NE of Area 5 RWMS ^a | Plot 28 ^b | Plot 28 ^b | Plot 28 ^c |
|---|--|--|------------------------|------------------------|------------------------|
| Location – Easting/Northing | 592937 E, 4079992 N | 594605 E, 4079688 N | 596258 E, 4079198 N | 596258 E, 4079198 N | 596258 E, 4079198 N |
| Date Sampled | 2001 | 2001 | 1963 | 1974 | 2002 |
| Total Shrub Cover | 21% | 18.60% | 14.68% | 17.95% | 8.64% |
| <i>Larrea tridentata</i> (creosote bush) | 12.6% | 2.42% | 5.92% | 7.15% | 5.69% |
| <i>Acamptopappus shockleyi</i> (Shockley goldenhead) | 4.83% | 4.28% | 2.08% | 4.62% | 0.03% |
| <i>Ambrosia dumosa</i> (white bursage) | 1.68% | 8.93% | 4.08% | 2.76% | 1.28% |
| <i>Lycium andersonii</i> (Anderson's wolfberry) | 1.68% | 0.93% | 0.00% | 0.00% | 0.00% |
| <i>Krameria erecta</i> (range ratany) | 0.42% | 0.93% | 0.12% | 0.21% | 0.40% |
| <i>Krascheninnikovia lanata</i> (winterfat) | 0.42% | 0.56% | 0.04% | 0.03% | 0.00% |

^aHansen and Ostler, 2003

^bBeatley, 1974 in Webb et al., 2003

^cWebb et al., 2003

CHAPTER 2

EXISTING WORK

Significant work was reviewed for each segment of interest in the disciplines of unsaturated zone hydrology, climate prediction and plant community development. Completed studies of relevance to this project are summarized below.

Area 5 Vadose Zone Flow Modeling

The high level of interest in the behavior of deep vadose zone flow systems in arid environments is evident by the number of studies that have been undertaken in the region. The Area 5 Radioactive Waste Management Site, in particular, has been the focus of much research; as an area on the edge of the climatological regime, it is a site of great interest for exploring the potential responses in the face of climate change. The system is well understood to be dominated by high surface evaporation rates, very low annual precipitation, low soil moisture content, and strongly negative matric potentials at the root zone, indicating a slight net upward hydraulic gradient. Significant work influencing how regional hydrology is understood was initiated by Winograd and Thordarson (1975), and expanded and refined by several others.

Phillips (1994)

Phillips reviewed environmental tracer data, specifically bomb pulse tritium (^3H), chlorine-36 (^{36}Cl), and meteoric chloride data from several sites in the southwestern U.S. to look for regional similarities in the depth profiles that would indicate larger flow patterns. This work identified similar ^{36}Cl bulges in the upper 2.5 m (8 ft) of the soil at all seven sites

where data were available, in spite of geographically separated sites with varying soils. The consistency between sites implies that a large scale, spatially uniform, one-dimensional conceptual flow model may reliably describe the behavior of the system on a decadal time scale. Chloride mass balance calculations predicted location of the bomb pulse concentration reasonably well, indicating ^{36}Cl behaves conservatively and does not exhibit preferential flow as compared to meteoric Cl. In addition, the ^3H profile had migrated further into the profile than the bomb pulse chlorine, in spite of its later deposition, indicating the role of thermally induced vapor transport. Evidence supported the idea that all sites were subject to a common control by climate change, resulting in regional cessation of net recharge 12 to 16 thousand years ago.

Deep chloride profiles representing much longer time scales were interpreted using the chloride mass balance approach. Phillips stated that deep soil-moisture flux throughout the entire region has decreased by a factor of 20, suggesting that deep vadose zone moisture conditions and chemistry are influenced by Pleistocene conditions, and are not in equilibrium with the more shallow soil. He also suggested that shallow, downward flux from the surface is likely dominated by desert vegetation extracting nearly all available soil water from the profile.

Interpretation of the environmental tracer data presented by Philips indicates the presence of a widespread, climatically driven change in water balance, resulting in little to no water available for percolation into the deep vadose zone. This interpretation is reflective of the underlying assumption of downward-only liquid flow implied in the chloride mass balance calculation. As a result, all flux estimates generated as a result of this approach will be positive downward, in the direction of the water table.

Tyler et al. (1996)

The work by Tyler et al. (1996) expanded the use of environmental tracers in the southwestern U.S., including carbon-14 (^{14}C) for dating soil pore water and stable isotope data ($\delta^{18}\text{O}$ and $\delta^2\text{H}$) from Area 5 RWMS samples collected at depth (>230 m), in addition to ^{36}Cl and chloride, to reconstruct soil water fluxes over the last 120,000 years. Tyler et al. compared the inferred paleohydrology from tracer data to climate history from ice cores and found a strong correlation between recharge and climate. The data further supported the idea that recharge is not occurring under current conditions, and last occurred during the Pleistocene epoch. They proposed a Gaussian model to fit the deep chloride profile data and developed dispersion coefficients and estimated recharge rates of 7.6 mm/yr and 5.9 mm/yr for each of the boreholes. Consistent differences between locations indicate that, in addition to the dominant role of climate change to the overall profile, local conditions such as surface topography, soil texture and hydraulic properties will have an effect on recharge rates.

Similar to the work presented by Phillips (1994), interpretation of the data rely on the governing assumption of piston-like, downward advective flow through the deep vadose zone to fit the deep chloride profile. However, this approach for determining paleorecharge rates does not explain the near-surface elevated chloride concentrations in the PW wells, nor does it address any of the recent processes that might have contributed to the development of the modern chloride bulge.

Walvoord et al. (2002a, 2002b)

Walvoord et al. documented conceptual models for understanding arid climate vadose zone behavior that have been postulated and applied in various previous studies, and presented an alternative explanation to account for disparity between existing conceptual models and chlorine profile and soil potential data. The conceptual model, termed as the Deep Arid System Hydrodynamic (DASH) Model, links vegetation changes that occurred

during the transition from the cooler, wetter Pleistocene epoch to drier Holocene epoch, and presented how vegetational shift could provide the driving forces for observed liquid and vapor fluxes in the deep profile. The vegetational transition is hypothesized to have created a zone of strongly negative soil moisture potential, effectively dampening occasional infiltration events. This conceptual model is supported by data showing that fluctuations due to surface conditions are rarely felt below the root zone.

Walvoord et al. identified the importance of the climatic transition to modern-day arid conditions, and found that including a paleovegetation component, that compliments paleoclimate as a major driver in the flow system, can better account for observed chloride profiles and matric potentials through the entire profile. Their work demonstrates that vapor flow is currently primarily upward in response to a fixed root zone matric potential. The revised conceptual model emphasized the importance of the root zone to arid zone systems, suggesting that plant characteristics that might factor into the force exerted at the root zone deserve further exploration.

Wolfsberg and Stauffer (2003)

This research focused on developing a detailed process model for upward liquid and vapor flow in the near surface environment to provide fluxes for the Area 5 RWMS Performance Assessment models. The liquid and vapor fluxes in the shallow UZ are upwardly advective, but very small, and of less consequence than the diffusive solute fluxes which are downward in response to solute concentration gradients in the presence of available water. Advective forces acting on the movement of soil moisture include gravity driven percolation (downward), capillary suction (upward) and vapor gradients (upward).

Like the Walvoord et al. work, hydraulic conditions resulting from root zone influence are represented using a fixed low matric potential (model) node at the base of the root zone (in this case, located three meters below the surface). Effective precipitation is represented as

a constant flux surface boundary condition. The Wolfsberg and Stauffer research demonstrates the importance of diffusive fluxes and vapor gradients, given the very low water contents and consequently small advection occurring at the site.

Yin et al. (2008)

The work of Yin et al. emphasizes the importance of interrelationships between environmental factors and the flow system in arid environments. This research simulated paleoclimate from 18,000 years ago to present using a series of case studies to test effects of root water uptake, precipitation intensity, extreme precipitation events, seasonal canopy structure, root growth, and root zone distribution. Results indicate that depth of chloride accumulation in the profile is a function of both climate and depth of the root zone. Additionally, recharge rates below the root zone are essentially zero as a result of plant water uptake, even in more a pluvial climate prior to the epochal transition, verifying that aspect of the conceptual model proposed by Walvoord et al. (2002a, 2002b) and employed in Wolfsberg and Stauffer (2003). However, results demonstrate that when vegetation is removed, downward recharge below the root zone becomes significant.

This thesis follows several approaches and techniques presented in Yin et al. to describe the Area 5 study site, including temporal resolution (daily time step over a several thousand year simulation period), use of time-variable atmospheric boundary conditions to represent surface conditions (including daily precipitation and evapotranspiration rates), and distribution of transpiration over the root zone according to growth form. Linkages demonstrated in the Yin et al. work are explored further in the Chapter 5, "Conclusions."

Hydraulic Properties

Two sets of hydraulic properties are reported for this area. The original data published by Reynolds Electrical and Engineering Company (REECO, 1994) include van Genuchten –

Mualem (Mualem, 1976; van Genuchten, 1980) estimates (from soil water content – soil water potential relationships) of the soil retention and hydraulic conductivity curves for various samples collected from three deep pilot wells near Area 5, as well as direct measurements of matric potential, porosity, and bulk density. Young et al. (2002) present direct measurements of soil retention and hydraulic conductivity, on samples collected by REECo, using the Unsaturated Flow Apparatus (UFA) in Washington. The finite element heat and mass transfer (FEHM) modeling work by Wolfsberg and Stauffer (2003) used both the REECo and Young et al. data to develop eight distinct material distributions for their simulations (Catlett et al., 2003).

Future Climate Prediction

Miklas et al. (1995)

This paper reports the findings of a Nuclear Regulatory Commission (NRC) study which used a process of expert elicitation to identify and describe predicted climate conditions at Yucca Mountain, NV at 100, 300, 1000, 5000 and 10,000 years in the future. Each of a five-member panel of climatologists described future climate at each identified time step, including dominant controls and how these controls would likely influence mean temperature and precipitation, expected trends of temperature and precipitation over time, percentage of winter to summer precipitation, storm intensity and frequency. Generally, the region is dominated by the rain shadow effect of the Sierra Nevada Range, which limited precipitation increases under all future conditions. Median temperature change over the entire 10,000 year period was not predicted to increase or decrease by more than 2° C. Even under the extreme scenario of doubled precipitation, the area is predicted to remain arid or semi-arid. Future climate ranges presented in the Miklas et al. paper provide the initial bounds upon which the

bioclimatic scenarios developed in this thesis are based. Descriptions of the +100, +300 and +1,000 year time steps are detailed in Chapter 3, "Modeling Methods."

Sharpe (2003)

Sharpe (2003) adapted a methodology developed by the United States Geological Survey (USGS) (Houseworth, 2001) for predicting future climate out 10,000 - 1,000,000 years after present. This approach assumes the earth is subject to repeatable long-term climate cycles of approximately 400,000 years in duration, and establishes a series of climate states (i.e., Milankovitch astronomical forcing). Climate states are identified and described on the basis of paleoenvironmental records. According to the chronology established in this methodology, climatic conditions in the southwestern U.S. will cycle through Interglacial (current state), Intermediate/Monsoon, Glacial, and Intermediate, with each state defined by average precipitation quantities and patterns and solar characteristics with respect to the current climate.

Sharpe used geographic analog sites to generate data sets representative of upper and lower bounds for each of the described climate states based on earth's orbital and rotational (or axial) characteristics and their influence on paleoclimatic circulation patterns. This thesis implements the same approach of selecting modern analog climate data to represent future climate states, though results from the comparatively shorter time scale of interest in this thesis imply greater climate stability than considered in Sharpe's work; the degree of climatic variability expected over the 1,000 year simulation period in this thesis is much less than the range predicted by Sharpe. Still, some of the basic ideas identified in Sharpe (2003) are valuable in this thesis, specifically geographic proximity can be generally related to temporal proximity, and climate states may regularly switch between sub-states as often as every +1,000 years (± 500 years), within the scope of the simulation period.

Intergovernmental Panel on Climate Change (2007)

The Intergovernmental Panel on Climate Change (IPCC) Fourth Assessment Report: Regional Climate Analysis of North America (Chapter 11) indicates the southwestern United States is likely to experience reduced precipitation rates in response to global climate change over the next 100 years. This reduction in rainfall is likely to result from the comparatively smaller warming over the Pacific Ocean to warming over the continent, which will result in amplification and northward displacement of the tropical anti-cyclone which brings the summer monsoon rainfall, resulting in less precipitation for the southwest, although most other areas of North America will experience increases in precipitation.

Data from the regional climate model outputs of the IPCC 3rd Assessment Report published in 2001 have been made available through an online portal sponsored by the U.S. Vegetation/Ecosystem Modeling and Analysis Project (VEMAP) (Kitell et al., 2004). The VEMAP project represents a large collaborative effort to compile high resolution climate, soils, and vegetative data averaged over 0.5° latitude by 0.5° longitude grid cells for the conterminous United States. The project involved running an equilibrium model and a transient processes model. For this collaborative research, outputs from the Transient Processes Model generated using the Canadian Climate Center for Modeling and Analysis (CCC) model version 3 and the Hadley Climate Center (HADGCM) outputs were translated into the VEMAP grid and integrated forward. VEMAP data made the results available for individual grid cells identifiable by latitude and longitude, which provided the localized change ratios used in this thesis for developing future climatic model inputs.

Vegetation Profiling and Migration

Climate is widely accepted as the driving force for large-scale vegetation distribution (Kirilenko & Solomon, 1998), but disturbance events and atmospheric composition can also effect plant communities (Woolfenden, 1996). Paleobotanical records indicate changes in plant phenology as a result of these driving forces, and using these records as an analog of previously existing vegetation will capture past events. However, some research indicates potential problems with this approach; Capon (2003) proposes that vegetation compositions will differ as a function of wetting versus drying conditions. Also, species migration will be less likely to resemble past evolutionary patterns as a result of barriers to migration not present in the early Holocene. Intensive land development, biodiversity reduction and increased atmospheric carbon concentrations as a result of human activity may play a part in the reduction of species migration rates (Kirilenko & Solomon, 1998).

Schlesinger and Pilmanis (1998)

Work by Schlesinger and Pilmanis (1998) suggests that plant-climate interactions are doubly coupled, and changes in vegetation characteristics of deserts have strong feedbacks to atmospheric conditions. Arid lands with bare soils are a significant source of dust, which can effectively cool the atmosphere over the oceans, effecting global circulation patterns. Increased bare soil as grasslands are converted to desert shrubs will result in higher albedo in the desert and a higher flux of sensible heat from the surface. However, these cooling effects on the soil during the transition of grasslands to desert shrubs, as a result of reflected energy, are overridden by reduced transpiration resulting in elevated surface soil and air temperatures (Schlesinger and Pilmanis, 1998).

This vegetational progression implies that increased soil water evaporation, in response to increased temperature, results in less moisture available for plants (Balling, 1988), further promoting the expansion of desert shrublands. Canopy composition might be expected to

reflect reduced grass cover in favor of expanded shrub coverage with time, a potential scenario explored in the future case simulations of this thesis.

Thompson and Anderson (2000)

An extensive compilation of fossil pollen and plant (from packrat midden) data were developed and used to map biome occurrence based on Kuchler's classification scheme at 6,000 and 18,000 years in the past for the western United States. Results indicate that both the pollen and plant data sources show good agreement when used for biome reconstruction, and support the use of macrofossils as an indication of past vegetation classes.

Biomes constructed by Thompson and Anderson generally adhere well to Kuchler's classification scheme, upon which much current research is based. However, the macrofossil data examined by Thompson and Anderson suggest the presence of a separate classification for "open conifer woodland" biome, which they adopted. Biome distribution at 6,000 years ago is similar to current distributions, but environments appear to differ at 18,000 years ago, indicative of the transition from the Last Glacial Maximum to current Holocene conditions.

Biome tolerances expressed in Thompson and Anderson (2000) are used in this thesis to identify and describe compatible biomes for possible future climate scenarios, and the growth form - species catalog developed in their work is employed to delineate guild compositions for each of the bioclimatic analogs developed in Chapter 3.

CHAPTER 3

MODELING METHODS

Predictive modeling is often associated with uncertainty and error. The complexity of arid desert environments, including high variability in vegetation, climate zones, topography and orographic conditions, can make it difficult for general circulation models (GCMs) to predict trends in this region with high levels of confidence (Lioubimtseva, 2004). GCM and regional climate model (RCM) results indicate that areas of the western U.S. are subject to predicted higher variability than the rest of the country. The southern Sierra Nevada Range may experience generally higher precipitation rates, while Arizona and New Mexico may experience reduced precipitation rates (Kim, 2005; IPCC, 2007). Seemingly opposing seasonal temperature trends observed in the western U.S. complicate understanding of underlying circulation mechanisms (Abatzoglou and Redmond, 2007). Difficulty in resolving regional phenomena at a local scale compound the problem of projecting future conditions at a specific site, and at a site or area that differs in scale from the measurement scale.

To address some of these difficulties, this project is conducted in two phases with the intent to verify that the model successfully handles major interactions between atmospheric inputs, vegetation uptake and soil properties on flow before considering future cases. Phase I consists of an epochal reconstruction of the Holocene to present conditions, simulated forward in time from 13,000 years ago to present. Initial conditions are based on knowledge of the hydraulic transition between Pleistocene and Holocene. Environmental factors are

varied individually by known quantities through a series of tests. Phase II proceeds forward from the paleomodel developed in Phase I in short-term (centennial scale) time steps by applying conditions associated with bioclimatic scenarios developed as part of this work. A range of conditions are explored out to a period of +1,000 years.

Phase II incorporates two different approaches to predicting conditions at the site. The first approach relies on predicted scaling factors for climate parameters of net incident solar radiation, wind speed, temperature and precipitation generated by a well-documented RCM under doubled atmospheric carbon dioxide (CO₂) concentrations applied to the Area 5 meteorological data. Scaling factors obtained from Kittel et al. (2004) are presented as a monthly average for each climate variable; predicted temperature change is expressed as a difference between RCM temperature at current CO₂ levels – temperature predicted at doubled CO₂ levels. Change ratios for precipitation, solar radiation and wind speed are expressed as the ratio the value under doubled CO₂ levels/ the value at current CO₂ levels. (Access to the dataset used for this scenario was provided by the Climate System Modeling Program, University Corporation for Atmospheric Research, and the Ecosystem Dynamics and the Atmosphere Section, Climate and Global Dynamics Division, National Center for Atmospheric Research. Readers are encouraged to refer to Kittel et al. (2004) for additional information.) By scaling observed Area 5 site data, this approach maintains the inherent cyclic characteristic and other features of observed weather patterns.

The second approach employed in Phase II involves the development and application of a series of bioclimatic analogs. The use of geographic analog sites is defensible on the basis that climate is driven by atmospheric circulation, and these circulation patterns are influenced by the solar radiation resulting from the planet's orbital and rotational characteristics, which vary on a predictable cyclical pattern (Sharpe, 2003). The use of analog sites for representing future climate states provides a series of additional benefits for this project, by firstly

allowing resolution of weather events on daily scale that has been shown to influence flow patterns; secondly, providing inputs at a resolution that enable other model components (i.e. potential evapotranspiration) to be explicitly calculated; and thirdly, by providing a realistic representation of observed ranges and fluctuations in weather patterns. Each of the bioclimatic analogs developed in Phase II provide model inputs for a series of future climate scenarios, simulated in Cases 1-8.

Predicting the response of coupled environmental systems under varying future climate change is, by its nature, complex. Uncertainties inherent in developing inputs for predictive modeling need to be considered, particularly developing a sound and defensible methodology for future climate estimates. Controls employed in this work to limit uncertainties in describing potential climates include:

- 1.) Internal controls in the formal elicitation process (Miklas et al., 1995) used to describe future climate steps in this thesis. Internal process controls include solicitation of information from climatological researchers with appropriate backgrounds and levels of expertise, led by personnel with expertise in decision theory, probability theory and assessment to facilitate the process, and extensive training for researchers in recognizing and overcoming bias.
- 2.) Explicit project controls. Expert opinions are aggregated and characterized by probability distributions. These probabilities are compared to climate descriptors developed in this work for each predicted future climate scenario. Probabilities for each time step are given in Figure 3.1.
- 3.) Environmental controls resulting from the biogeographical characteristics of the study site. Climate in this region has been remarkably stable over thousands of years (Spaulding, 1990) as a result of the Sierra Nevada rain shadow, and is likely

to remain relatively so during the period of interest in this study, constraining the range of possibilities.

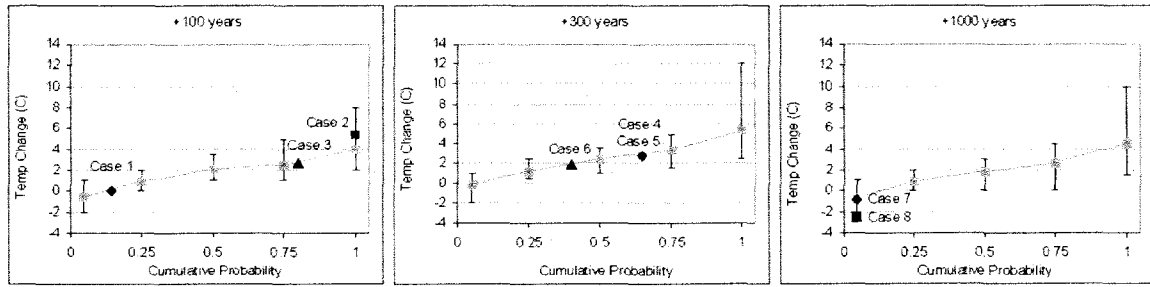


Figure 3.1a

Figure 3.1b

Figure 3.1c

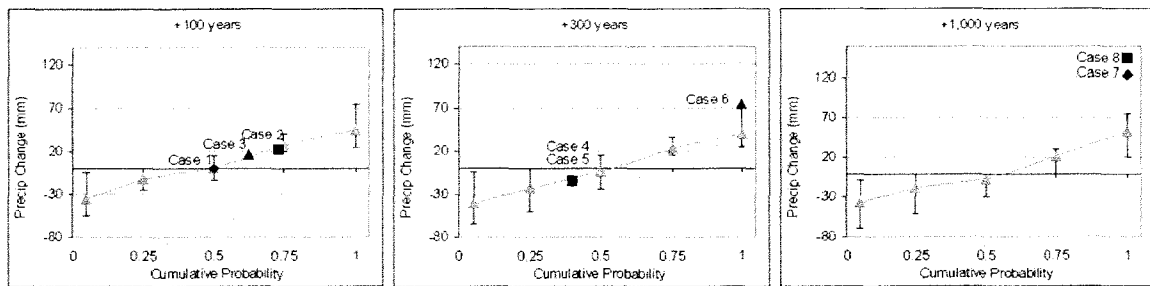


Figure 3.1d

Figure 3.1e

Figure 3.1e

Figure 3.1(a-e). Cumulative Probability Distributions for Predicted Changes in Temperature and Precipitation at the +100, +300 and +1,000 Year Time Step (Miklas et al., 1995)

- 4.) Verification against robust physically-based regional climate models (RCMs) when available. The +100 year, doubled CO₂ climate scenario developed in this thesis (Case 2) is compared with RCM temperature and precipitation projections (from Christensen et al., 2007) in Figure 3.2. Case 2 falls within the 25% - 75% quartile range of predicted precipitation for all seasons, and within the 50% quartile for summer and fall predicted temperature response. Winter and spring predicted temperature responses for Case 2 are outside the 75% quartile for the region, but still within predicted maximums for 14 of 21 averaged RCMs. Though these RCM outputs are averaged responses for the entire western United

States, these values demonstrate that Case 2 inputs represent predicted trends across the larger region.

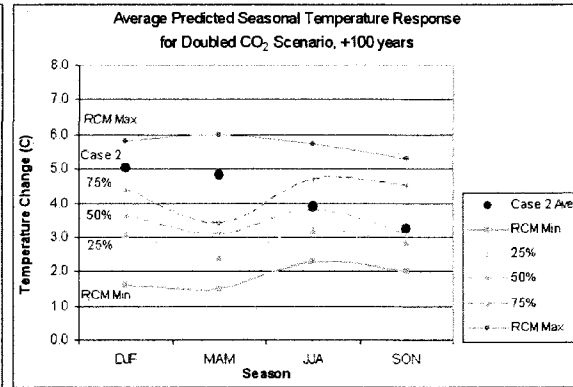
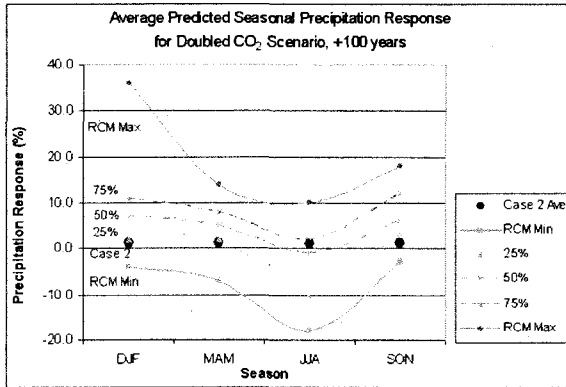


Figure 3.2a

Figure 3.2b

Figure 3.2. Projected Climate Responses at +100 Years Under a Doubled CO₂ Scenario for (a) Precipitation and (b) Temperature (Christensen et al., 2007).

It should be emphasized that future climate steps described in this work are not intended to be predictive in nature, but instead provide a methodology for testing a variety of realistic interdependent environmental conditions, while offering a view of how progressional changes might impact the flow system.

Phase I: Paleomodel

The paleomodel is constructed as a forward simulation of paleoclimatic conditions as they evolved through to present time (approximately 13,000 years). This provides the opportunity to examine the effects of changing climate and vegetation on flow conditions by independently testing individual processes, while allowing use of present-day observations for benchmarking purposes of the Base Case. In addition to the 13,000-year initial simulation (paleomodel Base Case), the paleomodel run series includes tests of:

- A.) Elevated evapotranspiration: Plant cover is increased from 20% total vegetation cover in the paleomodel Base Case to 90% deciduous shrub/ 90% grass cover. This is intended to simulate a very dense shrub cover with grass understory.
- B.) Reduced transpiration: Plants uptake is reduced to zero for 30 years every 100 years to simulate periods of widespread vegetation mortality, such as might be observed on a 100-year wildfire cycle.
- C.) Increased precipitation: Rainfall is doubled for the entire simulation, equivalent to a mean annual precipitation rate of 224 mm yr⁻¹.
- D.) Reduced precipitation: Rainfall is halved for the entire simulation, equivalent to a mean annual precipitation rate of 56 mm yr⁻¹.
- E.) Timing of precipitation: 80% of precipitation is compressed into an 8-hour period (08:00 – 16:00), 10% falling in early morning (0:00-08:00) and the remaining 10% falling in the evening (16:00-24:00). The allotted amount is randomly distributed within each block using an algorithm designed for this purpose (Appendix I). The model is run in hourly time steps.

Outputs from the Paleomodel Base Case provide initial conditions for the Phase II future case series.

Phase II: Future Cases

To represent future conditions in the model, this thesis couples the most probable climate states with supportable biomes based on climate conditions, vegetation tolerances, local soil conditions, topography and general suitability of each of the profiles for the Area 5 site. The suite of environmental factors used to provide the inputs for each case is termed a bioclimatic scenario; it is defined by climate characteristics and representative growth forms, which are

in turn used to develop root density profiles and ground coverage estimates following the methodology below:

- 1.) Identify and describe most probable future climate states;
- 2.) Select representative climate analog sites and process data sets;
- 3.) Determine appropriate biome for climate analog based on biome tolerances;
- 4.) Select representative vegetation for biome from field survey plots;
- 5.) Generate guild composition by classifying observed vegetation according to growth form;
- 6.) Parameterize guild composition for partitioning evapotranspiration (leaf area index, canopy cover) and root distributions.

Bioclimatic scenarios developed for this paper are outlined in Table 3.1, Table 3.2 and Table 3.3.

Selection of Probable Future Climates

A range of possibilities for the most probable scenarios are identified, providing high and low bounding conditions for each time step. Each future time step is treated as representative of that climatic state, avoiding difficulties associated with modeling highly uncertain transitional phenomenon. Findings of an expert panel debate for predicting future climate at Yucca Mountain (Miklas et al., 1995) are combined with work done by Sharpe (2003) outlining the use of orbital and rotational variations to predict long-term climate states to develop a series of probable climate states. Each climate state, identified by time of occurrence, is defined by the dominant controls influencing weather patterns, mean annual precipitation, and mean annual temperature. This work considers possible scenarios out to 1,000 years after present, with climatic transitions occurring at +100, +300 and +1,000 years.

Table 3.1. Bioclimatic Scenario - Climate Description

| Timing ^{a, b} | Dominant control ^b | Description ^a | Climate State ^a | Representative Locale | Mean Annual Precip (mm) ^c | Mean Annual Temp (C°) ^c | Growing Degree Days (Base 5°C) ^c | Mean Temp Coldest Month (C°) ^c | Moisture Index ^d |
|------------------------|--|--------------------------|----------------------------|---|--------------------------------------|------------------------------------|---|---|-----------------------------|
| 1. Present Day | Sierra Nevada Rainshadow | Current | Interglacial | Desert Rock Airport, NTS 9 years 8/1/98-7/31/07 | 112 | 18.6 | 5015 | 7.4 | -0.93 |
| 2. +100 years | -Rainshadow effect -Anthropogenic forcing -Doubled atmospheric CO ₂ | Much warmer/ wetter | Interglacial | DRA, scaled 9 years 8/1/98-7/31/07 | 134 | 23.9 | 6881 | 12.6 | -0.94 |
| 3. +100 years | -Rainshadow effect -Anthropogenic forcing | Warmer/ wetter | Interglacial- Monsoon | Calipatria, CA 15 years 8/1/90-7/31/05 | 128 | 21.3 | 5997 | 5.6 | -0.94 |
| 4. +300 years | -Rainshadow effect -Anthropogenic forcing | Warmer/ drier | Interglacial- Monsoon | Parker, AZ 18 years 1/1/87-7/31/05 | 97 | 21.4 | 5997 | 10.2 | -0.96 |
| 5. +300 years | -Rainshadow effect -Anthropogenic forcing | | | | | | | | |
| 6. +300 years | -Rainshadow effect -Anthropogenic forcing | Warmer/ wetter | Interglacial- Monsoon | Harquahala, AZ 9 years 8/1/97-7/31/06 | 186 | 20.5 | 5651 | 8.9 | -0.92 |
| 7. +1000 years | -Rainshadow effect -Anthropogenic forcing -Orbital variation | Cooler/ wetter | Intermediate | Riverside, CA 22 years 8/1/85-7/31/07 | 236 | 17.7 | 4648 | 12.3 | -0.87 |
| 8. +1000 years | -Rainshadow effect -Anthropogenic forcing -Orbital variation | Cooler/ wetter | Intermediate | Victorville, CA 13 years 3/1/94-7/31/07 | 257 | 16.1 | 4086 | 6.8 | -0.91 |

^aSharpe, 2003^bMiklas et al., 1995^cCalculated from raw weather data^dCalculated after Wilmott and Feddema, 1992

Table 3.2. Climatic Tolerances of Biomes in western North America

| Biome ^e | Min Mean Temp Coldest Month ^e | Max Mean Temp Coldest Month ^e | Min Growing Degree Days (GDD ₅) ^e | Max Growing Degree Days (GDD ₅) ^e | α Min ^e / α Min ^f | α Max ^e / α Max ^f |
|------------------------|--|--|--|--|--|--|
| Desert | 0 | 12.5 | 3000 | 6500 | 0.05/ -0.95 | 0.40/ -0.20 |
| Xerophytic woods/scrub | 2.5 | 12.5 | 2000 | 5000 | 0.30/ -0.40 | 0.70/ 0.40 |
| Grassland | -15.0 | 7.5 | 1500 | 5000 | 0.35/ -0.30 | 0.70/ 0.40 |
| Steppe | -10.0 | 0 | 1000 | 3000 | 0.15/ -0.70 | 0.55/ 0.1 |

^eThompson and Anderson, 2000; ^fCalculated after Wilmott and Feddema, 1992

Table 3.3. Bioclimatic Scenario - Vegetation Profile

| Timing | Biome ^g | Guild Composition ^h | Representative Species | Timing | Biome ^g | Guild Composition ^h | Representative Species |
|------------------------------------|--------------------|--|---|-------------------------------------|--------------------|--|--|
| 1. Present case | Desert | Evergreen - 7.1% Subshrub - 10.3% Grass - 2.7% Forb - 0.2% | <i>Larrea tridentata</i> <i>Ambrosia dumosa</i> <i>Oryzopsis hymenoides</i> <i>Mirabilis pudica</i> | 5. +300 years Warmer/ drier | Bare Soil | | Bare Soil |
| 2. +100 years Warmer/ wetter | Desert | Evergreen - 16.4% Subshrub - 20.1% Grass - 1.0% Forb - 0% | <i>Larrea tridentata</i> <i>Ambrosia dumosa</i> <i>Oryzopsis hymenoides</i> <i>Mirabilis pudica</i> | 6. +300 years Warmer/ wetter | Desert | Evergreen - 8.6% Subshrub - 15.5% Grass - 1.4% Forb - 0.1% | <i>Larrea tridentata</i> <i>Acamptopappus shockleyi</i> <i>Oryzopsis hymenoides</i> <i>Stanleya pinnata pinnata</i> |
| 3. +100 years Warmer/ wetter | Desert | Evergreen - 5.2% Subshrub - 15.3% Grass - 2.6% Forb - 0.1% | <i>Larrea tridentata</i> <i>Menodora spinescens</i> <i>Oryzopsis hymenoides</i> <i>Sphaeralcea emoryi</i> | 7. +1000 years Warmer/ wetter | Desert | Evergreen - 17.0% Subshrub - 19.9% Grass - 12.2% Forb - 0.0% | <i>Coleogyne ramosissima</i> <i>Grayia spinosa</i> <i>Stipa speciosa</i> <i>Delphinium parishii</i> |
| 4. +300 years Warmer/ drier | Desert | Evergreen - 4.0% Subshrub - 4.9% Grass - 0.1% Forb - 0.1% Succulent - 0.2% | <i>Larrea tridentata</i> <i>Psoralea fremontii</i> <i>Oryzopsis hymenoides</i> <i>Mirabilis pudica</i> <i>Opuntia ramosissima</i> | 8. +1000 years Cooler/ wetter | Xerophytic scrub | Evergreen - 21.0% Subshrub - 2.5% Grass - 9.8% Forb - 8.7% Conifer - 13.0% | <i>Artemisia nova</i> <i>Chrysothamnus viscidiflorus</i> <i>Sitanion hystrix</i> <i>Eriogonium ceasposum</i> <i>Pinus monophylla</i> |

^gPrentice et al., 1992; ^hKemp et al., 1997

Selection of Analog Climate Sites

Analog sites are chosen at varying geographical locations to provide proxy data for each of the specified climate states. The analog for each climate step is chosen primarily for its representativeness of the dominant indicators of precipitation and mean annual temperature. To be considered as an analog site, available data sets have to include a variety of atmospheric parameters to support the calculation of the Penman-Monteith reference evapotranspiration (ET_o), including net radiation, wind speed, mean temperature, and actual vapor pressure (or in its absence, daily minimum and maximum or hourly relative humidity). Alternatively, if station ET_o data was available, it is used.

It is reasonable to anticipate that analog sites for near-term climate steps would be geographically nearer to the current site than long-term climate analogs, thus the selection of representative locations begins in the southwest and western regions of the country. Weather data networks sourced for potential sites include the California Irrigation Management Information System (CIMIS), Arizona Meteorological Network (AZMET), National Oceanic and Atmospheric Administration Surface Radiation Budget Network (SURFRAD), and University of Utah's Department of Meteorology MesoWest network. Preliminary analysis of each potential analog site determines length of record, mean annual temperature, mean annual precipitation and seasonal precipitation patterns. These basic indicators are compared to current conditions for relative changes expected in future climate steps.

Climate Inputs

As the length of available record is necessarily less than the period of simulation, climate data sets are generated for each case by incrementing the analog data into shorter segments and randomly generating longer climate cycles. For example, the 9-year present day climate data set used in the Paleoflow Base Case and Case 1 is incremented into 1-year, 3-year and 9-

year blocks and randomized for 27, 9 and 3 permutations, respectively. This results in a 350-year randomized cycle for the each simulation, which is in keeping with observed cyclic weather patterns (e.g., 100-year and 500-year weather events). This approach is preferable to setting fixed boundary conditions, such as a prescribed surface flux or infiltration rate used in other long-term models of the region (Kwicklis et al., 2006; Walvoord et al., 2004; Scanlon et al., 2003), allowing the model to resolve daily events of consequence (i.e., extreme weather events such as short but intense storms characteristic of this region). Extreme events could conceivably affect flow patterns but would be averaged out by using fixed, longer-term (i.e. monthly or yearly) averages. This approach also allows calculated plant uptake (a function of temperature, wind speed and vapor pressure) to be correlated with observed precipitation, incorporating a greater level of realism in the model. This method preserves the descriptive statistics of the data set, while offsetting artificial short-term trends or cycles that might otherwise be introduced.

Case 1, +100 Years: Present Day Conditions

Current climate conditions at the Area 5 RWMS are represented by meteorological and radiation data recorded at the Desert Rock Airport (DRA) in Mercury, NV, 26 km (16 mi) to the south. Although precipitation data are available from stations at the Area 5 RWMS, the necessary solar measurements required to develop reference evapotranspiration (ET_0) are not available; data from a single location was desired to reduce possible modeling errors as a result of mismatch between localized precipitation and solar radiation records. The selected meteorological data are from the DRA Surface Radiation Site, maintained by the SURFRAD network for the 9-year period 8/1/1998-7/31/2007. Mean annual precipitation during this period is 112 mm/yr, mean annual temperature is 18.6 °C, mean temperature for the coldest month is 7.4 °C, and growing degree days (GDD_5) is 5015. The Priestley-Taylor moisture availability, expressed on a scale of $-1 \leq \alpha \leq 1$, is -0.93. Case 1 is a continuation of the

Paleomodel Base Case, run for an additional 350-year simulation period to provide a point of reference for Cases 2-8; as a result, this scenario has reached steady state.

Case 2, +100 Years: Warmer/ Much Wetter, Doubled Atmospheric Carbon Dioxide

Projected future climate for Case 2 is developed from current climate data using monthly scaling factors developed and grid referenced by the VEMAP Project (Kittel et al., 2004) based on output from the nested regional climate model by the Canadian Center for Climate Modelling and Analysis (CCC) High Resolution GCM Experiment (Boer et al., 1992). Monthly scaling factors for net incident solar radiation, temperature and wind speed for the 0.5° latitude x 0.5° longitude grid cell associated with the Area 5 RWMS are applied to the DRA climate data set from Case 1 using “ETrefTCO2” (Appendix I) to calculate CO₂ adjusted reference evapotranspiration (ET_o). Monthly scaling factors for precipitation from the Kittel et al. (2004) RCM data set are applied directly to the DRA precipitation data. Mean annual precipitation during this period is 134 mm/yr, mean annual temperature is 23.9 °C, mean temperature for the coldest month is 12.6 °C, growing degree days (GDD_5) is 6881, and the moisture index is -0.94.

Case 3, +100 Years: Warmer/ Wetter

As an alternative to the scaled data set, the analog site exhibits warmer temperatures and higher precipitation relative to current conditions. The 15-year data set from CIMIS Station 41 (Calipatria, CA) has a mean temperature of 21.3 °C, mean annual precipitation of 123 mm/yr, mean temperature coldest month of 5.7 °C, 5965 GDD_5 and a moisture index of -0.94.

Cases 4 and 5, +300 Years: Warmer/ Drier

The 17-year data set from AZMET Station 08 (Parker, AZ) has a mean temperature of 21.4 °C, mean annual precipitation of 95 mm/yr, mean temperature coldest month of 10.3 °C, $GDD_5 = 5996$ and a moisture index of -0.95, the driest of all simulations.

Case 6: +300 years, Warmer/ Wetter

Analog AZMET station 23 (Harquahala, AZ) provides a 9-year data set averaging 20.5 °C, mean annual precipitation of 170 mm/yr, mean temperature coldest month is 8.8 °C, GDD₅ equal to 5646 and a moisture index of -0.92.

Case 7: +1,000 years – Warmer/ Wetter

Climate data from CIMIS Station 44 (Riverside, CA) span 20 years, and have a mean annual temperature of 24.6 °C, mean annual precipitation of 246 mm/yr, mean temperature coldest month of 12.2 °C, 4650 growing degree days, and a moisture index of -0.87. Proportionally wetter winters evidenced here are representative of atmospheric cooling affected by Milankovitch forcing and associated movements (Miklas et al., 1995).

Case 8: +1,000 years – Cooler/ Wetter

Climate data from analog site CIMIS Station 117 (Victorville, CA) has a mean temperature of 16.1°C, mean annual precipitation of 257 mm/yr, mean temperature coldest month of 6.8°C, 4086 growing degree days and a moisture index of -0.91, the wettest and coolest of all simulations.

Development of Representative Biomes

Data for each of the climate analogs selected in the previous step are examined in terms of mean annual temperature, mean annual precipitation, number of growing degree days (base 5° C), Priestley-Taylor moisture availability index (scaled to $-1 \leq \alpha \leq 1$, where -1 = extremely dry and +1 = extremely wet following the method proposed by Wilmott and Feddema, 1992) and summer versus winter precipitation patterns. Climate profiles are compared to tolerance levels for biomes of western North America developed in Thompson and Anderson (2000). The work in this thesis employs the extensive catalog of

representative species for each biome presented in Thompson and Anderson (2000) to facilitate a review of species for additional site limitations that would favor or discourage the establishment of that biome at the Area 5 site.

This thesis follows the growth form classification system presented by Reynolds et al. (1996) and used in recent arid zone research of interest (Kemp et al., 1997; Yin et al., 2008) to describe each biome in terms of guild composition. Vegetation occurring in the vicinity of the study site is classified into the following representative growth forms, or “guilds,” as they are sometimes referred to in the literature (Kemp et al., 1997): evergreen shrubs, deciduous winter-active shrubs and subshrubs, grasses, spring/summer-active perennial forbs, succulents, and drought-tolerant woodland conifers. Designating a particular species to a functional type follows the classification presented by Thompson and Anderson (2000) when available; otherwise, growth form was obtained from the USDA PLANTS database (USDA NRCS, 2008) or the Utah State University Range Plants database (Utah State University, 2008). Where multiple growth forms are possible, species are assigned to a guild based on activity patterns and physical form most likely to develop given the climate state. *Larrea tridentata* (creosote bush) is classified as an evergreen shrub on the basis of rooting patterns, seasonal activity and stomatal responses to low moisture as suggested by Kemp et al (1997).

Plant species identified in the Area 5 RWMS vegetation surveys (Hansen and Osler, 2003) and the extensive Nevada Test Site vegetation surveys (Webb et al., 2003; Beatley, 1974) are, on balance, representative of Thompson and Anderson’s (2000) desert biome classification. Nearly all are considered to be of the desert shrub plant functional type, except for the desert forb, *Mirabilis pudica* (four o’clock). Plants near Area 5 that are classified as occurring in other designated regions include *Atriplex confertifolia* (shadscale saltbush) and *Ceratoides lanata* (winterfat), which are considered steppe shrubs, and *Oryzopsis hymenoides* (Indian ricegrass), a grass, in spite of conditions well outside of

predicted climatic tolerance. This indicates a certain amount of flexibility in the ability of plants to adapt to conditions outside their designated biome.

Guild compositions are developed in this study from the NTS vegetation surveys (Webb et al., 2003) that allow observation plots to be tied to climate characteristics. Though caution must be exercised when extrapolating vegetation patterns to other locales, using this set of geographically related sites allows consideration of what is likely to develop given regional soil, climate patterns, faunal exposure and migratory probabilities. A representative vegetation plot is selected for each bioclimatic scenario based on the following criteria:

- 1.) Average annual precipitation at the plot must be within $\pm 10\%$ of predicted precipitation for the climate scenario;
- 2.) Soil must be representative of the study site; that is, composed primarily of alluvium or sandy alluvium with no subsurface formation that would structurally impair root growth, thereby influencing the vegetation that has developed there;
- 3.) Location must be primarily undisturbed.

Surveyed plant species are grouped according to their guild, and the most common species from each guild is selected as its representative for leaf area index (defined as total leaf surface divided by land area) and rooting distribution. Guild composition is calculated using the 1970's ground cover data for each plot (Beatley, 1974). The 1970's data is selected in favor of the large percentage of dead and dormant vegetation observed in the 2002 data set resulting from an extreme drought in 1989-1991, and lesser droughts in 1996 and 2002 (Webb et al., 2003). Developed guild compositions and leaf area index (LAI) for all cases are referenced in Tables 3.4 – 3.10.

Table 3.4. Guild Composition, Case 1

| Guilds | % Ground Cover ^e | Representative species | Leaf Area Index |
|-------------------------|-----------------------------|--|-------------------|
| Evergreen Shrub | 7.1% | <i>Larrea tridentata</i> (creosote bush) | 0.65 ^a |
| Deciduous Subshrub | 10.3% | <i>Ambrosia dumosa</i> (white bursage) | 5.7 ^b |
| Grasses | 2.7% | <i>Oryxopsis hymenoides</i> (Indian ricegrass) | 3.6 ^c |
| Perennial Forbs | 0.2% | <i>Mirabilis pudica</i> (four o'clock) | 2.37 ^d |
| Total live ground cover | 20.3% | | |

Table 3.5. Guild Composition, Case 2

| Guilds | % Ground Cover ^f | Representative species | Leaf Area Index |
|-------------------------|-----------------------------|--|-------------------|
| Evergreen Shrub | 16.4% | <i>Larrea tridentata</i> (creosote bush) | 0.65 ^a |
| Deciduous Subshrub | 20.1% | <i>Ambrosia dumosa</i> (white bursage) | 5.7 ^b |
| Grasses | 1.0% | <i>Oryxopsis hymenoides</i> (Indian ricegrass) | 3.6 ^c |
| Perennial Forbs | 0% | <i>Mirabilis pudica</i> (four o'clock) | 2.37 ^d |
| Total live ground cover | 37.5% | | |

Table 3.6. Guild Composition, Case 3

| Guilds | % Ground Cover ^g | Representative species | Leaf Area Index |
|-------------------------|-----------------------------|---|-------------------|
| Evergreen Shrub | 5.2% | <i>Larrea tridentata</i> (creosote bush) | 0.65 ^a |
| Deciduous Subshrub | 15.3% | <i>Mindora spinescens</i> (spiny hopsage) | 5.7 ^b |
| Grasses | 2.6% | <i>Oryxopsis hymenoides</i> (Indian ricegrass) | 3.6 ^c |
| Perennial Forbs | 0.1% | <i>Sphaeralcea emoryi</i> (Emory's globemallow) | 2.37 ^d |
| Total live ground cover | 23.2% | | |

Table 3.7. Guild Composition, Case 4

| Guilds | % Ground Cover ^f | Representative species | Leaf Area Index |
|-------------------------|-----------------------------|--|-------------------|
| Evergreen Shrub | 4.0% | <i>Larrea tridentata</i> (creosote bush) | 0.65 ^a |
| Deciduous Subshrub | 4.9% | <i>Ambrosia dumosa</i> (white bursage) | 5.7 ^b |
| Grasses | 0.1% | <i>Oryxopsis hymenoides</i> (Indian ricegrass) | 3.6 ^c |
| Perennial Forbs | 0.1% | <i>Mirabilis pudica</i> (four o'clock) | 2.37 ^d |
| Succulents | 0.2% | <i>Opuntia ramosissima</i> (diamond cholla) | 0.25 ^e |
| Total live ground cover | 9.3% | | |

Sources:

^{a,b,c,d} After Kemp et al., 1997.

^aLudwig et al., 1975; Barbour, 1977

^bLudwig et al., 1975; Deput and Caldwell, 1975

^cWilliamson et al., 1987

^dIBP, 1974.

^ePlot 28a, Webb et al., 2003

^fHousman et al., 2006

^gPlot 7, Webb et al., 2003

Table 3.8. Guild Composition, Case 6

| Guilds | % Ground Cover ^e | Representative species | Leaf Area Index |
|-------------------------|-----------------------------|---|-------------------|
| Evergreen Shrub | 8.6% | <i>Larrea tridentata</i> (creosote bush) | 0.65 ^a |
| Deciduous Subshrub | 15.5% | <i>Acamptopappus shockleyi</i> (Shockley's goldenhead) | 5.7 ^b |
| Grasses | 1.4% | <i>Oryxopsis hymenoides</i> (Indian ricegrass) | 3.6 ^c |
| Perennial Forbs | 0.1% | <i>Stanleya pinnata pinnata</i> (desert prince's plume) | 2.37 ^d |
| Total live ground cover | 25.5% | | |

Table 3.9. Guild Composition, Case 7

| Guilds | % Ground Cover ^f | Representative species | Leaf Area Index |
|-------------------------|-----------------------------|--|-------------------|
| Evergreen Shrub | 17.0% | <i>Coleogyne ramosissima</i> (blackbrush) | 1.35 ^h |
| Deciduous Subshrub | 19.9% | <i>Grayia spinosa</i> (spiny hopsage) | 5.7 ^b |
| Grasses | 12.2% | <i>Stipa speciosa</i> (desert needlegrass) | 3.6 ^c |
| Perennial Forbs | 0.02% | <i>Delphinium parishii</i> (desert larkspur) | 2.37 ^d |
| Total live ground cover | 49.1% | | |

Table 3.10. Guild Composition, Case 8

| Guilds | % Ground Cover ^f | Representative species | Leaf Area Index |
|---------------------------|-----------------------------|---|-------------------|
| Evergreen Shrub | 21.0% | <i>Artemisia nova</i> (big sagebrush) | 0.29 ^j |
| Deciduous Subshrub | 2.5% | <i>Chrysothamnus viscidiflorus</i> (yellow rabbitbrush) | 5.7 ^b |
| Grasses | 9.8% | <i>Sitanion hystrix</i> (bottlebrush squirreltail) | 3.6 ^c |
| Perennial Forbs | 8.7% | <i>Eriogonium ceasпитosum</i> (mat buckwheat) | 2.37 ^d |
| Drought Tolerant Conifers | 13.0% | <i>Pinus monophylla</i> (singleleaf pinyon juniper) | 3.4 ^k |
| Total live ground cover | 55.0% | | |

Sources:

^{a,b,c,d} After Kemp et al., 1997.

^aLudwig et al., 1975; Barbour, 1977

^bLudwig et al., 1975; Deputit and Caldwell, 1975

^cWilliamson et al, 1987

^dIBP, 1974.

^eBriones et al., 1996

^fPlot 33, Webb et al., 2003

^gPlot 57, Webb et al., 2003

^hSmith et al., 1995

ⁱPlot 47, Webb et al., 2003

^jElvidge and Chen, 1995

^kWarren et al., 2001

^lPlot 63, Webb et al., 2003

The biome for the elevated CO₂ scenario in Case 2 is developed based on work showing measurable increases in productivity and photosynthetic response among desert shrubs to elevated atmospheric CO₂, particularly during wetter periods (Hamerlynck et al., 2000; Housman et al., 2006). Productivity factors of 2.3 for evergreen shrubs and 1.95 for deciduous subshrubs derived from Housman et al. (2006) are applied to Case 1 guild compositions to develop the biome for Case 2. Grass coverage is reduced by nearly 40% to account for the dynamics of shrubland expansion associated with drying conditions (Balling, 1988; Schlesinger and Pilmanis, 1998).

Case 4 demonstrates greatly reduced vegetation, and Case 5 tests the effects of soil evaporation only, thus guild compositions and root distributions = 0. Case 6 reflects similar proportions of high deciduous subshrubs and the perennial evergreen *Larrea tridentata* as seen in Case 3. The biome also represents an increase in coverage of grasses under increasing precipitation, as their rapid migratory properties allow them to move in and take advantage of increased available soil moisture (Prentice et al., 1992).

Case 7 is represented by total ground cover increases of nearly 50% in what is essentially a pluvial period in a semi-arid region. *Larrea tridentata* is replaced by *Coleogyne ramosissima* (blackbrush), *Grayia spinosa* (spiny hopsage) becomes the most abundant single species on the landscape, and an attendant increase in the grass population is seen. Leaf area index for *Coleogyne ramosissima* is updated with observations made under periods of low water stress by Smith et al. (1995). LAI for *stipa speciosa* (desert needlegrass) was held constant, due to the similarity in form and activity to previous representative species *Oryxopsis hymenoides* (Indian ricegrass) (Pavek, 1993).

In Case 8, total vegetation cover was increased to 55%. The biome indicators demonstrate the potential for tolerance of xerophytic scrub plants; the appearance of some of these species, most notably, *Pinus monophylla*, represent the introduction of drought-tolerant

woodland conifers guild to the biome. Leaf area index is 3.4 (Classen et al., 2005) (averaged for healthy pinyon juniper), in line with averaged observations by Warren et al. (2001) of 3.7 and 3.6 for *Pinus pinus* and *Pinus radiata*, respectively. LAI for *Artemisia nova* is 0.29, from measurements of full-foliage *Artemisia tridentata* (big sagebrush) (Elvidge and Chen, 1995).

Calculation of Evapotranspiration

Potential plant evapotranspiration, or reference evapotranspiration (ET_o), is calculated for each biome using the Penman-Monteith method as detailed by the Food and Agriculture Organization (FAO) (Equation 3.1) (Allen et al., 1998).

$$ET_o = \frac{0.408\Delta(R_n - G) + \gamma \frac{900}{T + 273} * u_2(e_s - e_a)}{\Delta + \gamma(1 + 0.34u_2)} \quad (3.1)$$

where Δ = slope vapor pressure curve [$\text{kPa } ^\circ\text{C}^{-1}$], R_n = net radiation at the crop surface [$\text{MJ m}^{-2} \text{ day}^{-1}$], G = soil heat flux density [$\text{MJ m}^{-2} \text{ day}^{-1}$], γ = psychrometric constant [$\text{kPa } ^\circ\text{C}^{-1}$], T = mean daily air temperature at 2 m height [$^\circ\text{C}$], u_2 = wind speed at 2 m height [m s^{-1}], e_s = saturation vapor pressure [kPa], e_a = actual vapor pressure [kPa] and $e_s - e_a$ = saturation vapor pressure deficit [kPa].

This thesis opts for the Penman-Monteith approach over other available methods for calculating ET_o in an effort to use a physically-based approach that explicitly accounts for meteorological parameters (specifically wind speed, solar radiation and temperature) that may be affected by climatic variations. In addition, this method was developed with the intention of serving as a standard in agricultural applications; as a result, many data networks are beginning to supply daily ET_o with currently available datasets, facilitating cross-network data comparison. A comparison between Penman-Monteith and Hargreaves (Wu, 1997;

Hargreaves and Allen, 2003) estimates of ET_o for the Case 1 climate data set indicates a good correlation ($r^2 = 0.7302$) between the two methods (Figure 3.3), so in practice the selection of the calculation method would have comparatively little impact on the flow model. Calculated ET_o results were compared to seasonal evapotranspiration data for *Larrea tridentata* (creosote bush) reported in literature (Sammis and Gay, 1979; Scott et al., 2006) and were in line with the magnitude and variation of field observations.

A Fortran program “ETrefTave”, developed for this project to facilitate preprocessing and calculation of ET_o from the extensive SURFRAD data set (which are available as daily files, written every three minutes), is included in Appendix I. Day of year, daily mean temperature and ET_o are written to an output file used to develop the variables $tAtm(i)$, $rSoil(i)$ and $rRoot(i)$, respectively, for HYDRUS upper boundary condition input file “ATMOSPH.IN.”

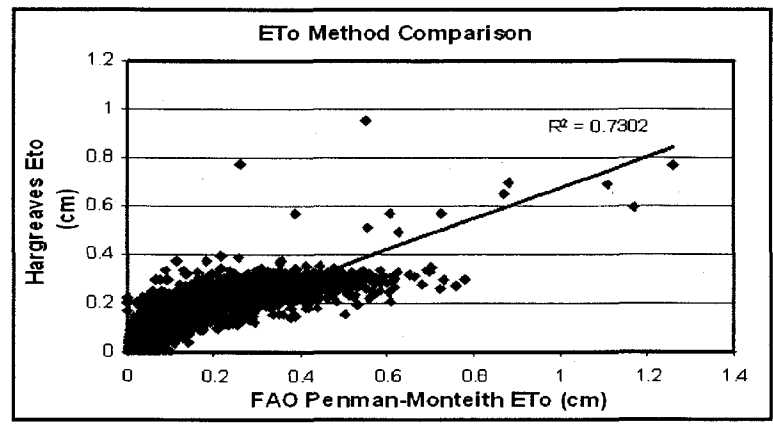


Figure 3.3. Comparison of Reference Evapotranspiration (ET_o) Calculation Methods using the Case 1 Climate Data Set.

Partitioning of ET_o into potential evaporation (E_{pot}) and potential transpiration (T_{pot}) is accomplished externally in Microsoft Excel using an approach described in Kemp et al. (1997) and employed in work by Yin et al. (2008):

$$T_{pot} = ET_o * (1 - e^{-k*LAI}) \quad (3.2)$$

$$E_{pot} = ET_o * e^{-k*LAI} \quad (3.3)$$

where ET_o = reference evapotranspiration [L], LAI = leaf area index [-], available from the literature and k [-] is a parameter accounting for radiation extinction by the canopy and varies with sun angle, leaf distribution and leaf arrangement (Kemp et al., 1997).

Total soil evaporation values for the biome are calculated by adding the guild values weighted by percent vegetation cover:

$$B_{evap} = \sum_{i=1}^g E_{pot_i} * GC_i \quad (3.4)$$

where B_{evap} refers to the total potential transpiration and potential evaporation for the biome [L], g = the number of guilds occurring in the biome and GC = percent ground cover [%]. Potential transpiration (T_{pot}) and potential evaporation (E_{pot}) are not seasonally adjusted by guild; all guilds are assumed to be annually active.

This method is selected over the crop coefficient (K_c) based method, proposed by Allen et al. (1998), because crop coefficients inherently assume that vegetation are unstressed; thus, this approach is inapplicable to plants with a high degree of stomatal control, which is not very compatible with natural arid systems (Mata-Gonzalez et al., 2005). In practice, the crop coefficient method is difficult to implement for desert vegetation and K_c for an individual species can show great variability; *Larrea tridentata* can exhibit field behavior described by K_c ranging from 0.3 to 1.25 (Saucedo et al., 2005).

Root densities for evergreen shrubs, subshrubs, forbs and grasses are obtained from Kemp et al. (1997), succulents from Briones et al. (1996) field surveys, and conifers from the equation published by Jackson et al. (1996) for temperate coniferous forests; these are listed in Table 3.11. Existing data indicate that most root profiles, even among plants of varying

physiological types and geographical locations, share common root distribution, densities and biomass (Jackson et al., 1996; Schenk, 2005). Composite distributions are developed by weighting the root distribution by guild ground cover:

$$\sum_{i=1}^g = \sum_{j=1}^x r_i * GC_i \quad (3.5)$$

where g = the number of guilds occurring in the biome, x = root zone depth [L], r = total root density for the interval $x_j - x_{j-1}$ [%] and GC = percent ground cover [%]. Root distributions are assumed constant over the duration of the simulation. Given the tendency for primary roots of perennial plants to reach depth relatively quickly and persist throughout the year, a fixed distribution is reasonable for this system. Grasses and forbs are combined into one group due to similarities in rooting patterns. Composite root distribution for all cases except Case 5 are shown in Figure 3.4.

| Depth (cm) | Evergreen Shrub ^a | Deciduous Subshrub ^a | Grasses/ Perennial Forbs ^a | Succulents ^b | Drought Tolerant Conifers ^c |
|------------|------------------------------|---------------------------------|---------------------------------------|-------------------------|--|
| 0 | 0 | 0 | 0.2 | 0.35 | 0 |
| 9 | 0 | 0.1 | 0.3 | 0.53 | 0.004 |
| 22 | 0.1 | 0.2 | 0.2 | 0.11 | 0.008 |
| 31 | 0.2 | 0.2 | 0.2 | 0.01 | 0.010 |
| 40 | 0.2 | 0.2 | 0.1 | - | 0.011 |
| 62 | 0.3 | 0.2 | - | - | 0.013 |
| 80 | 0.1 | 0.05 | - | - | 0.014 |
| 98 | 0.1 | 0.05 | - | - | 0.014 |
| 106 | - | - | - | - | 0.014 |
| 588 | - | - | - | - | 0.007 |
| 610 | - | - | - | - | - |

Source:

^aKemp et al., 1997

^bBriones et al., 1996

^cJackson et al., 1996

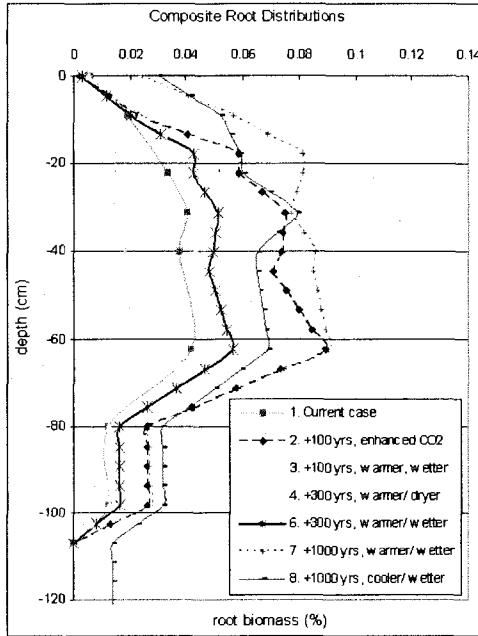


Figure 3.4a

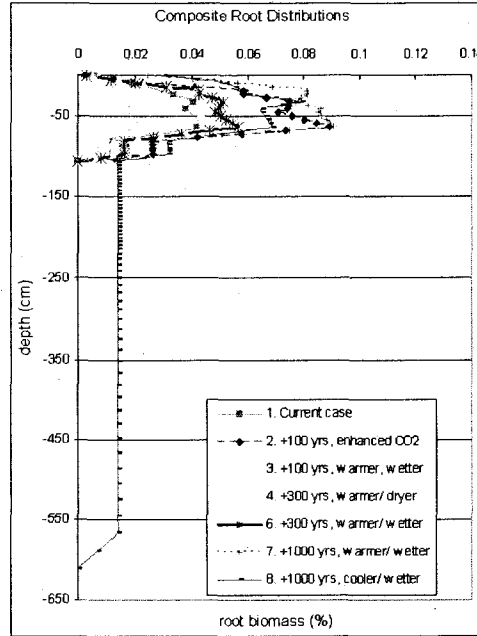


Figure 3.4b

Figure 3.4: Composite Root Distribution for Cases 1-8 for (a) depth = -1.2 meters and (b) depth = -6.5 meters

Numerical Flow Model Description

HYDRUS-1D (Simunek et al., 2005) is a one-dimensional numerical modeling package that includes coupled liquid water, water vapor and energy transport. It has been selected for its accessibility as a public-domain package, capability to account for vapor flux, and flexibility of analytical hydraulic properties models (including Brooks and Corey (1966), van Genuchten (1980) or Vogel & Cislrova (Vogel et al., 1991) hydraulic property calculation schemes), which can be important when considering soil conditions in extremely arid regions. HYDRUS uses Darcy's law to describe liquid water flux, Fick's law of diffusion to describe vapor flux, and a convection-dispersion equation for heat transport. Water flow is solved using Richard's equation in the form:

$$\frac{\partial \theta}{\partial t} = \frac{\partial}{\partial z} \left[K \left(\frac{\partial h}{\partial z} + 1 \right) \right] - S \quad (3.6)$$

where θ is volumetric water content [L^3L^{-3}], t is time [T], h is pressure head [L], z is a spatial coordinate (in this case, profile depth) [L], K is hydraulic conductivity [$L T^{-1}$], and S [T^{-1}] is the sink term representing plant water uptake (Simunek et al., 2005).

Although HYDRUS offers a variety of water retention functions to develop hydraulic properties as mentioned above, all of these relationships suffer from fundamental limitations inherent in using Richard's equation under conditions of very low or very high water contents (such as those encountered in extremely arid environments or saturated conditions). Under these conditions, the assumption of laminar flow (defined as the flow of adjacent layers of fluid are not turbulent relative to one another) required by Darcy's law may no longer be valid (Hillel, 1998). At very low water contents, water can bind to the soil particle surface as a result of adsorptive forces, resulting in non-viscous flow that is no longer proportional to the hydraulic gradient (Hillel, 1998). At very high water contents in association with large soil pores, high flow velocity may become turbulent, which also renders Darcy's law invalid (Hillel, 1998). Though these limitations are hardly unique to HYDRUS, it is worthwhile to identify it as a possible source of error. Another potential disadvantage of this numerical code is the assumption that advective vapor phase flow is negligible, which may not necessarily be true in the presence of some environmental conditions (e.g. high atmospheric pressure gradients) (Choi et al., 2002). This work does not explicitly address advective vapor flux resulting from barometric pumping or other surface atmospheric conditions.

Time Discretization and Scaling

The major climate states are predicted to occur on the order of 10,000 years, and in some cases transitional ages might vary by thousands of years. Yet the processes of interest occur on very short time scales. To resolve these different temporal scales, short term variations are emphasized, and results from each case simulation are to be considered a moment in time. Inputs are on a daily time scale except paleomodel Test E, which considers the impact of

hourly versus daily time step. Since this work does not model the transitional period between climate states and biome changes, it is assumed that the biome compositions are well established and will not change significantly over the course of the scenario.

Model Structure

In the model, the site is represented as a one-dimensional soil column with a depth to water table of 235 meters, represented by a fixed head lower boundary condition. Soil is assumed to be unsorted and homogeneous throughout the column. Though some research indicates that soil heterogeneity may play a more significant role in lateral flow than conservative estimates allowed for (Yucel and Levitt, 2001), the available soil properties data indicates that the alluvium is unconsolidated and poorly sorted, and virtually homogeneous throughout the profile (Bechtel Nevada, 2005a, 2005b). Thus, not only is the assumption of homogeneity in this work appropriate, but it simplifies analysis of the effects of environmental conditions on the deep hydraulic gradient by preventing flow that is solely a consequence of soil properties. In addition, the bulk of research suggests that on a longer time horizon of interest in this study, a one-dimensional conceptualization is also appropriate (Tyler et al., 1996, Walvoord et al., 2002a, 2002b, 2004).

The system is represented by a 500-node telescoping column, with higher densities of 0.5 cm (0.2 in) at the surface and through the root zone, estimated at a depth of 1.2 m (4 ft) based on work by Hansen and Ostler (2003) identifying maximum rooting depth for Area 5 vegetation of 95.5 to 115.8 cm. Nodal density at the bottom of the profile is 23.5 cm (9.2 in).

Soil Properties

Soil hydraulic properties used as model inputs are described in Table 4.1, and are obtained from Area 5 Pilot Well data for Ue5PW3. Although some research indicates hydraulic properties will change as the soil surface ages (Young et al., 2004), this work opts to hold soil properties constant throughout the simulation in all cases due to the

comparatively short forward simulation period relative to the time scale of measurable soil change.

| | |
|---|--------|
| [†] Residual Water Content (θ_r) [$\text{cm}^3 \text{cm}^{-3}$] | 0.045 |
| [†] Saturated Water Content (θ_s) [$\text{cm}^3 \text{cm}^{-3}$] | 0.303 |
| [†] van Genuchten alpha (α) [cm^{-1}] ² | 0.028 |
| [†] van Genuchten n (n) [-] | 1.38 |
| [†] Saturated hydraulic conductivity (K_{sat}) [cm day^{-1}] | 141.22 |
| [‡] Tortuosity factor (l) | 0.5 |

[†]Bechtel Nevada, 2005b

[‡]Soil textural properties catalogue for sand and loamy sand, Carsel and Parrish, 1988

Initial and Boundary Conditions

The entire profile is assigned an initial head of -10 m (33 ft) representative of wetter conditions found at the end of the Pleistocene, with the bottom of the column assigned a constant head of 0 m, consistent with the location of the water table. Minimum allowable head in the profile is -1000 m. The initial temperature gradient assigned to the profile is $34.5 \text{ }^\circ\text{C km}^{-1}$, with the water table temperature at $26.5 \text{ }^\circ\text{C}$ and an initial surface temperature of $18.4 \text{ }^\circ\text{C}$ at the time of transition (Walvoord et al., 2004). Water table and surface temperatures are held constant during the base case at $26.5 \text{ }^\circ\text{C}$ and $21.4 \text{ }^\circ\text{C}$, representative of the warmer surface conditions developing through the Holocene and creating an upward thermal gradient.

Plant Water Uptake

Plant water uptake is explicitly accounted for in HYDRUS-1D as an additional sink term in the water flow equation (3.2) above:

$$S(h) = \alpha(h)S_p \quad (3.7)$$

where the root-water uptake stress response function $\alpha(h)$ is a dimensionless function of pressure head h ($0 \leq \alpha \leq 1$), and S_p is the possible water uptake rate (Simunek et al., 2005). Potential plant transpiration is provided as an externally partitioned input (see equation 3.1) via the atmospheric input file ATMOSP.H. The actual uptake for the given time step is partitioned over the root zone in accordance with the prescribed root density. The HYDRUS model allows for adjustment of the uptake volume due to plant stress function using one of two available schemes, though all scenarios were run using the stepwise water stress response function developed by Feddes et al. (1978) (as described in Simunek et al., 2005). This assumes that water uptake is equal to zero close to saturation ($h_1 = 0$) and when exceeding the wilting point ($h_4 = \text{wilting point}$). Uptake is optimal between h_2 and h_3 , and decreases linearly as the system approaches either saturation or the wilting point (Simunek et al., 2005).

Feddes parameters for Cases 1 – 6 for *Larrea tridentata* (Figure 3.5a) were obtained from Franco et al. (1994); potential transpiration rates are from Hupet et al. (2002). As significant climatic changes lead to alterations in vegetation communities, plant parameters are updated to reflect dominant vegetation. For Case 7, uptake parameters (Figure 3.5b) ($\Psi_{min} = -6.0$ MPa; $\Psi_{max} = -1.0$ MPa) are taken from observations of xylem water potential of *Coleogyne ramosissima* by Gebauer and Ehleringer (2000), which are in line with observations for *Ephedra nevadensis* (Mormon tea) from a *Coleogyne ramosissima*-*Ephedra nevadensis*-*Grayia spinosa*-*Haplopappus cooperi* assemblage (Smith et al., 1995) similar to this biome ($\Psi_{min} = -6.5$ MPa; $\Psi_{max} = -1.6$ MPa). For Case 8, Feddes parameters for *Pinus monophylla* (Figure 3.5c) ($\Psi_{min} = -2.6$ MPa; $\Psi_{max} = -1.1$ MPa) are obtained from Jaindl et al. (1995) observations made in a *Pinus monophylla* – *Artemisia tridentata* (singleleaf pinyon – big sagebrush) community. Pressure potentials are converted to head of water [cm] for model parameters.

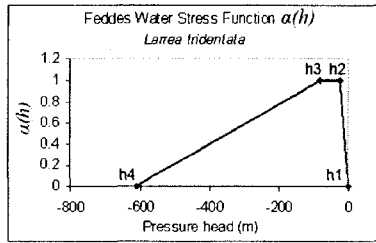


Figure 3.5a

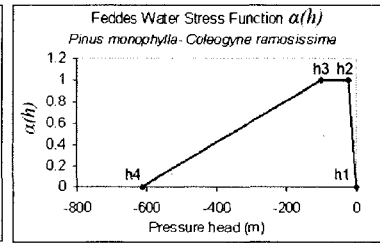


Figure 3.5b

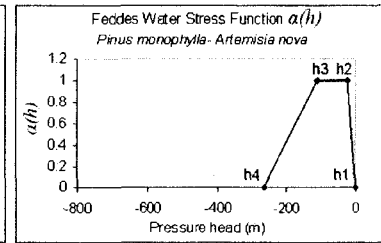


Figure 3.5c

Figure 3.5: Feddes Plant Uptake Parameters. (a) Cases 1-6; (b) Case 7; (c) Case 8

Model Performance Measures

Validation of model performance is complicated by the high level of uncertainty associated with the interdependent processes of climate change, vegetation and soil evolution. In addition, the predictive nature of forward simulation makes it difficult to identify appropriate performance measures. To that end, this project uses the paleomodel developed in Phase I to project forward from known paleoclimatic inputs to present day output, and verifies results of the paleomodel against observed current soil potential and water content data for the Area 5 study site. The hydrologic reversal from net downward to net upward flow associated with the transition from Pleistocene to Holocene conditions is well accepted by researchers (Walvoord et al., 2002a, 2002b; Edmunds and Tyler, 2002; Scanlon et al., 2003) and the timing of the transition is placed at approximately 12,000 to 16,000 years ago (Phillips, 1994). This work adopts the assumption that net flux = 0 approximately 13,000 years ago (Walvoord et al., 2004), and uses the developed inputs from paleoclimate simulations from previous work as initial conditions from the time of hydraulic transition to the present. All chronological forward steps are driven by potential outputs from the previous run. Model performance with respect to identified benchmarks is discussed in Chapter 4.

CHAPTER 4

RESULTS

Phase I Paleomodel Results

Paleomodel Base Case Results

Simulated soil water pressure head for the paleomodel initial simulation (Base Case) is shown in Figure 4.1. For all parameters of interest, the system responds very quickly and stabilizes within 3,500 years from initialization, with remarkable similarity at all time steps in the upper 10 m. Soil water potential becomes strongly negative in the upper 1 m of the soil profile under the influence of the root zone then becomes less negative immediately below,

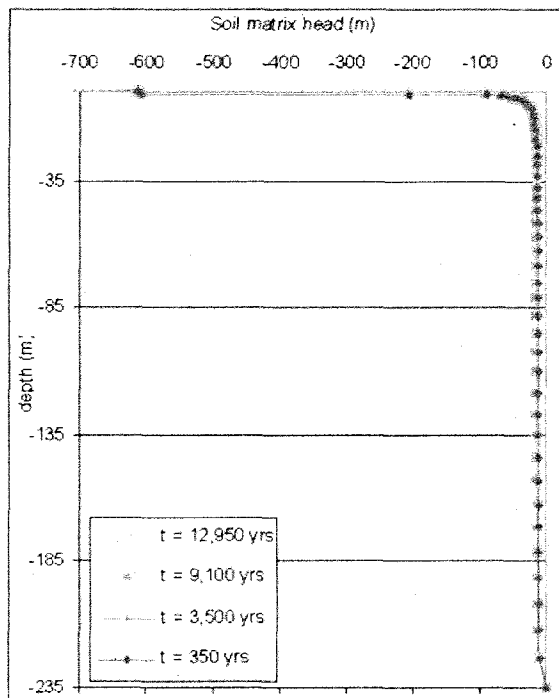


Figure 4.1a

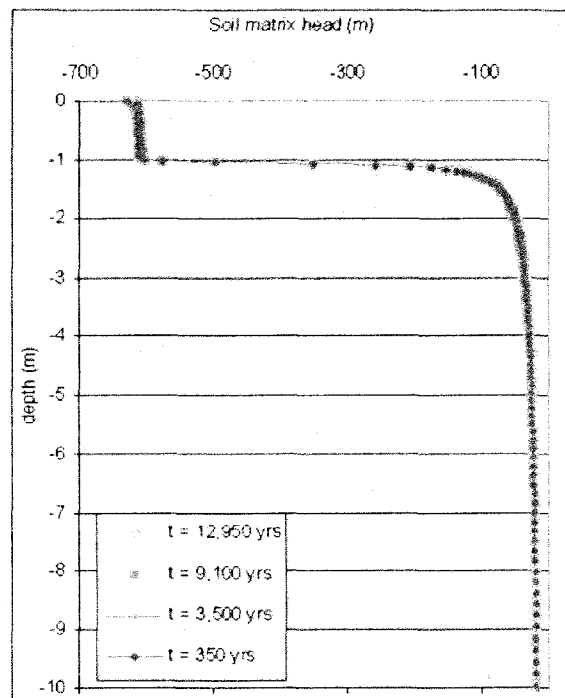


Figure 4.1b

Figure 4.1. Simulated Soil Matrix Head from 13,000 Years Ago to Present. (a) entire soil profile; (b) upper 10 meters.

where it remains constant around -14 m through the profile and down to the water table. This zone of constant head at depth indicates that the deep profile has reached unit gradient conditions, where pressure head contributes very little to the total hydraulic head and gravitational head dominates ($\Delta H/\Delta z = 1$). As a result, the downward flux approximately equals the unsaturated hydraulic conductivity (K) (Hillel, 1998); for the Base Case, $K = 0.0025 \text{ mm day}^{-1}$ (0.9 mm yr^{-1}) at $h = -14 \text{ m}$. Similarly, volumetric water content (Figure 4.2) increases at the base of the root zone and remains fairly constant through the profile until about 10 m above the water table, where it increases as the capillary fringe is encountered near the saturated lower boundary. Flux (Figure 4.3) is slightly positive (i.e. upward) through the top 10 cm in response to surface evaporation, and remains at or very nearly zero (-0.05 to 0.08 mm yr^{-1}) to a depth of approximately 1 m. Flux is upward from the base of the root zone ($\sim 105 \text{ cm}$) through 9.2 m. Below this point, flux becomes negative (i.e., in a downward direction) through to the base of the profile.

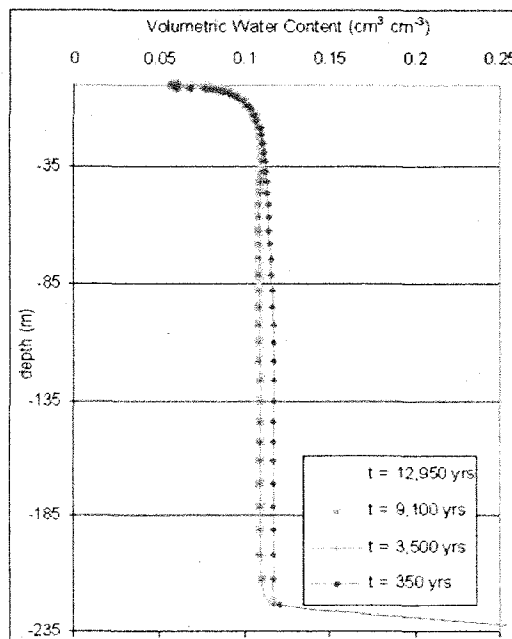


Figure 4.2a

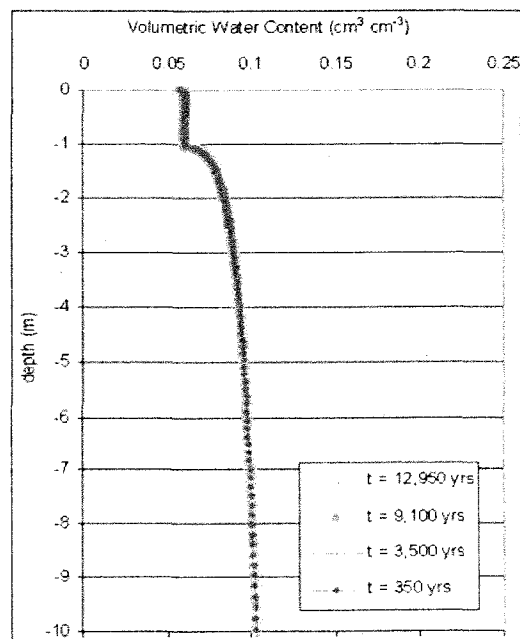


Figure 4.2b

Figure 4.2. Simulated Volumetric Water Content from 13,000 Years Ago to Present. (a) entire soil profile; (b) upper 10 meters.

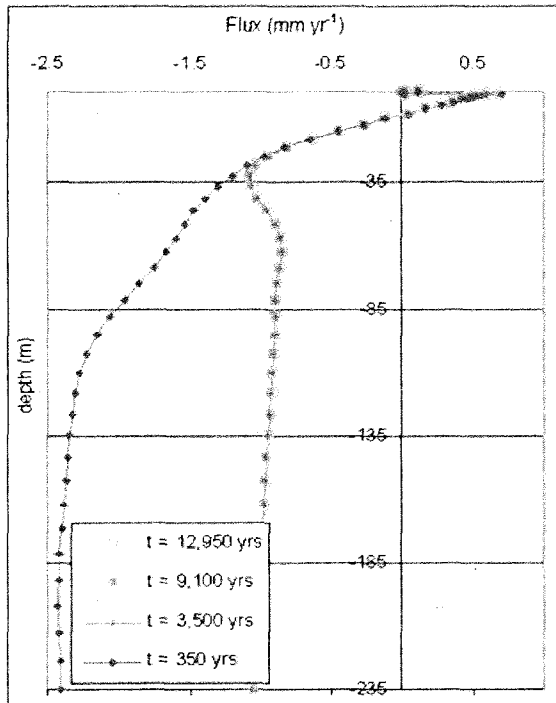


Figure 4.3a

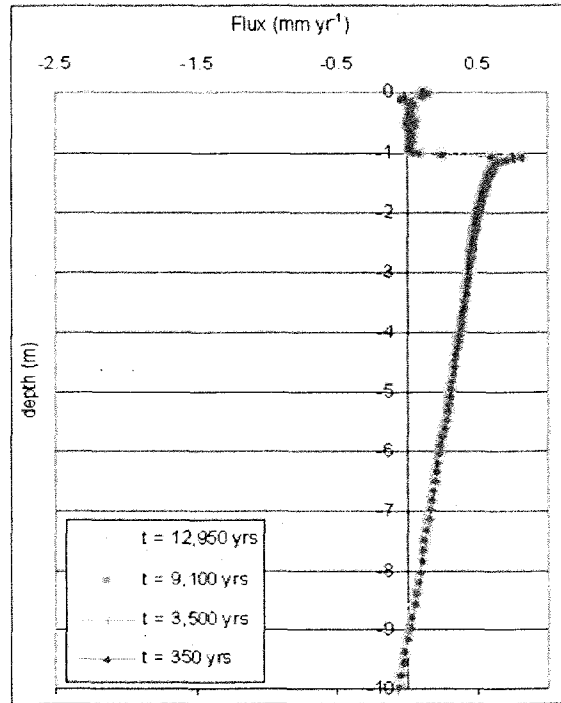


Figure 4.3b

Figure 4.3. Simulated Flux from 13,000 Years Ago to Present. (a) entire soil profile; (b) upper 10 meters.

Tests A – E Results

Soil water pressure heads and volumetric water contents for Base Tests A–E are shown in Figure 4.4. Test E results (i.e., compressed precipitation) for soil water pressure head, water content and flux are qualitatively indistinguishable from the Base Case. The most strongly negative heads are observed for Test D, where precipitation was reduced by 50% (equivalent to mean annual rainfall of 56 mm yr^{-1}). Head remains negative from the base of the root zone and increases to equilibrium values of approximately -31.1 m at a depth of around 85 m . Test A results (i.e., increased vegetation cover) exhibit similar features. Root water uptake led to more negative heads well below the base of the root zone and increasing to equilibrium values of -30.8 m at a depth of around 85 m . Both Tests A and D exhibit similar volumetric soil moisture profiles, averaging around 8% and 9%, respectively.

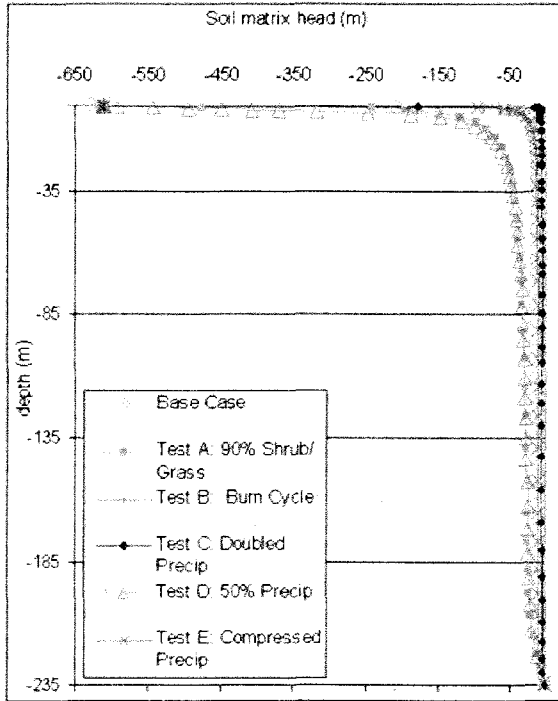


Figure 4.4a

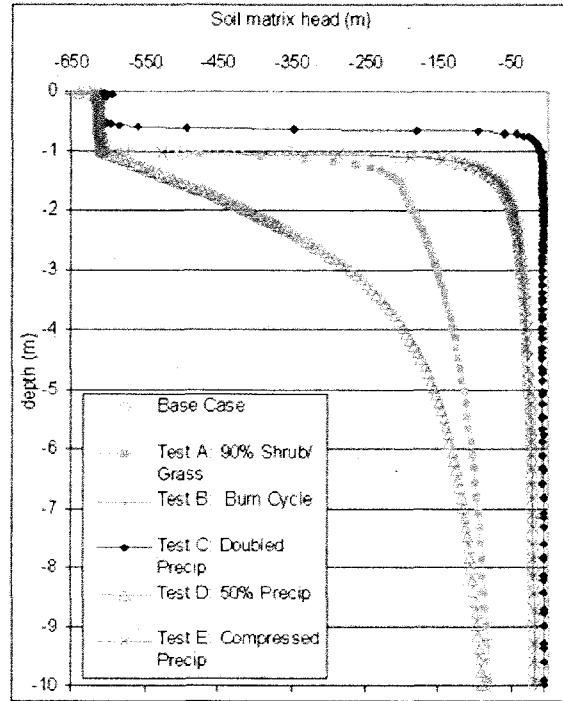


Figure 4.4b

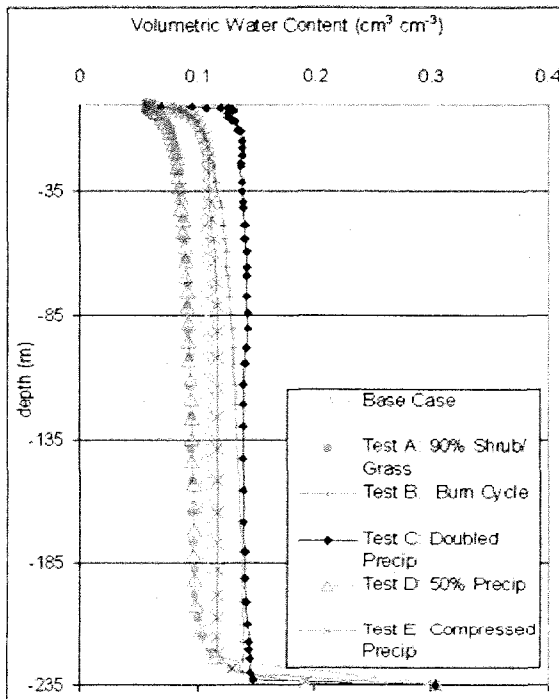


Figure 4.4c

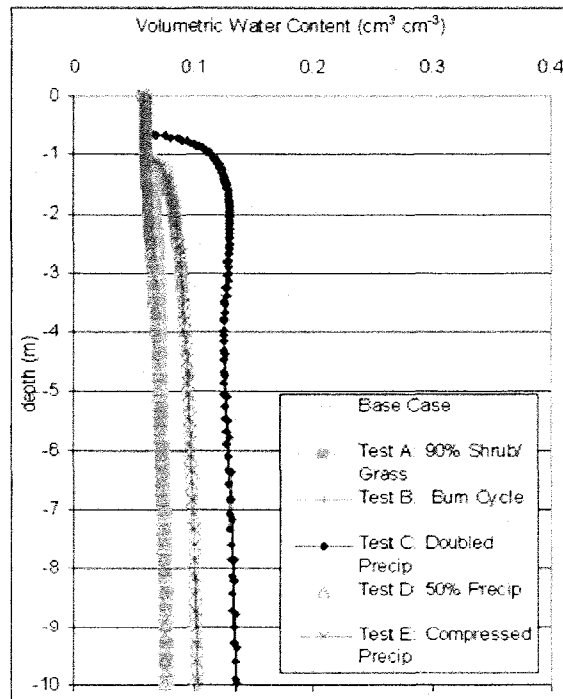


Figure 4.4d

Figure 4.4. Simulated Soil Matrix Head and Volumetric Water Content for Paleomodel Test Series. (a) Soil matrix head for entire soil profile; (b) soil matrix head for upper 10 meters; (c) volumetric water content for entire soil profile; (d) volumetric water content for upper 10 meters.

Results from Test B (i.e., wildfire scenario) and Test C (i.e. precipitation doubled to 224 mm yr⁻¹) demonstrate the opposite trend, with less negative heads through the deep vadose zone relative to the Base Case. Both Tests B and C show pressure heads of approximately -5 m at unit gradient. Soil water heads in Test B (wildfire scenario) begin to diverge from those predicted in the Base Case at around 20 m depth, becoming gradually less negative through the base of the profile. Similarly, water contents increase slightly around 20 m depth and continue to rise as the water table is encountered, indicating that periodic deep percolation is occurring during periods of vegetation removal. Test C (i.e., doubled precipitation) shows a slight bulge in water content near the soil surface (0.6 m – 4 m) which is reflected in the elevated positive (downward) fluxes over this depth (Figure 4.5). Fluxes for Test C are 150 times greater in the downward direction at the base of the profile in response to greater water availability.

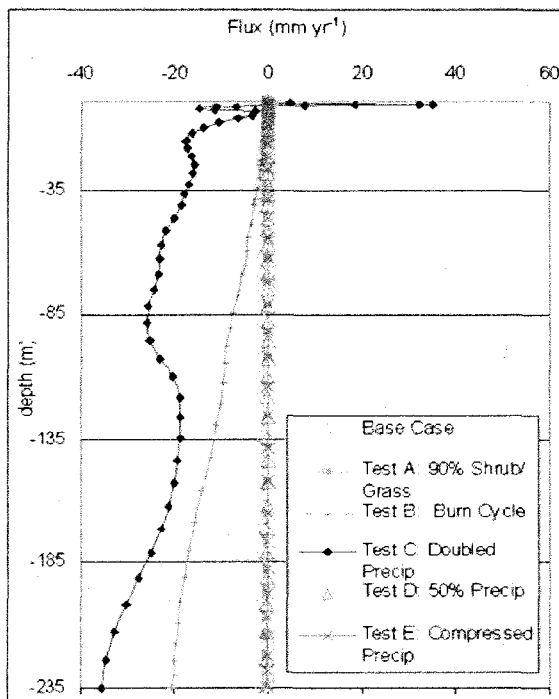


Figure 4.5a

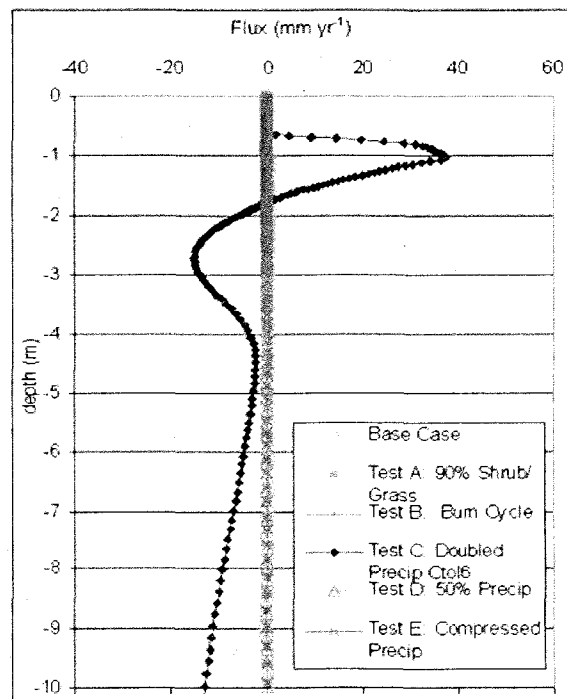


Figure 4.5b

Figure 4.5. Simulated Flux for Paleomodel Test Series. (a) entire soil profile; (b) upper 10 meters.

All tests display the characteristically highly negative pressure heads near the root zone, rapidly increasing to a unit gradient condition in the deeper portion of the profile where gravitational flow dominates ($\Delta H/\Delta z = 1$). In all tests, fluxes are upward toward the soil surface in the upper portion of the profile and downward through the majority of the deep vadose zone. The plane of zero flux (as defined by Hillel, 1998) in the Base Case is 9.2 m (± 0.12 m), Test A is 35.9 m (± 0.11 m), Test B is 10.3 m (± 0.05 m), Test C is 1.8 m (± 0.06 m), Test D is 37.6 m (± 0.12 m) and Test E is 8.9 m (± 0.28 m).

Water balance outputs at the end of the paleomodel simulation for test conditions A – E are presented in Table 4.2. Reducing precipitation values by 50% in Test D results in the driest soil column at the end of the simulation period, nearly matched by the effects of increased evapotranspiration in Test A; Tests A and D result in reductions of soil moisture storage compared to Case 1 of 13.8% and 14.0%, respectively. The other three tests (B, C and E) predictably lead to conditions wetter than Case 1. Periodic vegetation mortality represented in Test B shows increased storage of 18.2% compared to Case 1, while doubled precipitation results in the wettest simulated profile, with a 28.5% increase in stored water.

The effect of time step on calculation of net infiltration (precipitation – potential evapotranspiration) is demonstrated in Test E, which results in an increased total soil moisture in the profile of +5.3% at $t_f = 13,000$ years, relative to using daily precipitation inputs (as in the Base Case). Fluxes out of the profile decreased from -0.31 mm yr^{-1} to -0.14 mm yr^{-1} as concentrating precipitation resulted in proportionally greater precipitation relative to ET. This supports findings presented in Scanlon et al. (2002) that treatment of the upper boundary condition in HYDRUS 1D results in a slight overestimation of evaporation when using daily precipitation inputs. However, examination of changes to the water balance for the Base Case and Test E indicate no difference between change in stored water over the last

350 years, where it remained -0.1 cm for both cases. Given that any underestimation of water storage resulting from time step over a 350-year simulation period is less than the precision of the model, the effect of time step on water balance is not significant on the centennial time scale used in the Future Cases.

| | Paleo-model Base Case | Test A: Increased ET | Test B: Wildfire Cycle | Test C: Doubled Precip | Test D: 50% Precip | Test E: Compressed Precip |
|--|-----------------------|----------------------|------------------------|------------------------|--------------------|---------------------------|
| Plane of zero flux depth [m] | 9.2 m | 35.9 m | 10.3 m | 1.8 m | 37.6 m | 8.9 m |
| Actual surface flux (Precip- ET_{pot}) [cm] | 2416.1 | 1466.2 | 2698.0 | 5266.4 | 1042.4 | 2378.2 |
| Plant uptake [cm] | 2390.0 | 1468.5 | 1739.7 | 2350.3 | 1045.8 | 2332.0 |
| Bottom flux [cm] | 36.9 | 7.9 | 962.5 | 2920.4 | 7.9 | 58.1 |
| Net flux (- indicates outflow) [$mm\ yr^{-1}$] | -0.3 | -0.3 | -0.1 | -0.1 | -0.3 | -0.01 |
| Water in profile [cm] | 2598.5 | 2241.2 | 3071.4 | 3337.9 | 2235.1 | 2737.1 |
| Change in soil water storage relative to Base Case [%] | - | -13.8% | +18.2% | +28.5% | -14.0% | +5.33% |
| Absolute water balance error [cm] | 12.0 | 10.9 | 4.9 | 5.8 | 11.7 | 28.2 |
| Relative water balance error [%] | 0.16% | 0.17% | 0.07% | 0.04% | 0.33% | 0.39% |

Note: Absolute error is not related to the water volume in the flow domain, but instead to the sum of maximum change in water content and the sum of all boundary fluxes (Simunek et al., 1995).

Phase II Future Case Results

Future cases developed in Chapter 3 and listed in Table 3.1 are summarized below in Table 4.3. A schematic of scenario pathways, relation to the timeline, simulation times and observational points is presented in Figure 4.6. For all cases, findings are compared at the end of the ~350-year climate cycle (ending on August 31).

| | Timing (Years After Present) | Description | Total Ground Cover | Ave Annual Precip (mm yr ⁻¹) | Average Annual Temp (°C) | Total Ground Cover |
|---------|------------------------------|--------------------|--------------------|--|--------------------------|--------------------|
| Case 1. | 0 | Present Conditions | 20.3% | 112 | 18.6 | 20.3% |
| Case 2. | +100 yrs | Warmer/ wetter | 37.5% | 134 | 23.9 | 37.5% |
| Case 3. | +100 yrs | Warmer/ wetter | 23.2% | 128 | 21.3 | 23.2% |
| Case 4. | +300 yrs | Warmer/ drier | 9.2% | 97 | 21.4 | 9.2% |
| Case 5. | +300 yrs | Warmer/ drier | 0% | 97 | 21.4 | 0% |
| Case 6. | +300 yrs | Warmer/ wetter | 25.5% | 186 | 20.5 | 25.5% |
| Case 7. | +1000 yrs | Cooler/ wetter | 49.1% | 236 | 17.7 | 49.1% |
| Case 8. | +1000 yrs | Cooler/ wetter | 55.0% | 257 | 16.1 | 55.0% |

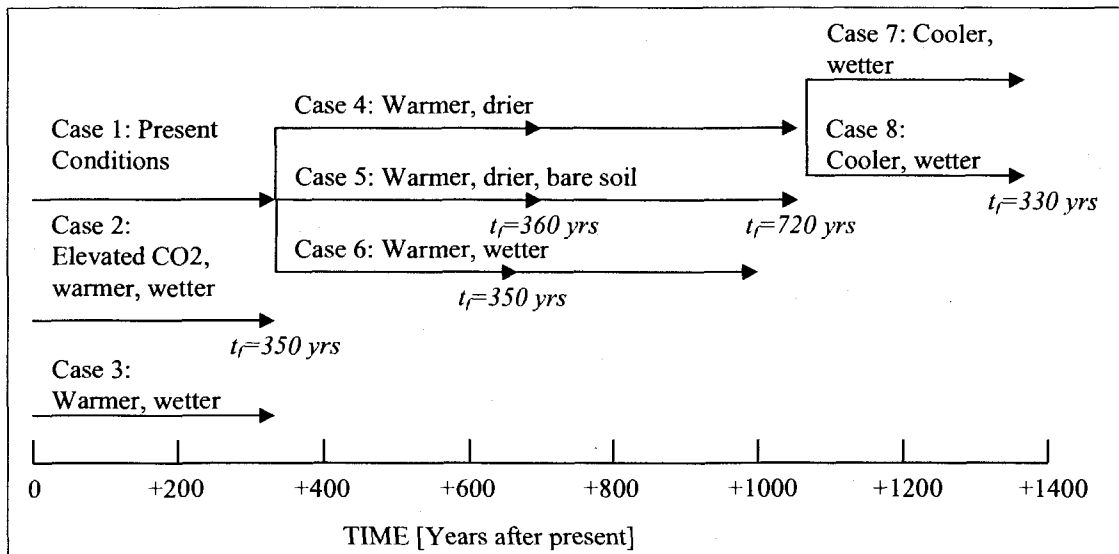


Figure 4.6. Timeline for Cases 1-8. Arrows indicate case observation points. Initial conditions are obtained from the preceding run. Initial conditions for Cases 1-3 are from the paleomodel Base Case outputs.

Present Conditions: Case 1

Case 1 is stepped forward from the Paleomodel Base Case under current climate and vegetation conditions to provide a reference for other future cases. Conditions have reached steady state, thus results are nearly identical to the Paleomodel Base Case detailed above.

+100 Years: Cases 2-3

At the +100 year time step, the elevated carbon dioxide scenario (Case 2) shows the development of a slight bulge of increased head from the base of the root zone to around 20 m depth, in response to the 16% increase in average annual precipitation (Figure 4.7). Interestingly, Case 3 having only a 13% increase in precipitation demonstrated a stronger response to the available water, with heads becoming less negative to a depth of 120 m. This indicates a response to the change in vegetation between these two scenarios; Case 2 has a total 38% ground cover, compared to 23% in Case 3. It is possible that the difference in uptake by vegetation cover and distribution has crossed some threshold whereby all available soil moisture is removed by plants, preventing deep percolation observed in Case 3, from occurring in Case 2. This is reflected in the water balance for Cases 2 and 3 (Table 4.4). For the +100 year scenario, Case 2 demonstrates an overall slight reduction in water storage of -0.37% at the end of the simulation period relative to current conditions, in response to the higher vegetation uptake, in spite of the 13% increase in precipitation. Case 3 shows an increase of +30.19% in water storage during the same period in response to the 16% increase in precipitation under vegetation cover that is similar to Case 1. Net upward flux for Case 2 is -1.9 mm yr^{-1} out of the profile, compared to the Case 3 downward flux of $+18.0 \text{ mm yr}^{-1}$ into the profile over the 350-year simulation period.

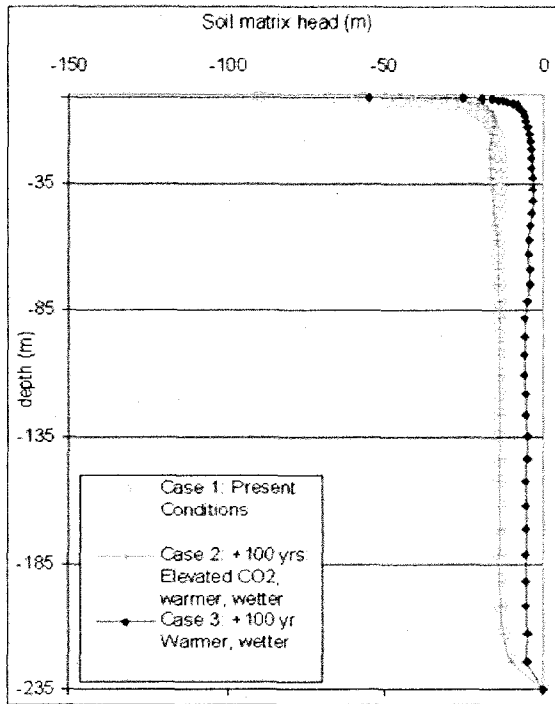


Figure 4.7a

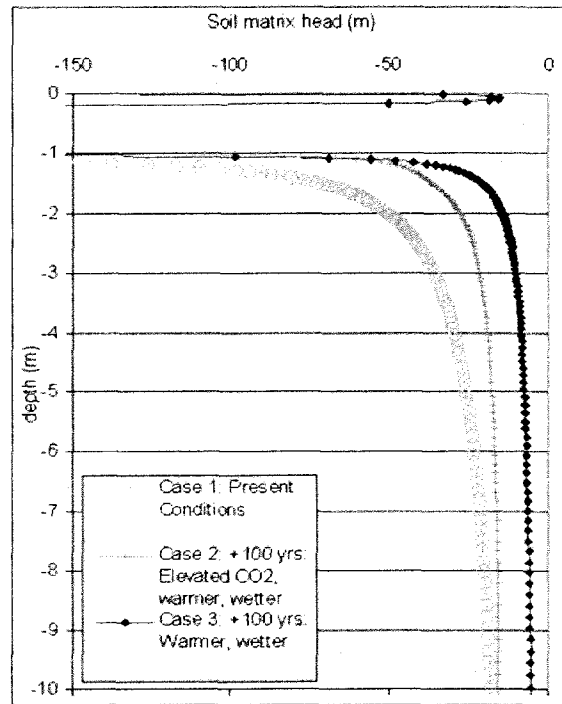


Figure 4.7b

Figure 4.7. Simulated Soil Matrix Head for Cases 1-3, +100 Years. (a) entire soil profile; (b) upper 10 meters.

| | Case 1 | Case 2 | | | Case 3 | | |
|---|--------|--------|--------|--------|--------|---------|---------|
| | t=350 | t=100 | t=180 | t=350 | t=100 | t=180 | t=350 |
| Time [years after present] | | | | | | | |
| Actual surface flux (Precip- ET_{pot}) [cm] | 2416.1 | 842.8 | 1498.0 | 2840.1 | 901.1 | 1644.0 | 3199.1 |
| Plant uptake [cm] | 2390.0 | 852.2 | 1510.8 | 2867.9 | 694.5 | 1255.4 | 2479.2 |
| Bottom flux [cm] | 36.9 | 10.6 | 19.2 | 37.4 | 10.7 | 19.0 | 70.5 |
| Net flux (-ve indicates outflow) [$mm\ yr^{-1}$] | -0.3 | -2.0 | -1.8 | -1.9 | +19.6 | +20.5 | +18.0 |
| Water in profile [cm] | 2598.5 | 2597.1 | 2598.4 | 2588.9 | 2802.8 | 2983.3 | 3383.0 |
| Change in soil water storage relative to Case 1 [%] | - | -0.05% | 0% | -0.37% | +7.86% | +14.81% | +30.19% |
| Absolute water balance error [cm] | 12.0 | 18.7 | 32.2 | 56.7 | 9.3 | 16.3 | 24.5 |
| Relative water balance error [%] | 0.16% | 0.74% | 0.71% | 0.66% | 0.40% | 0.39% | 0.30% |

Note: Absolute error is not related to the water volume in the flow domain, but instead to the sum of maximum change in water content and the sum of all boundary fluxes (Simunek et al., 1995).

The difference in availability of soil water in the profile between Cases 2 and 3 is evident in the simulated volumetric water contents (Figure 4.8), where the propagation of the wetting front to a depth of 87 m is visible in Case 3. The bulge in increased water content in the upper 18 cm of the soil profile is a result of a precipitation events 3 and 4 days immediately prior to the end of the simulation. The higher water contents are reflected in the flux profiles for Cases 2 and 3 (Figure 4.9), where high water contents in Case 2 result in less flux in high gradient zones as a result of reduced hydraulic conductivity as compared to increased fluxes in Case 3. The plane of zero flux is located at 5.2 m for Case 2 and 4.4 m for Case 3, demonstrating the plant uptake zone of influence of plant uptake is deeper in Case 2.

Slight variations within each case at $t = 100$ yrs, $t = 180$ years and $t = 360$ years are a result of differences in time-dependant boundary conditions in the ~350-year climate cycle.

+300 Years: Cases 4-6

At the +300 year time step, differences in Cases 4 and 5 (Case 4 = 9% vegetation cover, Case 5 = bare soil, identical climatic conditions) clearly show the impact of vegetation on soil water pressure heads (Figure 4.10). Case 4, which considers the effect of low vegetation cover under dry conditions, demonstrates the characteristic negative soil water heads associated with the root water uptake, with a zone of slightly less negative head and water content at the base of the root zone (from 1 to 4 m depth). Below the plane of zero flux at 3.8 m, soil water begins to percolate downward toward the water table. Flux for Case 4 is -0.7 mm yr^{-1} out of the profile, resulting in a decrease in soil water storage of -0.42% relative to current conditions represented in Case 1 (Table 4.5).

Case 5 is the wettest of the +300 year cases through the entire profile with heads averaging -5 m through $12 - 190 \text{ m}$. The effect of evaporation is dampened at 20 cm . A zone of slightly higher potentials and water content has developed at depths from 20 cm to 8.5 m below ground surface, demonstrating deep percolation in the absence of active root up-

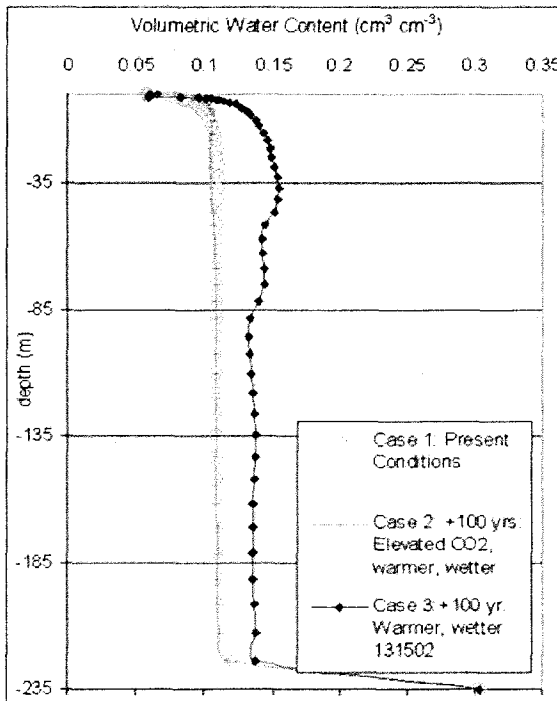


Figure 4.8a

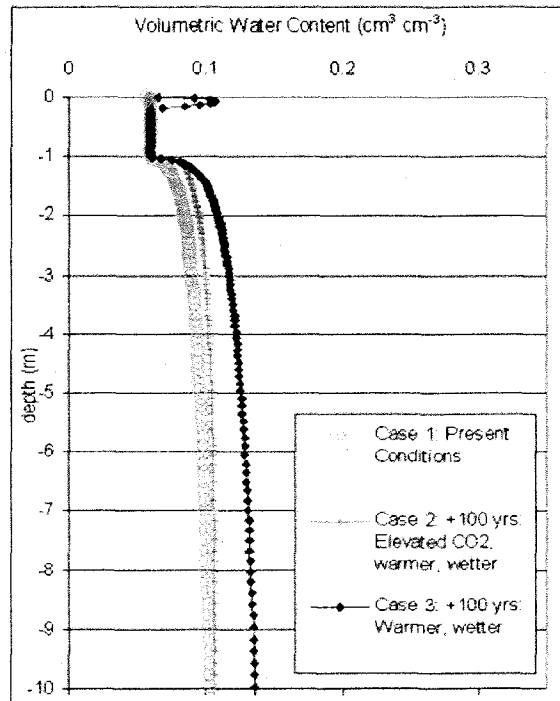


Figure 4.8b

Figure 4.8. Simulated Volumetric Water Content for Cases 1-3, +100 Years. (a) entire soil profile; (b) upper 10 meters.

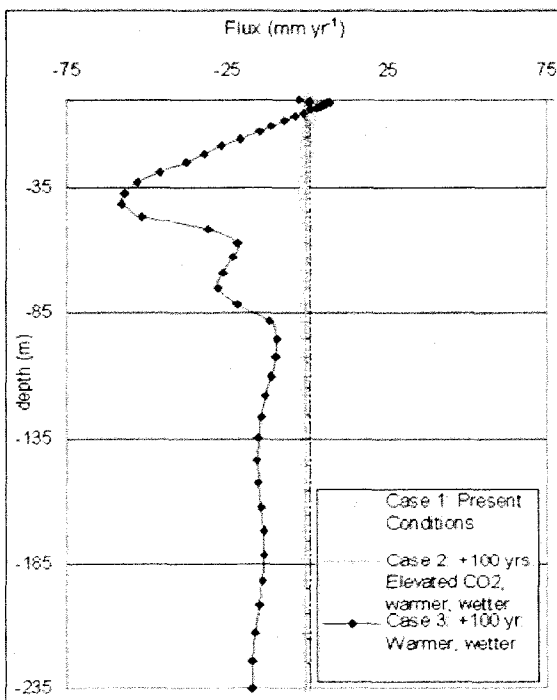


Figure 4.9a

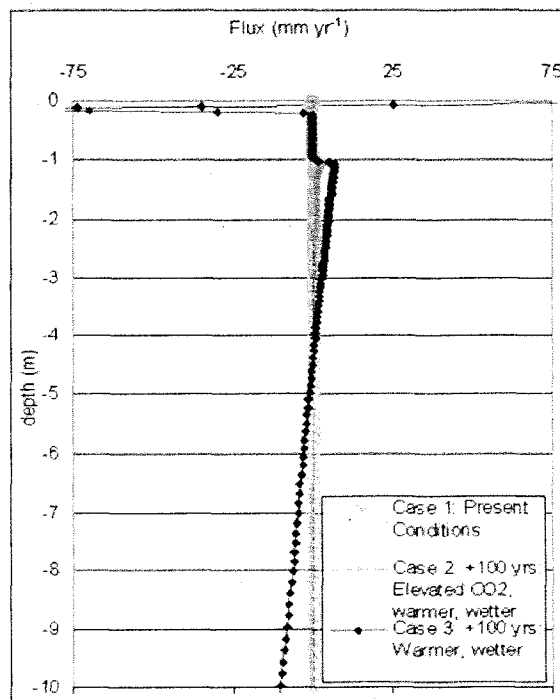


Figure 4.9b

Figure 4.9. Simulated Flux for Cases 1-3, +100 Years. (a) entire soil profile; (b) upper 10 meters.

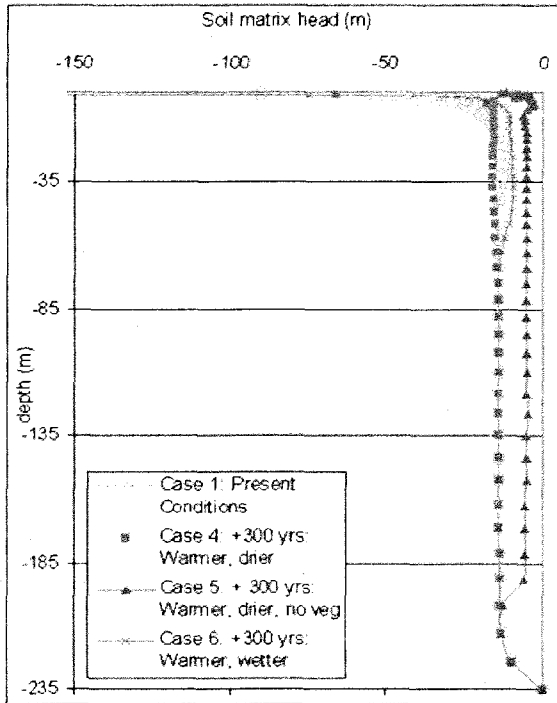


Figure 4.10a

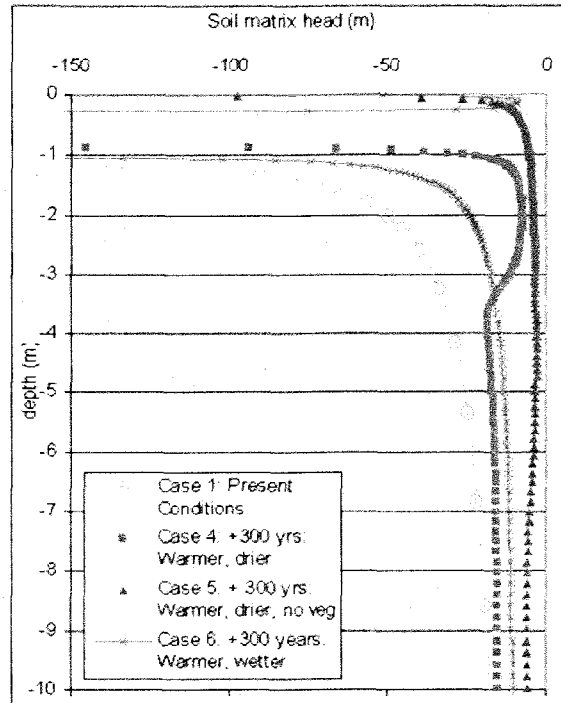


Figure 4.10b

Figure 4.10. Simulated Soil Matrix Head for Cases 4-6, +300 Years. (a) entire soil profile; (b) upper 10 meters.

| | Case 1 | Case 4 | Case 4 | Case 5 | Case 5 | Case 6 | Case 6 |
|---|--------|--------|--------|---------|---------|--------|--------|
| Time [years after present] | t=350 | T=360 | t=720 | t=360 | t=720 | t=350 | t=700 |
| Actual surface flux (Precip- ET_{pot}) [cm] | 2416.1 | 2128.7 | 2128.5 | 620.8 | 309.8 | 3197.7 | 3197.5 |
| Plant uptake [cm] | 2390.0 | 2115.4 | 2124.7 | 0 | 0 | 3198.0 | 3204.1 |
| Bottom flux [cm] | 36.9 | 37.7 | 37.6 | 37.7 | 530.5 | 36.0 | 36.5 |
| Net Flux (-ve indicates outflow) [$mm\ yr^{-1}$] | -0.3 | -0.7 | -0.9 | +16.3 | +2.2 | -1.0 | -1.2 |
| Water in Profile (cm) | 2598.5 | 2587.6 | 2587.6 | 3186.2 | 3265.1 | 2654.3 | 2702.4 |
| Change in Soil Water Storage over Simulation Period (%) | - | -0.42% | -0.42% | +22.62% | +25.65% | +2.15% | +4.0% |
| Absolute Water Balance Error [cm] | 12.0 | 22.7 | 22.7 | 4.1 | 0.2 | 93.7 | 93.3 |
| Relative Water Balance Error [%] | 0.16% | 0.35% | 0.35% | 0.07% | 0.00% | 0.93% | 0.92% |

take. It is notable that, although Case 6 is the wettest climate condition tested (annual precipitation of 128 mm yr^{-1} versus 97 mm yr^{-1} for Cases 4 and 5), the soil profile is drier than the Case 5 in terms of water content (Figure 4.11), with higher heads throughout the entire profile depth. This supports findings of others (Gee et al., 1994) that without plants, percolation will occur regardless of precipitation amount.

Case 6 results indicate root water uptake exceeds influx from precipitation, and net flux of -1.2 mm yr^{-1} indicates water is leaving the profile, yet stored water in the profile increases by $+2.15\%$. This implies that periodic percolation below the root zone is taking place in response to the higher precipitation events associated with this wetter climate; this is the only case where soil water increases are observed under net drying conditions.

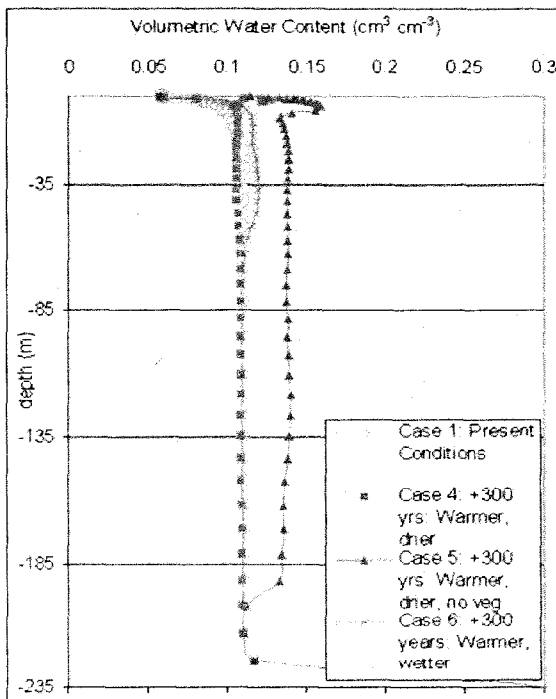


Figure 4.11a

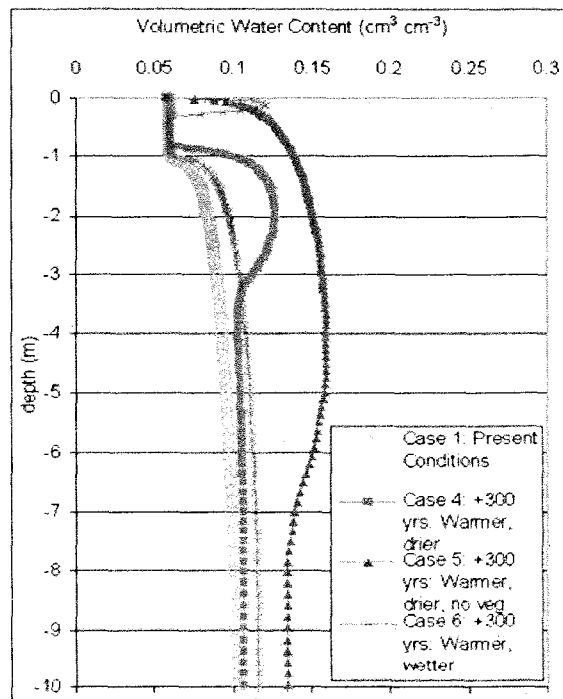


Figure 4.11b

Figure 4.11. Simulated Volumetric Water Content for Cases 4-6, +300 Years. (a) entire soil profile; (b) upper 10 meters.

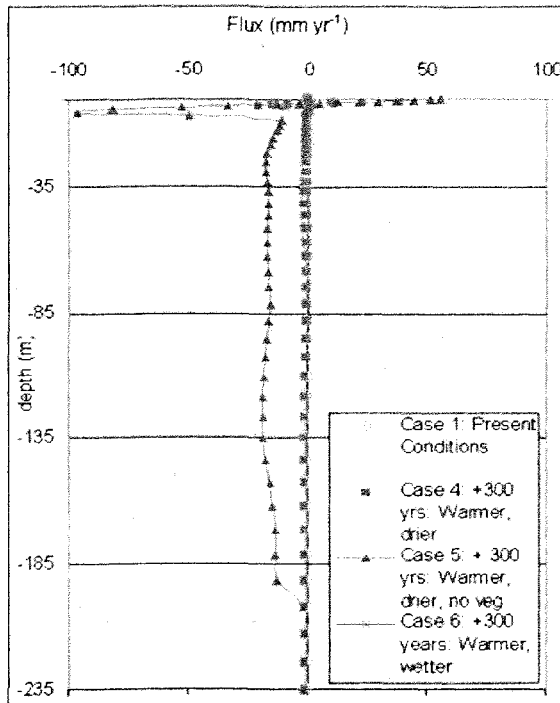


Figure 4.12a

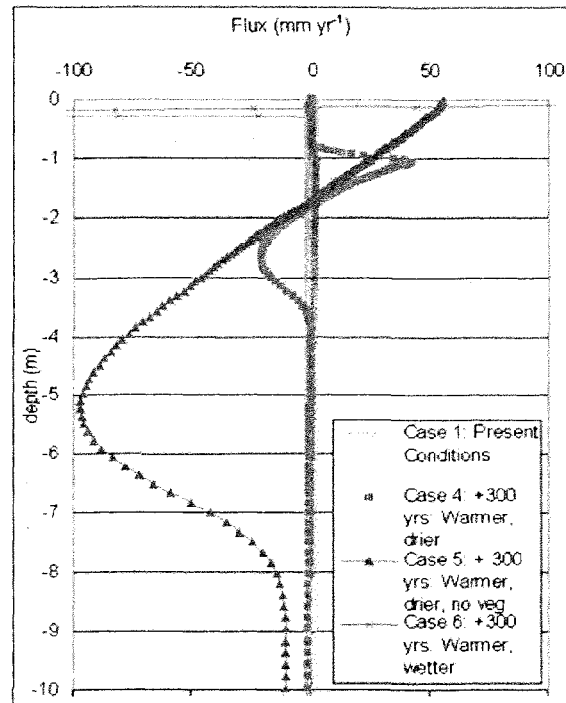


Figure 4.12b

Figure 4.12. Simulated Flux for Cases 4-6, +300 Years. (a) entire soil profile; (b) upper 10 meters.

+1000 years: Cases 7-8

Of all the cases presented, Cases 7 and 8 have the highest (least negative) pressure heads and highest water contents in the deep vadose zone (Figures 4.13 and 4.14). The most notable difference in the near-surface environment is the extension of the root zone as a result of expanding the biome to include deeper rooting vegetation in Case 8, resulting in more negative heads to a depth of 7 m. Though the top 1 m of the rooting zone is by far the largest proportion of root biomass, an increase in head is observed from depths of 0 to 40 cm. When taken in context with the water content, soil water appears to reach the upper 40 cm of the profile in response to the elevated precipitation rates.

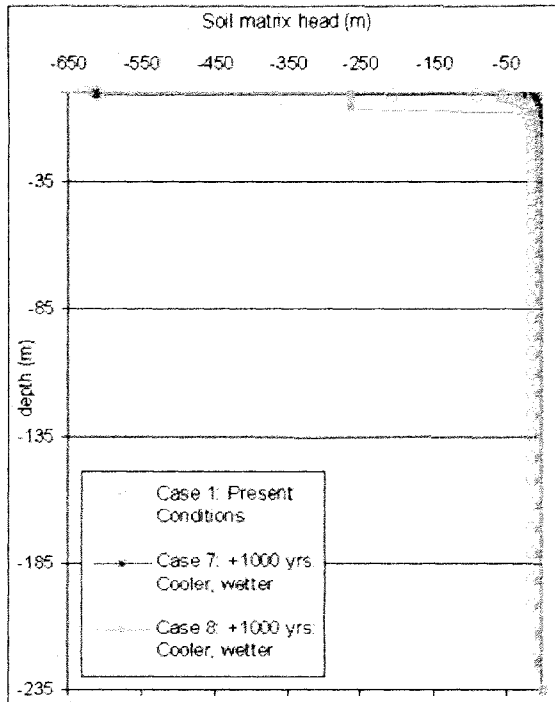


Figure 4.13a

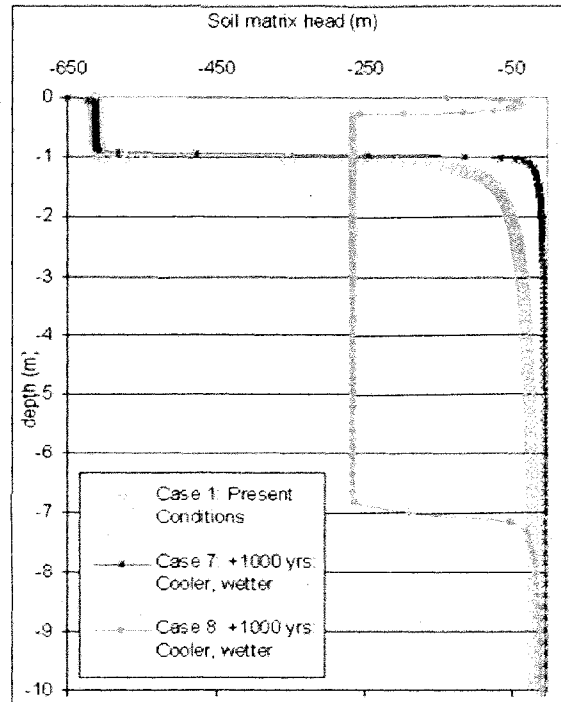


Figure 4.13b

Figure 4.13. Simulated Soil Matrix Head for Cases 7-8, +1000 Years. (a) Soil moisture head for entire soil profile; (b) soil moisture head for upper 10 meters.

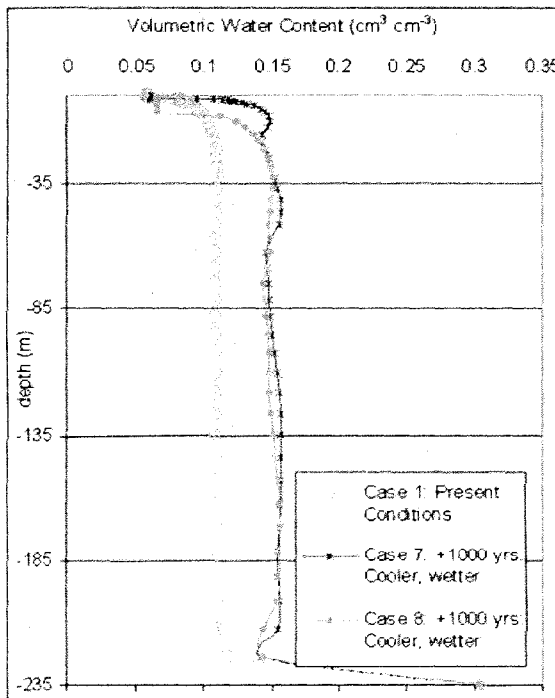


Figure 4.14a

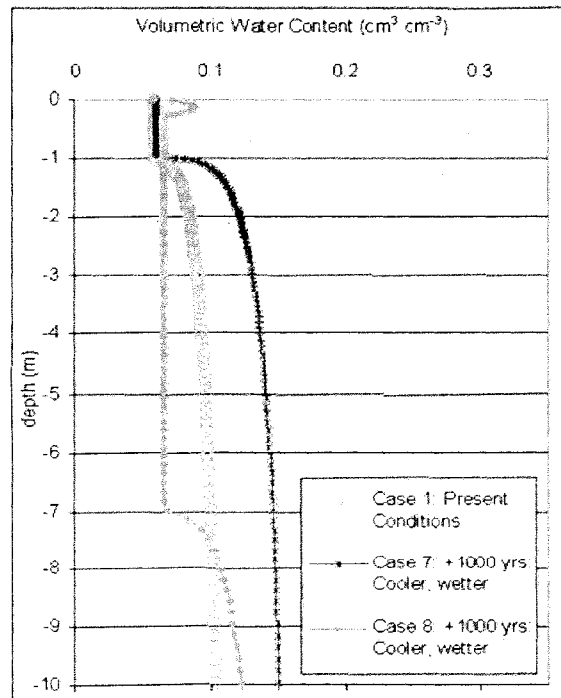


Figure 4.14b

Figure 4.14. Simulated Volumetric Water Content for Cases 7-8, +1000 Years. (a) volumetric water content for entire soil profile; (d) volumetric water content for upper 10 meters.

Both Cases 7 and 8 demonstrate an overall positive flux, indicating net water flow is into the column over the duration of the simulation, with fluxes of +27.7 and +25.6 mm yr⁻¹, respectively (Table 4.6). Change in soil water storage compared to current conditions is +37.7% and +24.7%. Flux profiles demonstrate the plane of no flux is located at 3.8 m depth in Case 7 and 10.8 m in Case 8 (Figure 4.15).

| Table 4.6. Water Balance for Future Cases 7-8, +1000 Years | | | |
|--|--------|--------|---------|
| | Case 1 | Case 7 | Case 8 |
| Time [years after present] | t=350 | t=330 | t=330 |
| Actual surface flux (Precip- ET_{pot}) [cm] | 2416.1 | 5021.6 | 6999.9 |
| Plant uptake [cm] | 2390.0 | 4073.2 | 6033.8 |
| Bottom flux [cm] | 36.9 | 32.0 | 119.6 |
| Net Flux (-ve indicates outflow) [mm yr ⁻¹] | -0.3 | +27.7 | +25.6 |
| Water in Profile (cm) | 2598.5 | 3577.6 | 3457 |
| Change in Soil Water Storage over Simulation Period (%) | - | +37.68 | +24.668 |
| Absolute Water Balance Error [cm] | 12.0 | 75.5 | 24.7 |
| Relative Water Balance Error [%] | 0.16% | 0.57% | 0.16% |

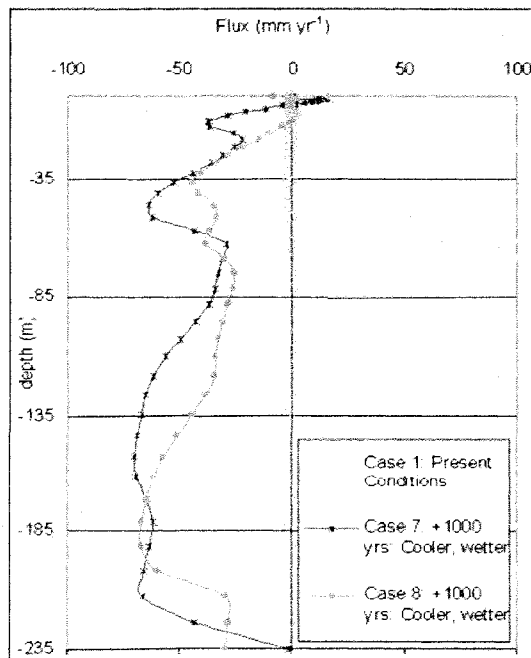


Figure 4.15a

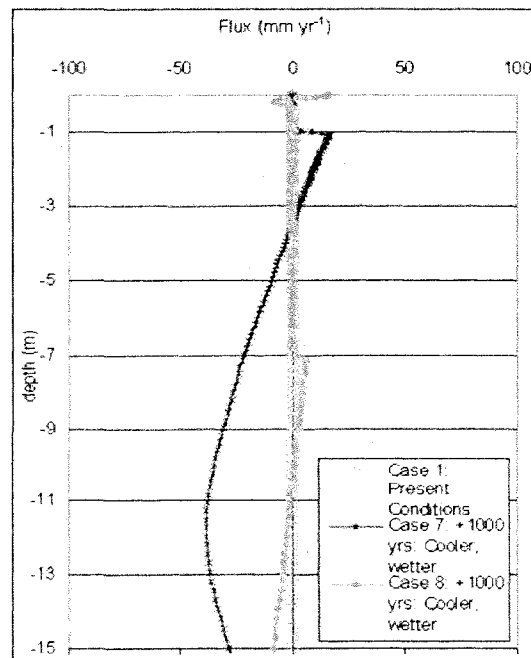


Figure 4.15b

Figure 4.15. Simulated Flux for Cases 7-8, +1000 Years. (a) entire soil profile; (b) upper 10 meters.

Model Validation and Performance

Fit of model outputs to observed field data for soil water pressure heads and volumetric water content is evaluated using Root Mean Square Error (RMSE) as a measure of variance between modeled results and field data. RMSE was calculated using the following equation (after Link et al., 1993):

$$RMSE = \sqrt{\left[\frac{\sum_{i=1}^n (X_{\text{modeled}} - X_{\text{observed}})_i^2}{n} \right]} \quad (3.8)$$

where X = the data point of interest (i.e. pressure head or water content) and n = number of observations.

Results for soil water pressure head and volumetric water content profiles for the paleoflow model (Base Case) and Case 1 show reasonably good agreement against observed soil water heads for the Area 5 PW wells (Bechtel Nevada, 2005b), with a Root Mean Square Error (RMSE) of 12 m for the PW-1 data set (Figure 4.16). Differences between the modeled profile and the field data are higher for the PW-2 and PW-3 data sets with a RMSE of 200 m for PW-2 and 149 m for PW-3 heads. The RMSE for all three wells is 118 m.

Though these error values seem high relative to the modeled heads, they are influenced by (1), the large head gradients in the profile (e.g., the transition from root zone to unit gradient) that exaggerate the difference between observed and modeled values in regions of rapid change, and (2), the large spread in the observed head data set. The descriptive statistics for the PW Wells field data listed in Table 4.7 indicate a wide range in values, with a coefficient of variance as high as 218% for the PW-3 well data set.

Simulated volumetric water content shows good agreement with the observed contents, with an RMSE of 0.03% for PW-1, 0.05% for PW-2, and 0.06% for PW-3. RMSE for all three wells is 0.04%, which is less than the precision of the reported water contents.

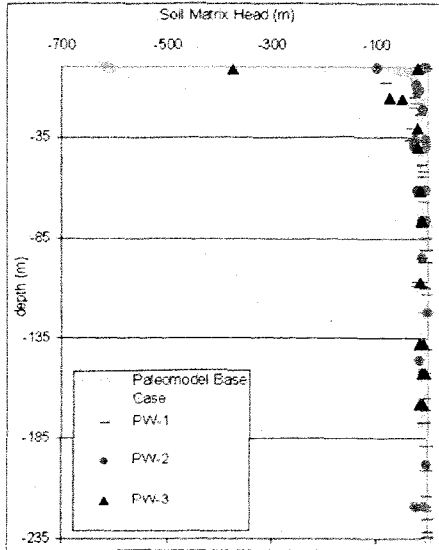


Figure 4.16a

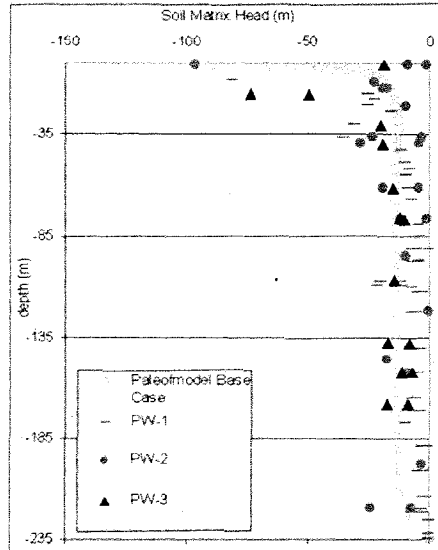


Figure 4.16b

Figure 4.16. Paleomodel Performance: Pilot Well Matrix Heads. (a) Simulated soil water head and field data to head = -700 m; (b) Simulated soil water head and field data to head = -150 m

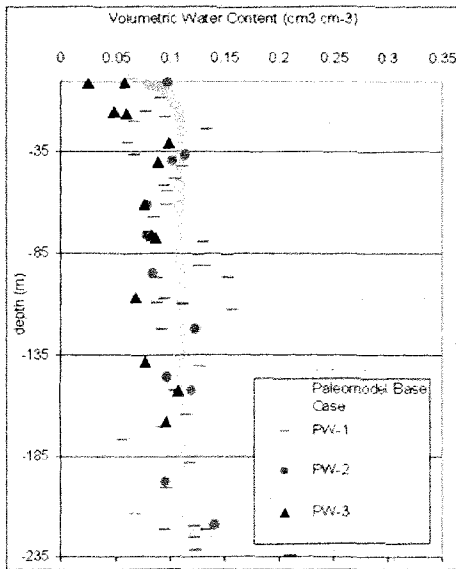


Figure 4.17. Paleomodel Performance: Pilot Well Volumetric Water Content

| Table 4.7. Descriptive Statistics for PW Wells Soil Water Head and Volumetric Water Content Data.* | | | | | |
|--|------------|----------|-----------|--------------------|------------------------------|
| | Minimum | Maximum | Mean | Standard Deviation | Coefficient of Variation [%] |
| PW-1 Head | -831.28 m | -0.31 m | -91.80 m | 124.43 m | 136.03 |
| PW-2 Head | -883.30 m | -3.06 m | -147.90 m | 177.48 m | 119.99 |
| PW-3 Head | -3822.88 m | -69.36 m | -398.81 m | 2230.18 m | 218.65 |
| PW-1 Content | 5.6% | 28.6% | 12.0% | 4.7% | 39.27% |
| PW-2 Content | 7.3% | 21.0% | 10.9% | 3.0% | 27.37% |
| PW-3 Content | 2.6% | 13.2% | 7.9% | 2.3% | 29.73% |

*Source: Bechtel Nevada, 2005b

The model stabilizes at approximately 35 years after initialization, based on the change in water balance as observed at a 5-year and 25-years intervals (Figure 4.17). The rate of change in stored water over the entire profile is a constant -0.12 cm yr^{-1} ($\pm 0.02 \text{ cm}$).

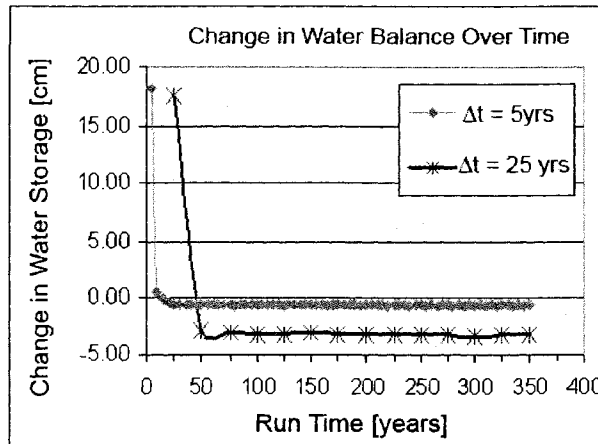


Figure 4.18. Model Performance Over Time. Changes to water stored in the profile are used to estimate simulation time to reach model equilibrium.

CHAPTER 5

CONCLUSIONS

Results from future case series demonstrate the importance of vegetation on the vadose zone flow system. Water balance findings indicate that certain combinations of vegetation and climate inputs will reverse the hydraulic gradient, as demonstrated by the net positive (downward) fluxes for the soil profile observed in Cases 3, 5, 7 and 8 (with corresponding values of $+18.0 \text{ mm yr}^{-1}$, $+16.3 \text{ mm yr}^{-1}$, $+27.8 \text{ mm yr}^{-1}$ and $+25.6 \text{ mm yr}^{-1}$, compared to net flux under current conditions of -0.03 mm yr^{-1}). These findings are supported by an increase in stored water volume of $+26\%$, $+23\%$, $+38\%$ and $+33\%$ relative to current conditions for each of the net infiltration cases.

Paleomodel treatments resulted in directional changes to the amount of soil water storage as would be expected. For example, increased vegetation cover in Test A and decreased precipitation in Test D resulted in less soil water storage compared to the Base Case, while reduced vegetation in Test B and increased precipitation in Test C resulted in more soil water storage compared to the Base Case. Though none of the treatments considered were sufficient to reverse net flux direction from upward to downward, the characteristics of the flow regime under wet tests B and C were significantly altered, as evidenced by the increase of downward water flux from the bottom boundary. Downward percolation to the water table becomes the dominant flow direction during periods of high moisture availability.

Though the current understanding of vadose zone flow at Area 5 of NTS is such that effects of individual environmental variables might be intuitively and qualitatively

describable, more complex interactions between climate, vegetation, and their effects on water balance are more difficult to predict. In other words, while it is reasonable to expect that more precipitation will result in greater soil moisture availability, it is more difficult to anticipate how an increase in precipitation might alter the composition and amount of ground cover, which affects how much available moisture remains in the profile. This is illustrated by the +100 Year scenarios (Cases 2 and 3), both representing a warmer climate, higher precipitation rates and expanded vegetation. The greater expansion of vegetation in Case 2 results in evapotranspiration removing all of the available water, reducing the flux compared to both Cases 1 and 3. Although Case 3 received less rainfall than Case 2, the vegetation was insufficient to maintain the current upward flux, so percolation occurred below the root zone; thus, the hydraulic gradient was reversed.

Reversal of the hydraulic gradient in Case 5, representing a warmer, much drier climate with bare soil, is attributable to the lack of root water uptake. Cases 7 and 8 both result in reversal of the hydraulic gradient as greater precipitation exceeds evapotranspiration, in spite of the expanded vegetation cover of 49% and 55%. In Case 8, water content has increased through the entire depth and drainage to the water table takes place.

Taken together, the future case findings show that changes associated with future climate scenarios can impact the hydrologic system in sometimes unanticipated ways by variably emphasizing the importance of different processes. This affect is enhanced by the fact that current conditions are extremely arid and fluxes are so low that the threshold for reversal can be crossed under conceivable future climate states.

Though the approaches used here to attempt to capture the possible environmental conditions were not strictly predictive in nature, and neglect some of the feedbacks inherent in complex climate-plant-soil systems such as soil temperature effects on atmospheric inputs, seasonal growth patterns, and plant community dynamics, they did successfully result in a

methodology for testing coupled environmental variables. The bioclimatic analogs developed and implemented in this study are appropriate for the intent of this work.

Simulations developed in this work incorporate the salient features of the conceptual model employed and verified elsewhere (Walvoord et al., 2002, 2004; Scanlon et al., 2003; Yin et al., 2008), including pressure head and water content responses to vegetation, upward fluxes in the near surface, and higher constant heads at depth. Some of the results developed in this study differed from the findings of others. For example, the prediction of the plane of zero flux at 9.8-m depth in the Paleomodel Base Case underestimates the depth of the zone of upward flux reported by others; Scanlon et al. (2004) modeled it at 38-m depth for the 13,000 year run, Kwicklis et al. (2006) modeled it at 65-m depth, and Bechtel Nevada (2005c) reported it at 40-m depth. Differences in the depth to the plane of zero flux might be attributed to the use of a fixed matric potential to represent the root zone, as opposed to the distributed transpiration explicitly accounted for in this work, where it was placed at a lower point in the profile. The studies referenced above implemented the fixed sink term at a depth of 2 m, as opposed to the 1.2 m depth of root zone employed here.

Generally, the high level of flux response to the potential range of climatic conditions, even on fairly short (e.g. centurial) time scales, render the use of a conceptual fixed no-flux boundary condition to any point in the profile inappropriate. To date, Area 5 modeling efforts that previously employed a fixed no-flux condition (Catlett et al., 2003; Neptune and Co, 2003) have been revised.

The findings of this work emphasize the importance of vegetation, represented in the model as daily potential transpiration and evaporation, on the behavior of the hydrologic system. The parameters used to calculate E_{pot} and T_{pot} values can be difficult to quantify at the field scale, and oftentimes a great deal of variability exists in literature-reported values for any particular species. For example, reported leaf area index (LAI) for *Coleogyne*

ramosissima include 0.02 in Schwinning et al.(2002) and 1.35 in Smith et al. (1995); this two order of magnitude difference in LAI results in a maximum reduction of potential transpiration of 0.12 cm for an LAI = 0.02 (assuming 17% shrub coverage), equivalent to a decrease in root water uptake of greater than 10% when using the value reported by Schwinning et al. (2002). Because arid systems, like at this study site, are sensitive to small changes in water content, the effects of uncertainty in plant descriptive parameters could have an impact on simulated results. This emphasizes the importance of strong representative parameters to describe vegetation profiles.

Future Work

This work relies heavily on the use of proxy sites and data sets for future scenarios, which assumes that future conditions can be determined by present or past conditions. How anthropogenically driven climate change might alter the use of past climate conditions to predict future climate is uncertain. The use of historical analog climate data does not address the potential for increased frequency of extreme hydrologic events resulting from elevated atmospheric CO₂ (Kim, 2005). It has been shown that extreme events can impact this flow system (Yin et al., 2008), and future work should incorporate large storms for comparison.

New research on plant community response to elevated atmospheric CO₂ indicates that responses are both structural (Obrist and Arnone, 2003) and behavioral (Hamerlynck et al., 2000), and can depend on a several interrelated factors including plant functional type, species, water availability and water use efficiency (Hamerlynck et al., 2000; Housman et al., 2006; Bradley and Fleishman, 2008), making it difficult to predict how future plant communities might develop over time. The approaches used in this work to incorporate the effects of CO₂ on plant development as done in Case 2 (application of productivity ratios to existing biome compositions) and Case 3 (use of nearby representative compositions based

on expected climate descriptors) are simplified. Future work at predictive modeling should seek to incorporate research focusing on new biome development and migration (Prentice et al., 1992; Kirilenko and Solomon, 1998; Melillo et al., 1993).

Additionally, this work does not account for seasonal variability in plant activity levels. This could be taken into account by simulating altered root distribution according to functional type at the appropriate time, and is recommended for future work. Inclusion of isotopic and chloride profiles could strengthen the ability to validate the model to observed data sets, as much existing research has been devoted to the use of environmental tracer data in this region.

APPENDIX I

COMPUTER CODE

```
program ETrefTav
implicit none
!
!Program written 1/15/06 by Amanda Brandt to read DRA rad files and
!extract parameters for use in calculating potential evapotranspiration
!using the Penman-Monteith method (Allen et al., 1998).

!Modified 6/11/08 to include Hargreaves and Allen PET calc for
!comparison purposes. Changed output to cm.
!
integer,parameter::nlines=3435
integer,parameter::un_radin=21,un_radout=26,un_fnamein=31
integer j,jcount,i,icount
!
character*80 station_name
character*80 filepath
!
integer year,month,day,jday,elevation,version
integer minute(nlines),hour(nlines)
real,parameter::seconds=0.864E5
real,parameter::mjfactor=1E-6
!
real latitude,longitude,dt(nlines),zen(nlines),direct(nlines)
real dw_psp(nlines),uw_psp(nlines)
real diffuse(nlines),dw_pir(nlines),dw_casetemp(nlines)
real dw_dometemp(nlines),uw_pir(nlines),uw_casetemp(nlines)
real uw_dometemp(nlines),uvb(nlines),par(nlines)
real netsolar(nlines),netir(nlines),totalnet(nlines)
real temp(nlines),rh(nlines),windspeed(nlines)
real winddir(nlines),pressure(nlines)
real dailynetsum_w,avedailynet_mj
!
integer qc_direct(nlines),qc_netsolar(nlines),qc_netir(nlines)
integer qc_dwpsp(nlines),qc_uwpsp(nlines),qc_diffuse(nlines)
integer qc_dwpir(nlines),qc_dw_casetemp(nlines)
integer qc_dw_dometemp(nlines),qc_uwpir(nlines)
integer qc_uw_casetemp(nlines),qc_uw_dometemp(nlines)
integer qc_uvbnlines),qc_parnlines)
integer qc_totalnet(nlines),qc_temp(nlines)
integer qc_rh(nlines),qc_windspeed(nlines),qc_winddir(nlines)
```

```

integer qc_pressure(nlines)
!
real tempmax,tempmin,rhmax,rhmin,avewspd,avewspd2
real VPmin,VPmax,VPsat,VPactual,VPCslope,psyccon
real pave,tempave,ETref,dailypsum,dailywspdsum
real ETrefnum,ETrefden,Kc,ETcrop,ETrefHarg
real transp,evap
real meantemp, dailytempsum
integer averadcount,avewspdcount,avepcount, avetempcount
!c
!THIS PROGRAM ALTERED ETref.f95 TO CALC MEAN TEMP*****
!c
open(unit=un_radout,file='c:/F/solarsum.dat',status='new')
!c
!c READ DATA FILE NAMES
open(unit=un_fnamein,file='c:/F/Data/radfiles.txt',status='old')
!c
jcount=0
do 20 j=1,3435,1
    read(un_fnamein,600)filepath
    600 format(a24)
    if (filepath.eq.'EOF')then
        print *, 'ALL RAD DATA FILES HAVE BEEN READ.'
        exit
    else
!        OPEN RAD DATA FILE
        open(UNIT=un_radin,file=filepath,status='old')
!c
!c READ DAILY RAD DATA FILE
        read(un_radin,100)station_name
    100 format(1x,a)
        read(un_radin,*)latitude,longitude,elevation
!c
        Kc=0.9
        icount=0
        avedaily_net_mj=0
        daily_net_sum_w=0
        averadcount=0
        tempmin=999
        tempmax=0
        meantemp=0
        avetempcount=0
        dailytempsum=0
        rhmax=0
        rhmin=999
        dailywspdsum=0
        avewspdcount=0
        avewspd=0
        avewspd2=0
        dailypsum=0
        avepcount=0
        VPmin=0
        VPmax=0
        VPsat=0
        VPactual=0
        tempave=0
        psyccon=0
    
```

```

ETref=0
ETrefHarg=0
ETrefnum=0
ETrefden=0
ETcrop=0
transp=0
evap=0
!
do 10 i=1,nlines
!c
    read(un_radin,300,end=400)year,jday,month,day,hour(i),&
    minute(i),dt(i),zen(i),dw_psp(i),qc_dwpsp(i),uw_psp(i),&
    qc_uwpsp(i),dirct(i),qc_direct(i),diffuse(i),&
    qc_diffuse(i),dw_pir(i),qc_dwpir(i),dw_casetemp(i),&
    qc_dw_casetemp(i),dw_domtemp(i),qc_dwdomtemp(i),&
    uw_pir(i),qc_uwpir(i),uw_casetemp(i),qc_uw_casetemp(i),&
    uw_domtemp(i),qc_uwdomtemp(i),uvb(i),qc_uvbi(i),&
    par(i),qc_par(i),netsolar(i),qc_netsolar(i),netir(i),&
    qc_netir(i),totalnet(i),qc_totalnet(i),temp(i),&
    qc_temp(i),rh(i),qc_rh(i),windspeed(i),qc_windspeed(i),&
    winddir(i),qc_winddir(i),pressure(i),qc_pressure(i)
300    format(1x,i4,1x,i3,4(1x,i2),1x,f6.3,1x,f6.2,&
    20(1x,f7.1,1x,i1))
!    Check validity of measurement, calc sum for NET RADIATION
    if (qc_totalnet(i).eq.0) then
        dailynetsum_w=dailynetsum_w+totalnet(i)
        averadcount=averadcount+1
    endif
!
!    Check temp for max and min, record associated rh for Tmax and Tmin
    if (qc_temp(i).eq.0) then
        if (temp(i).gt.tempmax)then
            tempmax=temp(i)
            if(qc_rh(i).eq.0)then
                rhmax=rh(i)
            endif
        endif
        if (temp(i).lt.tempmin)then
            tempmin=temp(i)
            if(qc_rh(i).eq.0)then
                rhmin=rh(i)
            endif
        endif
        dailytempsum=dailytempsum+temp(i)
        avetempcount=avetempcount+1
    endif
!
!    Windspeed
    if (qc_windspeed(i).eq.0) then
        dailywspdsum=dailywspdsum+windspeed(i)
        avewspdcount=avewspdcount+1
    endif
!    Pressure
    if (qc_pressure(i).eq.0)then
        dailypsum=dailypsum+pressure(i)
        avepcount=avepcount+1
    endif

```



```

!
      icount=icount+1   !line read counter
10    continue
400  print *,filepath,icount,' records read'
!    END OF DAY PROCEDURES
!    Check to see if any rad records were contained in the daily file
!    then calculate ave net radiation and write to file SOLARSUM.DAT
      if (averadcount.ne.0) then
          avedaily_net_mj=daily_netsum_w/averadcount*seconds*mjfactor
!         average net radiation [MJ/m2/day] = average W/m2 *86400
!         sec/day * 10^-6 MJ/J
      end if
!    Average daily windspeed
      if (avewspdcount.ne.0)then
          avewspd=dailywspdsum/avewspdcount
          avewspd2=avewspd*0.748 !convert 10m windspeed to 2m
      endif
      if (avepcount.ne.0)then
          pave=daily_psum/avepcount
      endif
!    MEAN temperature
      if (avetempcount.ne.0)then
          meantemp=dailytempsum/avetempcount
      endif
!    Actual vapor pressure (ea) from RH data
      VPmin=0.6108*exp((17.27*tempmin)/(tempmin+237.3))
      VPmax=0.6108*exp((17.27*tempmax)/(tempmax+237.3))
      VPsat=(VPmin+VPmax)/2.
      VPactual=((VPmin*rhmax/100)+(VPmax*rhmin/100))/2.
      tempave=(tempmax+tempmin)/2.
      VPCslope=(4098.*(0.6108*exp((17.27*tempave)/&
&(tempave+237.3))))/(tempave+237.3)**2
!    psychrometric constant - convert P from mbar to kPa
      psycon=0.665E-3*pave*0.1
!    Calculate ETo using Penman-Monteith
      ETrefnum=(0.408*VPCslope*avedaily_net_mj)+((psycon*900)/&
&(tempave+273))
      ETrefden=VPCslope+(psycon*(1+0.34*avewspd2))
      ETref=((ETrefnum*avewspd2*(VPsat-VPactual))/ETrefden)*0.1
!    ETref is output in mm/day, converted to cm/day for HYDRUS input
!    Calculate ETo using Hargreaves
      ETrefHarg=0.0135*(meantemp+17.78)*avedaily_net_mj*(238.8/&
&(595.5-(0.55*meantemp)))
!    Write output file
      write(un_radout,500)month,day,year,jday,ETref,ETcrop,meantemp,&
&ETrefHarg
500  format(i2,'/',i2,'/',i4,i5,f14.8,f14.8,f14.8,f14.8,f14.8,f14.8)
      end if !End of file check IFTHEN statement
!c
      jcount=jcount+1
20    continue
End

```

```

program ETrefCO2
implicit none
!
!Program to read input data from DRA daily atmospheric rad
!data (from SURFRAD network instrumentation), calculate daily
!means and totals, and use these inputs to develop a daily
!reference ET using the Penman-Monteith equation.
!Amanda Brandt, 3/4/06
!
!Modified to adjust atmospheric data according to predictive factors
!for a doubled CO2 climate scenario based on CMM climate model outputs.
!
!Modified 6/11/08 to include Hargreaves and Allen PET calc for
!comparison purposes. Removed ET partitioning and Kc info. Changed ETo
output to cm.
!
integer,parameter::nlines=3435
integer,parameter::un_radin=21,un_radout=26,un_fnamein=31
integer j,jcount,i,icount
!
character*80 station_name
character*80 filepath
!
integer year,month,day,jday,elevation,version
integer minute(nlines),hour(nlines)
real,parameter::seconds=0.864E5
real,parameter::mjfactor=1E-6
!
real latitude,longitude,dt(nlines),zen(nlines),dirct(nlines)
real dw_psp(nlines),uw_psp(nlines)
real diffuse(nlines),dw_pir(nlines),dw_casetemp(nlines)
real dw_dometemp(nlines),uw_pir(nlines),uw_casetemp(nlines)
real uw_dometemp(nlines),uvb(nlines),par(nlines)
real netsolar(nlines),netir(nlines),totalnet(nlines)
real temp(nlines),rh(nlines),windspeed(nlines)
real winddir(nlines),pressure(nlines)
real dailynetsum_w,avedailynet_mj
!
integer qc_direct(nlines),qc_netsolar(nlines),qc_netir(nlines)
integer qc_dwpsp(nlines),qc_uwpsp(nlines),qc_diffuse(nlines)
integer qc_dwpir(nlines),qc_dw_casetemp(nlines)
integer qc_dwdometemp(nlines),qc_uwpir(nlines)
integer qc_uw_casetemp(nlines),qc_uwdometemp(nlines)
integer qc_uvbnlines),qc_parnlines)
integer qc_totalnet(nlines),qc_temp(nlines)
integer qc_rh(nlines),qc_windspeed(nlines),qc_winddir(nlines)
integer qc_pressure(nlines)
!
real tempmax,tempmin,rhmax,rhmin,avewspd,avewspd2
real VPmin,VPmax,VPsat,VPactual,VPCslope,psycon
real pave,tempave,ETref,dailypsum,dailywspdsum
real ETrefnum,ETrefden,ETrefHarg
real meantemp,dailytempsum

```

```

real  srad_co2,temp_co2,ws_co2
integer  averadcount,avewspdcount,avepcount, avetempcount
!c
!THIS PROGRAM ALTERED ETref.f95 TO CALC MEAN TEMP*****
!c
open(unit=un_radout,file='c:/F/solarsum.dat',status='new')
!c
!c  READ DATA FILE NAMES
open(unit=un_fnamein,file='c:/F/Data/radfiles.txt',status='old')
!c
jcount=0
do 20 j=1,3435,1
  read(un_fnamein,600)filepath
  600  format(a24)
  if (filepath.eq.'EOF')then
    print *,'ALL RAD DATA FILES HAVE BEEN READ.'
    exit
  else
!    OPEN RAD DATA FILE
    open(UNIT=un_radin,file=filepath,status='old')
!c
!c  READ DAILY RAD DATA FILE
    read(un_radin,100)station_name
  100  format(lx,a)
    read(un_radin,*)latitude,longitude,elevation
!c
    icount=0
    avedailynet_mj=0
    dailynetsum_w=0
    averadcount=0
    tempmin=999
    tempmax=0
    meantemp=0
    avetempcount=0
    dailytempsum=0
    rhmax=0
    rhmin=999
    dailywspdsum=0
    avewspdcount=0
    avewspd=0
    avewspd2=0
    dailypsum=0
    avepcount=0
    VPmin=0
    VPmax=0
    VPsat=0
    VPactual=0
    tempave=0
    psycon=0
    ETref=0
    ETrefnum=0
    ETrefden=0
!
    srad_co2=1
    temp_co2=1
    ws_co2=1
!

```

```

do 10 i=1,nlines
!c
    read(un_radin,300,end=400)year,jday,month,day,hour(i),&
    minute(i),dt(i),zen(i),dw_psp(i),qc_dwpsp(i),uw_psp(i),&
    qc_uwpsp(i),dirct(i),qc_direct(i),diffuse(i),&
    qc_diffuse(i),dw_pir(i),qc_dwpir(i),dw_casetemp(i),&
    qc_dwcase temp(i),dw_dometemp(i),qc_dwdometemp(i),&
    uw_pir(i),qc_uwpir(i),uw_casetemp(i),qc_uwcase temp(i),&
    uw_dometemp(i),qc_uwdometemp(i),uvb(i),qc_uv b(i),&
    par(i),qc_par(i),netsolar(i),qc_netsolar(i),netir(i),&
    qc_netir(i),totalnet(i),qc_totalnet(i),temp(i),&
    qc_temp(i),rh(i),qc_rh(i),windspeed(i),qc_windspeed(i),&
    winddir(i),qc_winddir(i),pressure(i),qc_pressure(i)
300 format(1x,i4,1x,i3,4(1x,i2),1x,f6.3,1x,f6.2,&
    &20(1x,f7.1,1x,i1))
!
!
!
Select monthly scaling values for CO2x2 scenario based on
Julian Day
select case(day)
    case(1:31)
        srad_co2=0.991
        temp_co2=5.2
        ws_co2=1.025
    case(32:59)
        srad_co2=0.994
        temp_co2=5.5
        ws_co2=1.052
    case(60:90)
        srad_co2=0.948
        temp_co2=5.7
        ws_co2=0.794
    case(91:120)
        srad_co2=0.960
        temp_co2=4.5
        ws_co2=0.783
    case(121:151)
        srad_co2=0.00979
        temp_co2=4.3
        ws_co2=0.846
    case(152:181)
        srad_co2=0.947
        temp_co2=4.4
        ws_co2=0.938
    case(182:212)
        srad_co2=0.984
        temp_co2=3.7
        ws_co2=1.115
    case(213:243)
        srad_co2=0.998
        temp_co2=3.6
        ws_co2=0.958
    case(244:273)
        srad_co2=0.966
        temp_co2=3.6
        ws_co2=0.965
    case(274:304)
        srad_co2=1.003

```

```

        temp_co2=3.0
        ws_co2=1.208
    case(305:334)
        srad_co2=0.972
        temp_co2=3.1
        ws_co2=1.073
    case(335:366)
        srad_co2=0.990
        temp_co2=4.4
        ws_co2=1.029
    end select
!
!
!   Check validity of measurement, calc sum for NET RADIATION
if (qc_totalnet(i).eq.0) then
    dailynetsum_w=dailynetsum_w+totalnet(i)
    averadcount=averadcount+1
endif
!
!   Check temp for max and min, record associated rh for Tmax and
!   Tmin
!
if (qc_temp(i).eq.0) then
    if (temp(i).gt.tempmax)then
        tempmax=temp(i)+temp_co2 !scale Tmax for CO2scenario
        if(qc_rh(i).eq.0)then
            rhmax=rh(i)
        endif
    endif
    if (temp(i).lt.tempmin)then
        tempmin=temp(i)+temp_co2 !scale Tmin for CO2scenario
        if(qc_rh(i).eq.0)then
            rhmin=rh(i)
        endif
    endif
    dailytempsum=dailytempsum+temp(i)+temp_co2 !scale
!                                               Tmean for CO2 scenario
    avetempcount=avetempcount+1
endif
!
!   Windspeed
if (qc_windspeed(i).eq.0) then
    dailywspdsum=dailywspdsum+windspeed(i)*ws_co2 !scale
!                                               WS for CO2 scenario
    avewspdcount=avewspdcount+1
endif
!   Pressure
if (qc_pressure(i).eq.0)then
    dailypsum=dailypsum+pressure(i)
    avepcount= avepcount+1
endif
!
    icount=icount+1 !line read counter
10    continue
400  print *,filepath,icount,' records read'
!
!   END OF DAY PROCEDURES

```

```

! Check to see if any rad records were contained in the daily file
! then calculate average net radiation and write to file
! SOLARSUM.DAT
! if (averadcount.ne.0) then
!     avedailynet_mj=dailynetsum_w/averadcount*seconds*mjfactor
!     average net radiation [MJ/m2/day] = average W/m2 *86400
!     sec/day * 10^-6 MJ/J
!     avedailynet_mj=avedailynet_mj*srad_co2 !scale daily radiation
!     for CO2 scenario
! end if
! Average daily windspeed
! if (avewspdcount.ne.0)then
!     avewspd=dailywspdsum/avewspdcount
!     avewspd2=avewspd*0.748 !convert 10m windspeed to 2m, already
!     scaled for CO2
! endif
! if (avepcount.ne.0)then
!     pave=dailypsum/avepcount
! endif
! MEAN temperature - JUST ADDED TO THIS PGM VERSION
! if (avetempcount.ne.0)then
!     meantemp=dailytempsum/avetempcount
! endif
! Actual vapor pressure (ea) from RH data
! VPmin=0.6108*exp((17.27*tempmin)/(tempmin+237.3))
! VPmax=0.6108*exp((17.27*tempmax)/(tempmax+237.3))
! VPsat=(VPmin+VPmax)/2.
! VPactual=((VPmin*rhmax/100)+(VPmax*rhmin/100))/2.
! tempave=(tempmax+tempmin)/2
! VPCslope=(4098.*(0.6108*exp((17.27*tempave)/&
! &(tempave+237.3))))/(tempave+237.3)**2
! psychrometric constant - convert P from mbar to kPa
! psycon=0.665E-3*pave*0.1
! Calculate ETo using Penman-Monteith
! ETrefnum=(0.408*VPCslope*avedailynet_mj)+((psycon*900)/&
! &(tempave+273))
! ETrefden=VPCslope+(psycon*(1+0.34*avewspd2))
! ETref=((ETrefnum*avewspd2*(VPsat-VPactual))/ETrefden)
! ETref is output in mm/day, converted to cm/day for HYDRUS input
!
! Calculate ETo using Hargreaves - output in cm/day
! ETrefHarg=0.0135*(meantemp+17.78)*avedailynet_mj*(238.8/&
! &(595.5-(0.55*meantemp)))*0.1
! Write output file
! write(un_radout,500)month,day,year,jday,ETref,ETrefHarg,meantemp
500 format(i2,'/',i2,'/',i4,i5,f14.4,f14.4,f14.4)
!
! end if
!
! jcount=jcount+1
20     continue
end

```

```

Program pcphourly10
implicit none
!
!
!Program written 6/21/08 to extract an hourly input file (ATMOSPH.IN)
!for compressed precipitation scenario (Test E) for hourly HYDRUS run.
!This program reads the current daily ATMOSPH.IN input file, partitions
!daily potential evap and trans values into hourly values, and
!distributes daily precipitation into 3 blocks, with 10% falling
!between 12:01AM - 6AM, 80% between 6AM - 12PM, and 10% between 12:01PM
!and 12AM. Rainfall is randomized within each block by hourly time
!step.
!Amanda Brandt
!
!
character(len=140) ::header1,header2,header3,header4
!
real,    dimension(:),allocatable ::Prec,rSoil,rRoot,rB,hB,ht
real,    dimension(:),allocatable ::tTop,tBot,Ampl,Conc,rRoot_hrly
real,    dimension(:),allocatable ::rSoil_hrly,cBot
real    ::Pcp_hrly(1:24)
!
real    ::Random@,RanArray1(6)
real    ::Random@,RanArray2(7:18)
real    ::Random@,RanArray3(19:24)
real    ArraySum1,ArraySum2,ArraySum3
!
integer  un_atmos_read,un_atmos_hrly,tfinal_hrly
integer  tfinal,i,j,k,l,hour,ioerr1,ioerr2,hCritS
integer,dimension(:),allocatable ::tAtm,tAtm_hrly,hCritA
!
ioerr1=0
ioerr2=0
!
un_atmos_read=2
un_atmos_hrly=3
!
!
header1="  "
header2="  "
header3="  "
header4="  "
tfinal=130000
tfinal_hrly=3120000
hour=1
hCritS=0
!
!
open(unit=un_atmos_read,file='c:/F/ATMOSPH.IN',status='old')
open(unit=un_atmos_hrly,file='c:/F/atmos_hourly.txt',status='new')
allocate(tAtm(1:tfinal),Prec(1:tfinal),rSoil(1:tfinal),rRoot(1:tfinal),
hCritA(1:tfinal))
allocate(rB(1:tfinal),hB(1:tfinal),ht(1:tfinal),tTop(1:tfinal),tBot(1:t
final),cBot(1:tfinal))

```

```

allocate(AMPL(1:tfinal),Conc(1:tfinal),rRoot_hrly(1:tfinal),rSoil_hrly(
1:tfinal))
allocate(tAtm_hrly(1:tfinal_hrly))
!
! Read ATMOSPH.IN
read(unit=un_atmos_read,fmt=100,iostat=ioerr1)header1,header2,&
&tfinal,header3,hCritS,header4
tfinal_hrly=tfinal*24
write(unit=un_atmos_hrly,fmt=100,iostat=ioerr2)header1,header2,&
&tfinal_hrly,header3,hCritS,header4
100 format(A120/,A120/,i7/,A120/,i7/,A140)
200 format(1x,i10,3(f12.5),i12,8(f12.4))
210 format(1x,i10,3(f12.5),i12,9(f12.4))
300 format("Problem with input ATMOSPH.IN!!! Error code",i5)
do i=1,tfinal
read(unit=un_atmos_read,fmt=200,iostat=ioerr1)tAtm(i),Prec(i),&
&rSoil(i),rRoot(i),hCritA(i),rB(i),hB(i),ht(i),tTop(i),tBot(i),&
&AMPL(i),Conc(i)
cBot(i)=0
if(ioerr1.ne.0)then
write(*,300)ioerr1
end if
!
do j=1,6
RanArray1(j)=Random@()
end do
do k=7,18
RanArray2(k)=Random@()
end do
do l=19,24
RanArray3(l)=Random@()
end do
!
ArraySum1=sum(RanArray1)
ArraySum2=sum(RanArray2)
ArraySum3=sum(RanArray3)
!
!Subdivide daily records into hourly
do hour=1,24
select case(hour)
case(1:6)
j=hour
Pcp_hrly(hour)=(RanArray1(j)/ArraySum1)*Prec(i)*0.10
case(7:18)
k=hour
Pcp_hrly(hour)=(RanArray2(k)/ArraySum2)*Prec(i)*0.80
case(19:24)
l=hour
Pcp_hrly(hour)=(RanArray3(l)/ArraySum3)*Prec(i)*0.10
end select
rSoil_hrly(i)=rSoil(i)/24
rRoot_hrly(i)=rRoot(i)/24
tAtm_hrly(hour)=(tAtm(i)-1)*24+hour
!
!
write(unit=un_atmos_hrly,fmt=210,iostat=ioerr2)tAtm_hrly(hour),&
&Pcp_hrly(hour),rSoil_hrly(i),rRoot_hrly(i),hCritA(i),rB(i),hB(i),&

```



```
&ht(i),tTop(i),tBot(i),Ampl(i),Conc(i),cBot(i)
  if(ioerr2.ne.0)then
    stop
  end if
end do
end do
write(unit=un_atmos_hrly,fmt=410)
410 format("end")
!
end program
```

REFERENCES

- Abatzoglou, J.T. and Redmond, K.T. 2007. Assymetry between trends in spring and autumn temperature and circulation regimes over western North America, *Geophysical Research Letters*, 34: L18808, doi:10.1029/GL030891.
- Albright, W., Tyler, S., Chapman, J., Miller, M., Estrella, R. 1994. "Area 5 Site Characterization Project Report, FY 1994", DOE/NV/10845-T20, Prepared for U.S. DOE/NV Operations Office. Desert Research Institute, Water Resources Center: Reno, NV.
- Allen, R., Pereira, L.S., Raes, D., Smith, M. 1998. "Crop evapotranspiration – Guidelines for computing crop water requirements", FAO Irrigation Drainage Paper No. 56, Food and Agriculture Organization: Rome, Italy.
- Balling, R.C. 1988. The impact of summer rainfall on the temperature gradient along the United States-Mexico border, *Journal of Applied Meteorology*, 28: 304-308.
- Barbour, M.G. 1977. Terrestrial vegetation of California, 1002 pp. Wiley Interscience: New York, NY.
- Beatley, J. 1974. Effects of rainfall and temperature on the distribution and behavior of larrea tridentata (creosote-bush) in the Mojave Desert of Nevada, *Ecology*, 55(2): 245-261.
- Bechtel Nevada. 2001. "Composite Analysis for the Area 5 Radioactive Waste Management Site at the Nevada Test Site, Nye County, Nevada", DOE/NV-994, Prepared for U.S. DOE/NNSA/Nevada Operations Office: Las Vegas, NV.
- Bechtel Nevada. 2002. "2001 Waste Management Monitoring Report for Area 3 and Area 5 Radioactive Waste Management Sites", DOE/NV/11718-718, Prepared for U.S. DOE/NNSA/Nevada Operations Office: Las Vegas, NV.
- Bechtel Nevada. 2005a. "Hydrogeologic characterization data from the Area 5 shallow soil trenches", DOE/NV/11718-1060, Prepared for U.S. DOE/NNSA/Nevada Site Office: Las Vegas, NV.
- Bechtel Nevada. 2005b. "Hydrogeologic characterization and monitoring data from the Area 5 pilot wells", DOE/NV/11718-1067, Prepared for U.S. DOE/NNSA/Nevada Site Office: Las Vegas, NV.
- Bechtel Nevada. 2005c. "Characterization report: Operational closure covers for the Area 5 Radioactive Waste Management Site at the Nevada Test Site", DOE/NV/11718-758, Prepared for U.S. DOE/NNSA/Nevada Site Office: Las Vegas, NV.

- Boer, G.J., McFarlane, N.A., and Lazare, M. 1992. Greenhouse gas-induced climate change simulated with the CCC second generation general circulation model. *Journal of Climate*, 5(10): 1045-1077.
- Bradley, B.A. and Fleishman, E. 2008. Relationships between expanding pinyon-juniper cover and topography in the central Great Basin, Nevada, *Journal of Biogeography*, 35: 951-964.
- Briones, O., Montana, C. and Excurra, E. 1996. Competition between three chihuahuan desert species: evidence from plant size-distance relations and root distribution. *Journal of Vegetation Science*, 7(3): 453-460.
- Brooks, R.H. and Corey, A.T. 1966. Properties of porous media affecting fluid flow, *Journal of Irrigation and Drainage Engineering*, 72(IR2): 61-88.
- Capon, S. 2003. Plant community responses to wetting and drying in a large arid floodplain, *River Research and Applications*, 19: 509-520.
- Carsel, R.F. and Parrish, R.S. 1988. Developing joint probability distributions of soil water retention characteristics, *Water Resources Research*, 24(5): 755-769.
- Catlett, K., Sully, M., Tauxe, J., Stockton, T. and Black, P. 2003. "Unsaturated zone conceptual model for the NTS Area 5 RWMS GoldSim Model", Neptune and Co.: Los Alamos, NM.
- Choi, J.-W., Tillman, F.D., Smith, J.A. 2002. Relative importance of gas-phase diffusive and advective Trichlorethene Fluxes in the unsaturated zone under natural conditions, *Environmental Science and Technology*, 36(14): 3157-3164.
- Christensen, J.H., Hewitson, B., Busuioc, A., Chen, A., Gao, X., Held, I., Jones, R., Kolli, R.K., Kwon, W.-T., Laprise, R., Magana Rueda, V., Mearns, L., Menendez, C.G., Raisanen, J., Rinke, A., Sarr, A., and Whetton, P. 2007. 2007: Regional Climate Projections. In: *Climate Change 2007: The Physical Science Basis. Contribution of Working Group I to the Fourth Assessment Report of the Intergovernmental Panel on Climate Change*, eds. Solomon, S., D. Qin, M. Manning, Z. Chen, M. Marquis, K.B. Averyt, M. Tignor and H.L. Miller. Cambridge University Press: New York, NY.
- Classen, A.T., Hart, S.C., Whitman, T.G., Cobb, N.S., and Koch, G.W. 2005. Insect infestations linked to shifts in microclimate: important climate change implications, *Soil Science Society of America Journal*, 69: 2049-2057. doi:10.2136/sssaj2004.0396.
- Cook, P.W., Edmunds, W.M. and Gayne, C.B. 1992. Estimating paleorecharge and paleoclimate from unsaturated zone profiles, *Water Resources Research*, 23 (10): 2721-2731.
- Deput, E.J and Caldwell, M.M. 1975. Gas exchange of three cool semi-desert species in relation to temperature and water stress, *Journal of Ecology*, 63: 835-858.

- Edmunds, W.M. and Tyler, S.W. 2002. Unsaturated zones as archives of past climates: toward a new proxy for continental regions, *Hydrogeology Journal*, 10: 216-228.
- Elvidge, C.D. and Chen, Z. 1995. Comparison of broad-band and narrow-band red and near-infrared vegetation indices, *Remote Sensing of Environment*, 54: 38-48.
- Feddes, R.A., Kowalik, P.J. and Zaradny, H. 1978. *Simulation of Field Water Use and Crop Yield*, John Wiley & Sons: New York, NY.
- Franco, A.C., de Soyza, A.G., Virginia, R.A., Reynolds, J.F. and Whitford, W.G. 1994. Effects of plant size and water relations on gas exchange and growth of the desert shrub *Larrea tridentata*, *Oecologia*, 94: 171-178.
- Gaubauer, R.L.E. and Ehleringer, J.R. 2000. Water and nitrogen uptake patterns following moisture pulses in a cold desert community, *Ecology*, 81(5): 1415-1424.
- Gee, G.W., Wierenga, P.J., Andraski, B.J., Young, M.H., Fayer, M.J. Rockhold, M.L.. 1994. Variations in water balance and recharge potential at three western desert sites, *Soil Science Society of America Journal*, 58: 63-72.
- Hamerlynck, E., Huxman, T., Nowak, R. Reder, S., Loik, M. Jordan, D., Zitzer, S., Coleman, J., Seemann, J.R. and Smith, S. 2000. Photosynthetic responses of *Larrea tridentata* to a step-increase in atmospheric CO₂ at the Nevada Desert FACE Facility, *Journal of Arid Environments*, 44: 425-436.
- Hansen, D. and Ostler, W.K. 2003. "Rooting characteristics of vegetation near Areas 2 and 5 Radioactive Waste Management Sites at the Nevada Test Site", DOE/NV/11718-595, Prepared for U.S. Department of Energy/ National Nuclear Security Administration, Nevada Site Office: Las Vegas, NV.
- Hargreaves, G. and Allen, R. 2003. History and evaluation of Hargreaves evapotranspiration equation, *Journal of Irrigation and Drainage Engineering*, 129(1): 59-70.
- Hillel, D. 1998. *Environmental Soil Physics*, 771 pp. Academic Press, Inc.: New York, NY.
- Houseworth, J. 2001. "Future Climate Analysis", ANL-NBS-GS-000008-Rev 00 ICN 01, Prepared for U.S. DOE/ Office of Civilian Radioactive Waste Management, Yucca Mountain Project. U.S. Geological Survey: Denver, CO.
- Housman, D.C., Naumberg, E., Huxman, T.E., Charlet, T.N., Nowak, R.S., and Smith, S.D. 2006. Increases in desert shrub productivity under elevated carbon dioxide vary with water availability, *Ecosystems*, 9:371-375.
- Hupet, F., Lambot, S., Javaux, M., and Vanclooster, M. 2002. On the identification of macroscopic root water uptake parameters from soil water content observations, *Water Resources Research*, 38(12): 1300, doi:10.1029/2002WR001556.
- IBP (International Biological Program). 1974. *International Biological Program, Reports of 1973 Progress, vol. 2, Validation Studies*, 332 pp. Utah State University: Logan, UT.

- IPCC (Intergovernmental Panel on Climate Change). 2007. *Climate Change 2007: The Physical Science Basis. Contributions of Working Group I to the Fourth Assessment Report of the Intergovernmental Panel on Climate Change*, eds. Solomon, S., D. Qin, M. Manning, Z. Chen, M. Marquis, K.B. Averyt, M. Tignor and H.L. Miller. Cambridge University Press: New York, NY. <http://www.ipcc.ch/ipccreports/ar4-wg1.htm>.
- Jaindl, R.G., Eddleman, L.E. and Doescher, P.S. 1995. Influence of an environmental gradient on physiology of singleleaf pinyon, *Journal of Rangeland Management*, 48: 224-231.
- Jackson, R.B., Candadell, J., Ehleringer, J.R., Mooney, H.A., Sala, O.E. and Schulze, E.D. 1996. A global analysis of root distributions for terrestrial biomes, *Oecologia*, 108: 389-411.
- Kemp, P., Reynolds, J., Pachepsky, Y and Chen, J. 1997. A comparative modeling study of soil water dynamics in a desert ecosystem, *Water Resources Research*, 33(1), 73-90.
- Kim, J. 2005. A projection of the effects of the climate change induced by increased CO₂ on extreme hydrologic events on the Western U.S., *Climatic Change*, 68: 153-168.
- Kirilenko, A.P. and Solomon, A.M. 1998. Modeling dynamic vegetation response to rapid climate change using bioclimatic classification, *Climatic Change*, 38: 15-49.
- Kittel, TGF, N.A. Rosenbloom, J.A. Royle, C. Daly, W.P. Gibson, H.H. Fisher, P. Thornton, D.N. Yates, S. Aulenbach, C. Kaufman, R. McKeown, D. Bachelet, D.S. Schimel, and VEMAP2 Participants. 2004. VEMAP Phase 2 bioclimatic database. I. Gridded historical (20th) century climate for modeling ecosystem dynamics across the conterminous USA, *Climate Research*, 27(2):151-170.
- Kwicklis, E.M., Wolfsberg, A.V., Stauffer, P.H., Walvoord, M.A., and Sully, M.J. 2006. Multiphase, multicomponent parameter estimation for liquid and vapor fluxes in deep arid systems using hydrologic data and natural environmental tracers, *Vadose Zone Journal*, 5: 934-950.
- Link, S.O., Kickert, R.N., Fayer, M.J. and Gee, G.W. 1993. "A comparison of simulation models for predicting soil water dynamics in bare and vegetated lysimeters", PNL-8675/UC-902, Prepared for the U.S. DOE. Pacific Northwest Laboratory, Richmond, WA.
- Lioubimtseva, E. 2004. Climate change in arid environments: revisiting the past to understand the future, *Progress in Physical Geography*, 28: 1-29.
- Ludwig, J.A., Reynolds, J.F., and Whitson, P.D. 1975. Size-biomass relations of several Chihuahuan desert shrubs, *American Midland Naturalist*, 94: 451-461.
- Melillo, J.M., McGuire, A.D., Kicklighter, D.W., Moore III, B.M., Vorosmarty, C.J., and Schloss, A.L. 1993. Global climate change and terrestrial net primary production, *Nature*, 636: 234-240.

- Miklas, M.P. Jr., Norwine, J., DeWispelare, A.R., Herren, L.T., and Clemen, R.T. 1995. Future climate at Yucca Mountain, Nevada proposed high-level radioactive waste repository, *Global Environmental Change*, 5(3): 221-234.
- Meta-Gonzalez, R., McLendon, T., and Martin, D.W. 2005. The inappropriate use of crop transpiration coefficients (K_c) to estimate evapotranspiration in arid ecosystems: a review, *Arid Land Research and Management*, 19: 285-295.
- Mualem, Y. 1976. A new model for predicting the hydraulic conductivity of unsaturated porous media, *Water Resources Research*, 12(3): 513-521.
- Neptune and Co. 2003. A Radiological Performance Assessment Model of the Area 5 Radioactive Waste Management Site, Nevada Test Site, Version 2.0. [CD ROM] Neptune and Co.: Evergreen, CO.
- National Securities Technologies. 2007. "Closure Strategy Nevada Test Site Area 5 Radioactive Waste Management Site", DOE/NV/25946-153, U.S. DOE, Nevada Operations Office: Las Vegas, NV.
- Obrist, D. and Arnone III, J.A. 2003. Increasing CO₂ accelerates root growth and enhances water acquisition during early stages of development in *Larrea tridentata*, *New Phytologist*, 159: 175-184.
- Pavek, Diane S. 1993. *Achnatherum speciosum*. In: *Fire Effects Information System*, [Online]. U.S. Department of Agriculture, Forest Service, Rocky Mountain Research Station, Fire Sciences Laboratory. <http://www.fs.fed.us/database/feis>
- Phillips, F.M. 1994. Environmental tracers for water movement in desert soils of the American Southwest, *Soil Science Society of America Journal*, 58: 15-24.
- Prentice, I.C., Cramer, W., Harrison, S., Leemans, R., Monserud, R., and Solomon, A. 1992. A global biome model based on plant physiology and dominance, soil properties and climate, *Journal of Biogeography*, 19: 177-134.
- REECo (Reynolds Electrical and Engineering Company). 1994. "Site characterization and monitoring data from area 5 pilot wells, Nevada Test Site, Nye County, NV", DOE/NV/11432-74, U.S. DOE, Nevada Operations Office: Las Vegas, NV.
- Reynolds, J.F., Virginia, R.A., and Schlesinger, W.H. 1996. Defining functional types for models of desertification. In: *Functional Types*, eds. Smith, T.M., Shugart, H.H. and Woodward, F.I., p. 194-214. Cambridge University Press: New York, NY.
- Sammis, T.W. and Gay, L.W. 1979. Evapotranspiration from an arid zone plant community, *Journal of Arid Environments*, 2: 313-321.
- Saucedo, D., Sammis, T.W., Picchioni, G.A. and Mexal, J.G. 2005. Wastewater application and water use of *larrea tridentata*, *Agricultural Water Management*, 82: 343-353.

- Scanlon, B.R., Christman, M., Reedy, R.C., Porro, I., Simunek, J., and Flerchinger, G.N. 2002. Intercode comparisons for simulating water balance of surficial sediments in semiarid regions, *Water Resources Research*, 38(12): 1323, doi:10.1029/2001WR001233.
- Scanlon, B.R., Keese, K., Teedy, R., Simunek, J., and Andraski, B. 2003. Variations in flow and transport in the thick desert vadose zones in response to paleoclimatic forcing (0-90 kyr): Field measurements, modeling, and uncertainties, *Water Resources Research*, 39: 1179-1196.
- Scott, R.L., Huxman, T.E., Cable, W.L., and Emmerich, W.E. 2006. Partitioning of evapotranspiration and its relation to carbon dioxide exchange in a Chihuahuan Desert shrubland, *Hydrological Processes*, 20: 3227-3243.
- Schenk, H.J. 2005. "Vertical Vegetation Structure Below Ground: Scaling from Root to Globe" in *Progress in Botany, Vol. 66*, ed. Esser, K., p.341-373. Springer-Verlag Berlin, DEU: Springer, 2005.
- Schlesinger, W. H. and Pilmanis, A.M. 1998. Plant-soil interactions in deserts, *Biogeochemistry*, 42: 169-187.
- Schwinning, S., Davis, K., Richardson, L., and Ehleringer, J.R. 2002. Deuterium enriched irrigation indicates different forms of rain use in shrub/grass species of the Colorado Plateau, *Oecologia*, 130 (3): 345- 355.
- Sharpe, S. 2003. "Future Climate Analysis – 10,000 years to 1,000,00 years after present", MOD 01 001 Rev 01, U.S. Department of Energy, Nevada Operations Office, Las Vegas, NV.
- Shott, G., Sully, M., Muller, C., Hammermeister, D., Gianni, J. 1995. Site characterization and performance assessment for a low level radioactive waste management site in the American southwest, DOE/NV/11432-192. In: *Fifth international conference on radioactive waste management and environmental remediation -- ICM'95: Proceedings. Volume 2: Management of low-level waste and remediation of contaminated sites and facilities*. American Society of Mechanical Engineers: New York, NY.
- Simunek, J., M. Sejna, and van Genuchten, M.T. 2005. The HYDRUS-1D Software Package for Simulating the One-Dimensional Movement of Water, Heat and Multiple Solutes in Variably-Saturated Media, version 2.0, International Groundwater Modeling Center, Colorado School of Mines: Golden, CO.
- Smith, S.D., Herr, C.A., Leary, K.L., and Piorkowski, J.M. 1995. Soil-plant water relations in a Mojave Desert mixed shrub community: a comparison of three geomorphic surfaces, *Journal of Arid Environments*, 29: 339-351.
- Soule, D.A. 2006. Climatology of the Nevada Test Site. SORD Technical Memorandum SORD 2006-003, April 2006, NOAA Air Resources Laboratory, Special Operations and Research Division: Las Vegas, NV.

- Spaulding, W.G. 1990. Vegetational and climatic development of the Mojave Desert: The Last Glacial Maximum to the present. In: *Packrat Middens: The Last 40,000 Years of Biotic Change*, eds. J.L. Betancourt, T. R Van Devender and P.S. Martin, p. 166-199. University of Arizona Press: Tucson, AZ.
- Thompson, R.S. and Anderson, K.H. 2000. Biomes of western North America at 18,000, 6000 and 0 ^{14}C yr BP reconstructed from pollen and packrat midden data, *Journal of Biogeography*, 27, 555-584.
- Tyler, S.W., Chapman, J.B., Conrad, S.H., Hammermeister, D.P., Blout, D.O., Miller, J.J., Sully, M.J., Ginanni, J.M. 1996. Soil-water flux in the southern Great Basin, United States: Temporal and spatial variations over the last 120,000 years, *Water Resources Research*, 32: 1481-1499.
- US DOE (Department of Energy). 1997. "Environmental Assessment for the Area 5 Radioactive Waste Management Site Access Improvement at the Nevada Test Site", DOE/EA-1170. U.S. DOE, Nevada Operations Office: Las Vegas, NV.
- USDA NRCS (United States Department of Agriculture Natural Resources Conservation Service). 2008. The PLANTS Database. National Plant Data Center: Baton Rouge, LA. <http://plants.usda.gov>.
- Utah State University. 2008. Range Plants of Utah. Utah State University Cooperative Extension: Logan, UT. <http://extension.usu.edu/range/index.htm>.
- van Genuchten, M.Th. 1980. A closed form equation for predicting the hydraulic conductivity unsaturated soils, *Soil Science Society of America Journal*, 44, 892-898.
- Vogel, T., Cislerova, M. and Hopmans, J.W. 1991. Porous media with linearly variable hydraulic properties, *Water Resources Research*, 27(10): 2735-2741.
- Walvoord, M.A., Plummer, M.A., Phillips, F.M., Wolfsberg, A.V. 2002a. Deep arid system hydrodynamics 1. Equilibrium states and response times in thick desert vadose zones, *Water Resources Research*, 38: 1308-1323.
- Walvoord, M.A., Phillips, F.M., Tyler, S.W., Hartsough, P.C. 2002b. Deep arid system hydrodynamics 2. Application to paleohydrologic reconstruction using vadose zone profiles from the northern Mojave Desert, *Water Resources Research*, 38: 1291-1307.
- Walvoord, M.A., Stonestrom, D., Andraski, B., and Striegl, R. 2004. Constraining the Inferred Paleohydrologic Evolution of a Deep Unsaturated Zone in the Amargosa Desert, *Vadose Zone Journal*, 3: 502-512.
- Warren, C.R., McGrath, J.F., and Adams, M.A. 2001. Water availability and carbon isotope discrimination in conifers, *Oecologia*, 127: 476-486.
- Webb, R.H., Murov, M.B., Esque, T.C., Boyer, D.E., DeFalco, L.A., Haines, D.F., Oldershaw, D., Scoles, S.J., Thomas, K.A., Blainey, J.B. and Medica, P.A.. 2003.

- “Perennial vegetation data from permanent plots on the Nevada Test Site, Nye County, Nevada”, U.S. Geological Survey Open File Report 03-336: Tucson, AZ.
- Williamson, S.C., Detling, J.K. Dood, J.L. and Dyer, M.I. 1987. Nondestructive estimation of shortgrass aerial biomass, *Journal of Rangeland Management*, 40: 254-256.
- Wilmott, C.J., and Feddema, J.J. 1992. A more rational climatic moisture index, *Professional Geographer*, 44(1): 84-87.
- Winograd, I., and Thordarson, W. 1975. “Hydrogeologic and hydrochemical framework, South-central Great Basin, Nevada-California, with special reference to the Nevada Test Site”, U.S. Geological Survey Professional Paper 712-C. U.S. Geological Survey: Golden, CO.
- Wolfsberg, A. and Stauffer, P. 2003. “Vadose zone fluid and solute flux: Advection and diffusion at the Area 5 Radioactive Waste Management Site”, submitted to U.S. DOE/ National Nuclear Security Administration; Los Alamos National Laboratory, Earth and Environmental Sciences Division: Los Alamos, NM.
- Woolfenden, W.B. 1996. Quaternary vegetation history. In: *Sierra Nevada Ecosystem Project: Final report to Congress, vol II, Assessments and Scientific Basis for Management Options*. Davis: University of California, Centers for Water and Wildland Resources: Davis, CA.
- Wu, I. 1997. A simple evapotranspiration model for Hawaii: The Hargreaves model, *CTAHR Fact Sheet, Eng. Notebook, 106*. College of Tropical Agriculture and Human Resources, University of Hawaii, Manoa: Honolulu, HI. <http://www.ctah.hawaii.edu/oc/freepubs/pdf/EN-106.pdf>.
- Young, M., McDonald., E., Caldwell, T., Benner, S., and Meadows, D. 2004. Hydraulic properties of a desert soil chronosequence in the Mojave Desert, USA. *Vadose Zone Journal*, 3(3): 956-963.
- Young, M.H., Cooper, C., Sharpe, S., Miller, J., and Shafer, D. 2002. “Upward advection: Dynamic simulation of vadose zone moisture flux”, Desert Research Institute: Las Vegas, NV.
- Yin, J., Young, M.H., and Yu, Z. 2008. Effects of paleoclimate and time-varying canopy structure on paleowater fluxes, *Journal of Geophysical Research*, 113, D06013, doi:10.1029/2007JD009010.
- Yucel, V. and Levitt, D. 2001. Potential groundwater recharge and the effects of soil heterogeneity on flow at two radioactive waste management sites at the Nevada Test Site. DOE/NV/11718—609. 2002 *International Groundwater Symposium*. Berkeley, CA.

VITA

Graduate College
University of Nevada, Las Vegas

Amanda Marie Brandt

Local Address:

5317 Red Glory Drive
Las Vegas, NV 89130

Degrees:

Bachelor of Environmental Studies, 1999
York University
Toronto, Ontario, Canada

Thesis Title: Modeling the Unsaturated Zone at the Area 5 Radioactive Waste
Management Site: Effects of Climate Change and Vegetation on Flow Conditions

Thesis Examination Committee:

Chairperson, Dr. David Kreamer, Ph.D.
Committee Member, Dr. Gary Cerefice, Ph.D.
Committee Member, Dr. Michael Young, Ph.D.
Graduate Faculty Representative, Dr. Clifford McClain, Ph.D.